

Bioprospecting of Red Sea Sponges for Novel Antiviral Pharmacophores

Dissertation by

Aubrie Elise O'Rourke

In Partial Fulfillment of the Requirements

For the Degree of

Doctor of Philosophy

King Abdullah University of Science and Technology, Thuwal,

Kingdom of Saudi Arabia

© April 2015

Aubrie O'Rourke

All rights reserved

The dissertation of Aubrie Elise O'Rourke is approved by the examination committee.

Committee Chairperson: Dr. Christian R Voolstra

Committee Member: Dr. Uli Stingl

Committee Member: Dr. Niveen Khashab

Committee Member: Dr. Ruth Brack-Werner

ABSTRACT

Bioprospecting of Red Sea Sponges for Novel Antiviral Pharmacophores

Aubrie Elise O'Rourke

Natural products offer many possibilities for the treatment of disease. More than 70% of the Earth's surface is ocean, and recent exploration and access has allowed for new additions to this catalog of natural treasures. The Central Red Sea off the coast of Saudi Arabia serves as a newly accessible location, which provides the opportunity to bioprospect marine sponges with the purpose of identifying novel antiviral scaffolds. Antivirals are underrepresented in present day clinical trials, as well as in the academic screens of marine natural product libraries. Here a high-throughput pipeline was initiated by prefacing the antiviral screen with an Image-based High-Content Screening (HCS) technique in order to identify candidates with antiviral potential. Prospective candidates were tested in a biochemical or cell-based assay for the ability to inhibit the NS3 protease of the West Nile Virus (WNV NS protease) as well as replication and reverse transcription of the Human Immunodeficiency Virus 1 (HIV-1). The analytical chemistry techniques of High-Performance Liquid Chromatography (HPLC), Liquid Chromatography-Mass Spectrometry (LC-MS), and Nuclear Magnetic Resonance (NMR) were used in order to identify the compounds responsible for the characteristic antiviral activity of the selected sponge fractions. We have identified a 3-alkyl pyridinium from *Amphimedon chloros* as the causative agent of the observed WNV NS3 protease inhibition *in vitro*. Additionally, we identified debromohymenialdisine, hymenialdisine, and oroidin from *Stylissa carteri* as prospective scaffolds capable of HIV-1 inhibition.

ACKNOWLEDGMENTS

I would like to thank my Father for his love and support. I would like to thank my friends and family for their support as well. I would like to thank my committee members Dr. Uli Stingl, Dr. Niveen Khashab, and Dr. Ruth Brack-Werner. I would like to thank my advisor, Dr. Christian Voolstra, for recruiting, overseeing, and funding my research and allowing me to pursue my interest in Natural Products as antivirals, as well as my postdoc advisor, Dr. Stephan Kremb, who helped to coordinate experiments concerning his previous work with HIV, established the High Content Screening technique, and both for their frequent review of my progress. I am thankful for the HIV screening performed by colleagues, Dr. Markus Helfer and Theresa Maria Rock, in the lab of Dr. Ruth Brack-Werner. I am also thankful for the camaraderie of my labmates and Red Sea Research Center members, whose SCUBA prowess made replicate collection quite easy. I am very thankful for the friendly and knowledgeable personnel of the KAUST core labs, Misjudeen Raji, Salim Sioud, Najeh M. Kharbartia, and Abdel-Hamid Emwas, as well as the state-of-the-art instrumentation provided by KAUST. I am thankful to our Director, Dr. Xabier Irigoyen, for funding me to attend the 2014 GRC Natural Products conference, an event that proved to be a turning point in my research. I am thankful for the time Dr. Nicole deVoogd took to sit with me, where she helped with the identification of the unknown sponges in our collection. I am appreciative of the time Dr. William Gerwick gave to me to review and discuss my data. This work is dedicated to those who have been affected by viral Myocarditis, in memory of Caitlyn Vincent and for her family.

Table of Contents

APPROVAL BY THE EXAMINATION COMMITTEE	2
ABSTRACT	3
ACKNOWLEDGMENTS	4
LIST OF ABBREVIATIONS.....	9
LIST OF FIGURES.....	11
LIST OF TABLES	13
INTRODUCTION	14
Natural Products versus Synthetics as Pharmacophores	14
The need for novel Antiviral Pharmacophores and targets	15
Marine natural products and bioactivity	19
Marine sponges and their antiviral potential.....	20
OBJECTIVE	23
REFERENCES	24
CHAPTER 1: Bioprospecting of a Central Red Sea Sponge Library	27
1.1 Abstract	27
1.2 Introduction.....	28
1.2.1 High Content Screening using pre-fractionated Marine extracts.....	29
1.2.2 <i>High Content Screening for the identification of novel Antivirals</i>	30
1.3 Materials and Methods.....	32
1.3.1 <i>Red Sea Sponge Specimen collection</i>	32
1.3.2 <i>Red Sea Sponge Specimen Identification</i>	32
1.3.3 <i>Compilation of a Red Sea Sponge Screening Library</i>	33
1.3.4 <i>High Content Screening of a Red Sea Sponge Library</i>	34
1.4 Results.....	36
1.4.1 <i>Sponge Taxonomy</i>	36
1.4.2 <i>High Content Screening identifies antiviral candidates</i>	38
1.5 Discussion.....	39
1.6 Figures and Tables.....	45
1.7 References	55

CHAPTER 2: Identification of a 3-alkyl pyridinium from the Red Sea sponge Amphimedon chloros as an inhibitor of the West Nile Virus NS3 protease in vitro.....	59
2.1 Abstract	59
2.2 Introduction.....	60
2.3 Materials and Methods.....	62
2.3.1 <i>A. chloros</i> Sponge Collection.....	62
2.3.2 <i>A. chloros</i> Sponge Extraction.....	62
2.3.3 West Nile Virus NS3 Protease Inhibition Assay.....	63
2.3.4 HCV NS3 Protease Inhibition Assay.....	63
2.3.5 Thrombin serine protease inhibition assay	64
2.3.6 Cytotoxicity/HCA of <i>A. chloros</i>	64
2.3.7 LC-MS of <i>A. chloros</i> Bioactive compound.....	65
2.3.8 NMR of <i>A. chloros</i> 3-alkyl pyridinium.....	65
2.4 Results.....	65
2.4.1 <i>A. chloros</i> demonstrates inhibiton of West Nile Virus NS3 Protease	65
2.4.2 High-Content Screening reveals cytotoxic of <i>A.chloros</i> treatment	66
2.4.3 Analytical Chemistry reveals 3-alkyl pyridinium as bioactive compound.....	66
2.4.4 DOSY reveals the approximate size of the 3-alkyl pyridinium bioactive compound	67
2.5 Discussion.....	68
2.6 Figures and Tables.....	73
2.7 References	80
CHAPTER 3: Alkaloids from <i>Stylissa carteri</i> present prospective scaffolds for the inhibition of the Human immunodeficiency Virus-1 (HIV-1)	83
3.1 Abstract	83
3.2 Introduction.....	84
3.2.1 Human immunodeficiency virus -1 replication.....	85
3.2.2 Known compounds from <i>Stylissa carteri</i>	86

3.2.3 Brominated marine natural products.....	87
3.2.4 Reduction of viral pathogenesis by host regulation	87
3.2.5 Pharmacophores from a Red Sea Sponge.....	88
3.3 Materials and Methods.....	89
3.3.1 <i>S. carteri</i> Specimen collection and sample fractionation.....	89
3.3.2 Human Immunodeficiency Virus, full Virus Screening	90
3.3.3 MTT assay.....	91
3.3.4 Human Immunodeficiency Virus, Reverse transcriptase biochemical test.....	91
3.3.5 Analytical Chemistry of bioactive <i>S. carteri</i> fractions.....	92
3.3.6 Principle component analysis of molecular descriptors.....	92
3.3.7 <i>In silico</i> modeling.....	92
3.4 Results.....	93
3.4.1 Activity of <i>S. carteri</i> SPE fraction 1 on HIV-1 replication.....	93
3.4.2 Activity of <i>S. carteri</i> HPLC fractions on HIV-1 replication.....	93
3.4.3 Activity of <i>S. carteri</i> HPLC fractions 2 and 6 on HIV-1 RT activity <i>in vitro</i>	93
3.4.4 High Content Screening of <i>S. carteri</i> SPE fractions.....	94
3.4.5 Analytical Chemistry of active HPLC fractions.....	94
3.4.6 Principal Component Analysis of Molecular Descriptors for LOPAC reference compound, Sponge constituents, and approved HIV-1 Reverse Transcriptase drugs	95
3.4.7 Activity of single molecules on full-virus model HIV-1 replication.....	96
3.4.8 Activity of single molecules on HIV-1 reverse transcriptase assay	96
3.4.9 <i>In Silico</i> modeling of Oroidin on HIV-1 Reverse Transcriptase.....	96
3.5 Discussion.....	97
3.5.1 Previously described compounds from <i>S. carteri</i> as candidate inhibitors.....	98
3.5.2 Debromohymenialdisine and Hymenialdisine demonstrate a broad inhibition of HIV-1 while Oroidin targets the HIV-1 Reverse Transcriptase	101

3.5.3 PCA helps to propose the binding of Oroidin.....	102
3.5.4 In Silico modeling of Oroidin and the HIV-1 Reverse Transcriptase.....	103
3.5.5 Candidates show similarity to current marine alkaloid anti-HIV leads.....	103
3.6 Conclusion	105
3.7 Figures and Tables.....	107
3.8 References	128
Dissertation Conclusion.....	131
Manuscripts in preparation	132
Patent Applications Filed.....	132

LIST OF ABBREVIATIONS

HCS	High Content Screening
HPLC	High performance Liquid Chromatography
LC-MS	Liquid Chromatography Mass Spectrometry
NMR	Nuclear Magnetic Resonance
Poly-APS	poly-Alkyl pyridiniums
WNV	West Nile Virus
NS3	Nonstructural protein 3
ADC	Antibody Drug Conjugates
FDA	US Food and Drug Administration
logP	octanol-water partition coefficient
ADMET	Absorption, Distribution, Metabolism, Excretion and Toxicity
HCV	Hepatitis C Virus
HPV	Human Papilloma Virus
HIV-1	Human Immunodeficiency Virus -1
HTLV	Human T-Cell Lymphotropic Virus
HSV	Herpes Simplex Virus
AZT	Azidothymidine
HAART	Highly Active Antiretroviral Therapy
DAAs	Directly Acting Antivirals
DENV	Dengue Virus
YFV	Yellow Fever Virus
HP20SS	Highly porous 20 styrenic, small
FW	Fraction water or deionized water
IPA	Isopropanol

MeOH	Methanol
CBIQ	4-Chlorobenzo[F]isoquinoline
LTR	Long Terminal Repeat
NOS	Nitric Oxide Synthase
SIRT	Inhibitor of Sirtuin
EGF	Epidermal Growth Factor
DRG	Dorsal Root Ganglion
SPE	Solid Phase Extract
VSV	Vesicular Stomatitis Virus
NNRTI	Non-Nucleoside Reverse Transcriptase Inhibitor
CDK	Cyclin Dependent Kinase
B-P-2-AI	Brominated pyrrole-2-aminoimidazole
HD	Hymenialdisine
DBH	Debromohymenialdisine
NRTI	Nucleoside Reverse Transcriptase Inhibitor
Tat	HIV-1 Trans-activator of Transcription
ATP	Adenosine Triphosphate
RHRTI	RNase H Reverse Transcriptase Inhibitor

LIST OF FIGURES

Introduction:

Figure 1: Timeline highlighting the tripartite link between Cancer research, Marine natural products and Antivirals. (Dates compiled from literature.)..... 18

Figure 2: High-throughput approach for identifying novel antiviral inhibitors from a pre-fractionated Red Sea sponge library. 24

CHAPTER 1: Bioprospecting of a Central Red Sea Sponge Library

Figure 1. 1: Red Sea extract fractionation process..... 45

Figure 1. 2: Images of sponge species represented in the Red Sea sponge library. 47

Figure 1. 3: Sponge samples and the LOPAC library were clustered according to Spearman distance with complete linkage and displayed as a heat map..... 48

Figure 1. 4: Compounds which cluster with *A. chloros* fraction 2..... 49

Figure 1. 5: Compounds which cluster with *S. carteri* fraction 1. 50

CHAPTER 2: Identification of a 3-alkyl pyridinium from the Red Sea sponge *Amphimedon chloros* as an inhibitor of the West Nile Virus NS3 protease in vitro

Figure 2. 1: Replication steps of the WNV depicting fusion and entry (Steps 1 and 2), uncoating and release (Step 3), translation of the polyprotein and packaging of a mature virus (Steps 4-10). 73

Figure 2. 2: Activity of *A. chloros* on the WNV NS3 protease. 74

Figure 2. 3: Vitality of cells treated with HPLC fractions from the SPE fraction 2 (SPE F2) of *A. chloros*. 75

Figure 2. 4: Analytical chemistry of active SPE fraction 2 from *A. chloros*. 77

CHAPTER 3: Alkaloids from *Stylissa carteri* present prospective scaffolds for the inhibition of the Human Immunodeficiency Virus-1 (HIV-1)

Figure 3. 1: The nine virally encoded genes of HIV-1: *gag*, *pol*, *vif*, *vpr*, *rev*, *tat*, *nef*, *env* and the Long Terminal Repeat (LTR). (Figure adapted from Gottfredsson et al. 199735.) 107

Figure 3. 2: The HIV replication cycle including 1. Fusion, 2. Virus entry, 3. Reverse transcription, 4. Integration, 5. Packaging, 6. Budding, and 7. Maturation. (Image redrawn from NIAID illustration) 108

Figure 3. 3: Metabolites from <i>Stylissa carteri</i> , such as 10Z-hymenialdisine, debromohymenialdisine and sceptrin, with previously reported bioactivity are derivatives of the compound oroidin. (Figure adapted from Yarnold et al. 20124.)....	109
Figure 3. 4: Depiction of the EASY-HIT reporter scheme where the Tat protein drives transcription of the DsRed reporter harboring the p17/p24 elements of the HIV structural <i>gag</i> gene.....	110
Figure 3. 5: % Infection and % Cell Vitality of EASY-HIT assay after <i>S.carteri</i> SPE fraction 1 treatment.....	111
Figure 3. 6: % Infection and % Cell Vitality of EASY-HIT assay after <i>S.carteri</i> SPE fraction 1 HPLC fraction 1-11 treatment.....	112
Figure 3. 7: % Activity of the HIV-1 Reverse transcriptase after treatment with <i>S.carteri</i> SPE fraction 1, HPLC fraction 1, 2, 3, 4, and 6 treatment.....	113
Figure 3. 8: HCS Heat map and cell counts for HPLC fractions 1-10.....	114
Figure 3. 9: LC-MS chromatogram and spectra for <i>S.carteri</i> SPE fraction 1, HPLC fraction 2 and 6	115
Figure 3. 10: Compound procured from Enzo Life Sciences. (A) Debromohymenialdisine , (B) 10Z- Hymenialdisine and (C) Oroidin	116
Figure 3. 11: Principle component analysis was performed on data aggregated from the High Content Analysis (LOPAC, pink), EASY-HIT, RT biochemical test and LC-MS data (<i>Stylissa</i> , red) and known HIV RT inhibitors (NaRTI, yellow; NNRTI, blue; NtRTI, green; RHRTI, black).....	117
Figure 3. 12: % Infection and % Cell Vitality of EASY-HIT assay after debromohymenialdisine, hymenialdisine, and oroidin treatment.....	118
Figure 3. 13: Debromohymenialdisine, hymenialdisine, and oroidin screened on the biochemical HIV-1 reverse transcriptase assay	119
Figure 3. 14: In silico modeling of Oroidin with the HIV RT (PDB:1S1U) in Autodock vina..	120

LIST OF TABLES

CHAPTER 1: Bioprospecting of a Central Red Sea Sponge Library

Table 1. 1: Inventory of the Red Sea Sponge library includes the Call ID or sample number, available SPE fraction, the associated species name and point of collection. 51

Table 1. 2: Cellular stains used for High Content Screening (HCS) and parameters measure 53

CHAPTER 2: Identification of a 3-alkyl pyridinium from the Red Sea sponge *Amphimedon chloros* as an inhibitor of the West Nile Virus NS3 protease in vitro

Table 2. 1: HPLC gradient used to separate the *A. chloros* SPE fraction 2..... 79

CHAPTER 3: Alkaloids from *Stylissa carteri* present prospective scaffolds for the inhibition of the Human immunodeficiency Virus-1 (HIV-1)

Table 3. 1: HPLC gradient used to separate the *S. carteri* SPE fraction 1 into HPLC fractions 1-11..... 121

Table 3. 2: LC-MS gradient used to characterize the bioactive compounds of the *S. carteri* SPE fraction 1, HPLC fraction 2 and 6 (SPEF1_H2 and SPEF1_H6). 122

Table 3. 3: Molecular descriptors used for PCA analysis..... 123

Table 3. 4: Binding affinity values for molecular modeling of oroidin and HIV-1 RT. 126

Table 3. 5: Anti-HIV alkaloids reported in the literature to date. 127

INTRODUCTION

Marine natural products provide new avenues for drug discovery by offering a diversity of molecular scaffolds. The discovery and acquisition of natural product pharmacophores, constituted of novel “privileged scaffolds”, are important for the development of new pharmaceuticals. The atoms of pharmacophores have a chemical spatial arrangement, which elicit a known or predicted biological activity. Natural products have the potential to facilitate the hit to lead process because they act as starting points with unique chemical architectures that require less modification and optimization than what is necessary to achieve the same chemical novelty in a purely synthesized compound.

Natural Products versus Synthetics as Pharmacophores

A recent review of 100 natural products (NPs) (which includes compounds produced from natural product templates using semi-synthesis and synthetic compounds inspired by natural product templates) as well as the 33 Antibody Drug Conjugates (ADC) in clinical trials as of 2013, reveals the important role that natural products play primarily in the treatment of cancer and bacterial diseases and to a lesser extent in the treatment of viral, cardiovascular, metabolic, inflammatory and neurological disease. In total 25 natural product-related drugs have been approved since 2008 where on average 20-30 small molecules are approved per year, leaving natural product-related drugs to account for roughly 20% of the drugs approved from 2008-2013. The US Food and Drug Administration (FDA) reports that between the years 1981 and 2010, 34% of medicines were naturally derived ¹. This illustrates a slight drop off for natural products in the pharmaceutical realm and this could continue as only five of the natural product pharmacophores discovered in the past fifteen years are currently being investigated in clinical trials. A trend has emerged where academic and national research labs are the primary generators of novel natural

product pharmacophores. Pharmaceutical companies acquire these scaffolds from research laboratories and then develop the leads in the same way as synthetic molecules- to conform to the Lipinski 'Rule of Five'. The "Rule of Five" follows four assumptions involving multiples of five (no more than 5 hydrogen bond donors such as nitrogen or oxygen with one or more hydrogen atoms; no more than 10 hydrogen bond acceptors such as nitrogen or oxygen atoms alone; molecular mass, no less than 500 daltons; octanol-water partition coefficient ($\log P$), no greater than 5²). These qualifications have generated drug-like compounds with the ability to be absorbed, distributed, metabolized, excreted, and non-toxic (ADMET) to cells.

Natural products are often exceptions to the rule of five, yet they serve as effective drugs because of the diversified stereochemistry, or spatial arrangement of the atoms in the compound¹. Natural product chemistry provides a greater chemical space than the products that are achieved by synthetic or combinatorial chemistry. The application of an ADMET filter to a novel natural pharmacophore can generate an extremely effective new chemical entity³. Because chemical space is synonymous with multi-dimensional molecular descriptor space⁴ this also allows for new entities to be modeled *in silico* and aids in the design of new leads with novel scaffolds.

The need for novel Antiviral Pharmacophores and targets

Despite the combined screening efforts of synthetic libraries around the world, antiviral drug approvals continue to be elusive either for a lack of chemical novelty in the libraries or for a lack of diversity in assay targets. In the period of 2008 to 2013, Hepatitis C Virus (HCV) was the only viral target to be in clinical trials with a derivative of the natural product, cyclosporine A. This is in contrast to the 71 natural derivatives targeting cancers

for the same time period⁵. Cancer screening has a rich history with screening efforts that began in the 1950's. The screening setup is less sophisticated than what is required for antiviral screens, with a more simplistic criterion for hit consideration. Generally, a compound shows anticancer potential if it is cytotoxic with specificity to the cancerous cell type. A virus, on the other hand, is a non-living entity that relies on the host's cellular machinery for replication. Therefore, an antiviral needs to inhibit at least one step in the propagation of the virus without being cytotoxic to the host cell, and be capable of overcoming mutations conferring resistance, and not be immunosuppressive. This requires a near to complete understanding and characterization of the viral proteins in order to develop antiviral drugs specific to the virus.

The first antiviral drug was approved in 1962. It was a nucleoside analog, named Idoxuridine, for the treatment of Herpes simplex keratitis and was initially identified as a DNA synthesis inhibitor from an anticancer screen. Viruses with an association to cancer have been well studied and protease, reverse transcriptase, entry inhibitors, and maturation inhibitors among others have been approved. These viruses include the Human Papilloma Virus (HPV), Hepatitis C Virus (HCV), Human Immunodeficiency Virus-1 (HIV-1) by association to the first human retrovirus, Human T-Cell Lymphotropic Virus (HTLV), and Herpes Simplex Virus (HSV).

Retroviruses, named for their ability to reverse transcribe RNA to DNA, gained attention for their ability to cause neoplastic or tumor forming disease. Peyton Rous first observed this phenomenon in 1906. This observation propagated research efforts focused on describing the mechanism of transformation used by animal retroviruses. In the 1960's Howard Temins observed that the retrovirus, known to have a RNA genome could be

inhibited by actinomycin D, a DNA synthesis inhibitor. Later in 1975, Temins, David Baltimore and Renato Dulbecco shared the Nobel prize for discovering the retroviral reverse transcriptase. This is the polymerase that is capable of transcribing DNA from RNA, which helps retroviruses to incorporate into the host genome. Upon the advent of a lentivirus with a less oncogenic, yet chronic manifestation, HIV, the characterization of the “complex” retrovirus grew upon the foundation set from research efforts into the “simple” tumor-forming retroviruses⁶.

The National Cancer Institute recognized the need for an anti-AIDS division and incorporated antiviral screening into their program in 1983. This generated the necessary momentum, which led to the FDA approval of the first reverse transcriptase inhibitor, azidothymidine (AZT), in 1987. Since then a number of inhibitors targeting the viral protease and reverse transcriptase, among other virally encoded proteins, have been approved. Despite the number of inhibitors that currently exist there remains a constant demand for new drugs as new mutations arise on account of the error prone HIV reverse transcriptase and the quick replication rate of HIV, thus causing an arms race of sorts. The best weapon to date has been the Highly Active Antiretroviral Therapy (HAART) where a combination therapy is used in order to reduce viral load. However, it has been observed that latent reservoirs containing drug-resistant variants of the virus exist and exacerbate the problem and necessitate the need for new anti-retrovirals.

Timeline: Cancer research, Marine natural products, and Antivirals

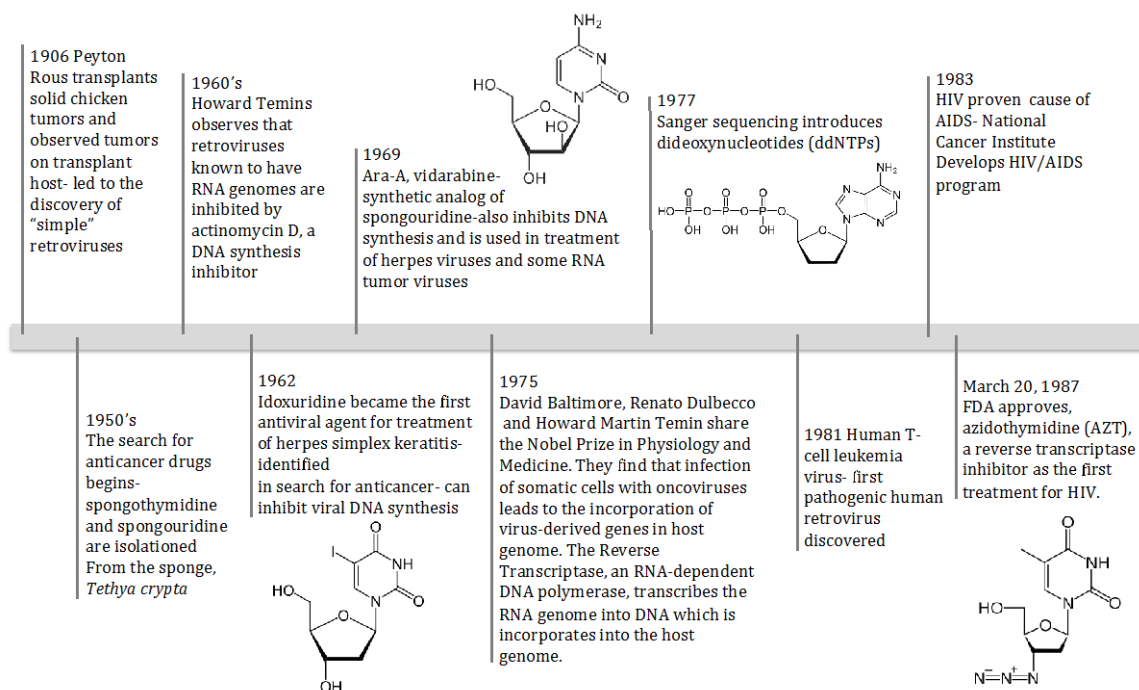


Figure 1: Timeline highlighting the tripartite link between Cancer research, Marine natural products and Antivirals. (Dates compiled from literature.)

Another virus with oncogenic ramifications that has made a substantial impact on the human population is the Hepatitis C Virus (HCV), which currently has more than 34 prospective antivirals in various clinical phases. Pegylated interferon and ribavirin were the first HCV medications available followed by the directly acting antivirals (DAAs): Boceprevir, Telaprevir, and Simprevir which target the viral protease and Sofsbuvir, a viral polymerase inhibitor. When the number of HCV approvals is compared to the West Nile Virus (WNV), also in the family *Flaviviridae*, which has no antivirals, the disparity among viruses in terms of screening efforts and drug approvals is apparent. The WNV has made a substantial impact on the citizens of developing countries and a low cost antiviral would benefit the global populations alike. In fact many of the RNA viruses aside from retroviruses

are without any antiviral remedy to date. This long list includes the Filoviruses, most notably Ebola; and the Picornaviruses, which includes the togaviruses encompassing the flaviviruses; the Arenaviruses, responsible for various hemorrhagic fevers; and the reoviruses, responsible for respiratory and intestinal infections. Other RNA viruses where the need for antiviral treatment is obviated by the existence of a vaccine include polio, hepatitis A, measles, mumps, and rabies, and influenza A, and yellow fever. Research into viruses that have been the subject of clinical trials, such as HPV, HCV, and HIV, must continue however pharmaceutical research needs to further extend its scope to viruses without a neoplastic ramification that impose a substantial global impact such as the neglected tropical disease-causing viruses of WNV and Dengue Virus (DENV).

Marine natural products and bioactivity

A statistical review preformed by Hu et al 2015⁷ analyzed the temporal trends of marine natural products discovered between the years 1985 to 2012. Every year anticancer activity has dominated the bioactivity spectrum. 25% of all novel compounds for all years have been associated with any bioactivity. The authors view this as an indicator that screening for bioactivity is not commiserate with the rate of discovery. Years where bioactivity reports exceed the 25% bioactivity average were years that included screens beyond cancer inhibition and included a diversity of antibacterial, antifungal, antiviral and pest resistance screens. Of the four thousand bioactive compounds surveyed, 56% had reported anticancer activity, 13% had antibacterial activity, and antivirals accounted for only 3% of the total. However, antiviral screenings comprised nearly 10% of all bioactivity in the year 1987 coincident with the approval of AZT for HIV, but has since decreased.

The most common compound category found for marine natural products are the terpenes at 40% of all known compounds followed by the alkaloids at approximately 25%. Other compound classes include the sterides, ketals, lactones, hydroxybenzenes, and peptides, in order of abundance. However, the peptides with an overall abundance of little more than 5% have the greatest proportion of bioactive compounds at 40%. This is compared to the terpenes that have the lowest proportion of bioactivity at 20% and the alkaloids, which have a proportion of bioactivity at 31%⁷. In summary there are a great number of marine natural product compounds with bioactivities, which remain to be discovered.

Marine sponges and their antiviral potential

Historically, 75% of all the known marine natural products have been isolated from marine invertebrates. The marine sponges are in the phylum Porifera, which accounts for 30% of all marine natural product compounds known to date. Of nearly 1800 compounds reported for Porifera, only 30% have a reported bioactivity⁷. Anticancer and antibacterial bioactivities also dominate the marine natural product pharmacophore landscape. This has been attributed to the observation that sessile marine organisms are under constant bombardment by marine microorganisms⁸. Marine bacteria exist in the ocean at an abundance of approximately 10^6 cells/ml and in order to avoid competition, some bacteria have found their ecological niche within sponges and generate secondary metabolites in defense against the ambient bacterial load. This has spurred the search for antibiotics from marine invertebrates.

However, it has been estimated that the abundance of marine viruses is 15-fold higher than that of bacteria and archaea, with approximately 15×10^6 /ml⁹ in the water

column¹⁰. Much of the focus of marine viral research is on bacteriophages because of their ability to shape marine microbial communities, and to a lesser extent, marine viruses have been implicated in disease among marine invertebrates and vertebrates. There are thought to be 10^{30} viruses in the ocean¹¹, which far outnumber the quantity found on land. It is then not hard to imagine that sessile marine invertebrates produce secondary metabolites that have an evolutionarily selected ability to inhibit viruses. These metabolites may exhibit a broad-spectrum antiviral capacity wherein they act upon the host proteins that the virus hijacks in order to increase pathogenesis rather than by directly inhibiting virally encoded proteins¹². However, marine organisms may harbor metabolites with the evolved capacity to act directly on the virus, given the evidence as “simple” sarcoma-causing retroviruses have been reported in molluscs¹³ and “herpes-like” viruses have been associated with corals¹⁴, as well as Rhabdoviruses in panaeid shrimp¹¹.

The search for marine derived antiviral pharmacophores is not without precedent. A review from Sagar et al. 2010¹⁵ summarizes antivirals leads derived from marine sponges. In the 1950s a nucleoside containing an arabinose sugar, spongouridine was isolated from the Caribbean sponge *Tethya crypta*¹⁶. The antiviral activity of its synthetic analog, Ara-A was later described¹⁷. It was found to inhibit viral DNA polymerases and synthesis of herpes and the varicella zoster viruses. Other antivirals derived from sponges include Mycalamide A and B active against the corona virus¹⁸, Herpes simplex type 1 and Polio type 1¹⁹ isolated from the genus, *Mycale*. Additionally, Avarol isolated in 1973 from *Disidea avara*²⁰ is shown to have an effect on human T-lymphotropic retrovirus (HTLV III) and HIV-1. The cyclic depsipeptides, papuamide A,B,C, and D from *Theonella mirabilis* and *Theonella swinhoei*²¹; and the large microspinosamide from *Sidonops microspinosa*²² are also recognized for anti-HIV activity²³. The alkaloids, 4-methylaaptamine from the marine

sponge *Aaptos sp.* showed anti HSV-1 activity ²⁴ as well as the bromoindole alkaloid, dragmacidin F, from the genus *Halicortex* which shows antiviral activity against HIV-1 and HSV-1²⁵. Finally, the first of the manzamines, Manzamine A was isolated from *Haliclona sp.*²⁶, a family of compounds with bioactivity ranging from antimicrobial, antiparasitic, antipesticidal, and anti-HIV-1 to anti-AIDS opportunistic infections ²⁶.

OBJECTIVE

Addressing the need for new antiviral leads by high-throughput screening

An image-based High Content Screening (HCS) cytological profiling approach is used in order to identify Red Sea sponges with antiviral promise and to assess their cytotoxicity. The candidate fractions generated by HCS in Chapter 1, are further investigated in Chapters 2 and 3. The aim of Chapter 2 is to determine which compound produced by the sponge, *Amphimedon chloros*, is able to inhibit the West Nile Virus (WNV) nonstructural protein 3 (NS3). The aim of Chapter 3 is to determine which compound from the sponge, *Stylissa carteri*, is capable of inhibiting the Human Immunodeficiency Virus-1 (HIV-1).

The West Nile Fever is considered a neglected tropical disease and is caused by the WNV. WNV is without antiviral treatment to date. It is a disease prevalent in Africa, the Middle East and around the Mediterranean Sea, as it is transferred to humans by a mosquito vector where it reaches a dead-end in its lifecycle and can manifest as encephalitis or meningitis in extreme cases. It is in the *Flaviviridae* family among Hepatitis C Virus (HCV), Dengue Virus (DENV) and Yellow Fever Virus (YFV) where HCV currently has two approved NS3 protease inhibitors on the market and the others have none. HCV is a disease common among injection drug users, a first world mosquito bite. Pharmacologically effective drugs are needed for the treatment of WNV and DENV as YFV has a vaccine and the others do not.

The HIV virus remains a promising antiviral target because of its previously displayed natural product druggability ²⁷; where despite, Highly Active Antiretroviral Treatment (HAART), HIV infections still represent a global threat with more than 34 million infected individuals worldwide and 2.5 million new infections in 2011 (UNAIDS report on the global AIDS epidemic, 2012). This is attributed to its tendency to accumulate drug-resistances, which creates the demand for new anti-HIV chemotherapies. This thesis

displays the potential of a Red Sea sponge library to be a natural reserve for novel antiviral pharmacophores for the treatment of the neglected tropical disease-causing WNV and HIV-1.

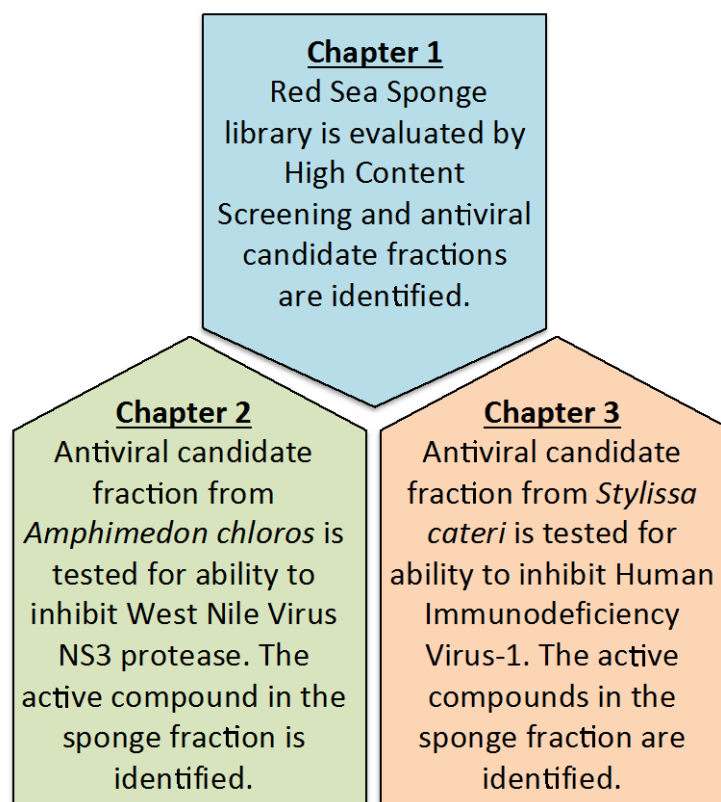


Figure 2: Smart-throughput approach for identifying novel antiviral inhibitors from a pre-fractionated Red Sea sponge library.

REFERENCES

1. Harvey, A. L.; Edrada-Ebel, R.; Quinn, R. J., The re-emergence of natural products for drug discovery in the genomics era. *Nat Rev Drug Discov* **2015**, *14* (2), 111-29.
2. Ortholand, J. Y.; Ganesan, A., Natural products and combinatorial chemistry: back to the future. *Current Opinion in Chemical Biology* **2004**, *8* (3), 271-280.
3. Harvey, A. L., Natural products in drug discovery. *Drug Discov Today* **2008**, *13* (19-20), 894-901.

4. Bender, A.; Fergus, S.; Galloway, W. R.; Glansdorp, F. G.; Marsden, D. M.; Nicholson, R. L.; Spandl, R. J.; Thomas, G. L.; Wyatt, E. E.; Glen, R. C.; Spring, D. R., Diversity oriented synthesis: a challenge for synthetic chemists. *Ernst Schering Res Found Workshop* **2006**, (58), 47-60.
5. Butler, M. S.; Robertson, A. A. B.; Cooper, M. A., Natural product and natural product derived drugs in clinical trials. *Natural Product Reports* **2014**, 31 (11), 1612-1661.
6. Cullen, B. R., Human-Immunodeficiency-Virus as a Prototypic Complex Retrovirus. *J Virol* **1991**, 65 (3), 1053-1056.
7. Hu, Y. W.; Chen, J. H.; Hu, G. P.; Yu, J. C.; Zhu, X.; Lin, Y. C.; Chen, S. P.; Yuan, J., Statistical Research on the Bioactivity of New Marine Natural Products Discovered during the 28 Years from 1985 to 2012. *Mar Drugs* **2015**, 13 (1), 202-221.
8. Hu, G. P.; Yuan, J.; Sun, L.; She, Z. G.; Wu, J. H.; Lan, X. J.; Zhu, X.; Lin, Y. C.; Chen, S. P., Statistical Research on Marine Natural Products Based on Data Obtained between 1985 and 2008. *Mar Drugs* **2011**, 9 (4), 514-525.
9. Bergh, O.; Borsheim, K. Y.; Bratbak, G.; Haldal, M., High Abundance of Viruses Found in Aquatic Environments. *Nature* **1989**, 340 (6233), 467-468.
10. Suttle, C. A., Viruses in the sea. *Nature* **2005**, 437 (7057), 356-361.
11. Suttle, C. A., Marine viruses - major players in the global ecosystem. *Nat Rev Microbiol* **2007**, 5 (10), 801-812.
12. Martinez, J. P.; Sasse, F.; Bronstrup, M.; Diez, J.; Meyerhans, A., Antiviral drug discovery: broad-spectrum drugs from nature. *Nat Prod Rep* **2015**, 32 (1), 29-48.
13. Poulet, F. M.; Casey, J. W.; Spitsbergen, J. M., Studies on the Transmissibility and Etiology of Orocutaneous Tumors of Brown Bullheads *Ictalurus-Nebulosus*. *Dis Aquat Organ* **1993**, 16 (2), 97-104.
14. Marhaver, K. L.; Edwards, R. A.; Rohwer, F., Viral communities associated with healthy and bleaching corals. *Environ Microbiol* **2008**, 10 (9), 2277-2286.
15. Sagar, S.; Kaur, M.; Minneman, K. P., Antiviral Lead Compounds from Marine Sponges. *Mar Drugs* **2010**, 8 (10), 2619-2638.
16. Bergmann, W.; Feeney, R. J., Contributions to the Study of Marine Products .32. The Nucleosides of Sponges .1. *Journal of Organic Chemistry* **1951**, 16 (6), 981-987.
17. Degarilhe, M. P.; Derudder, J., Effet De Deux Nucleosides De Larabinose Sur La Multiplication Des Virus De Lherpes Et De La Vaccine En Culture Cellulaire. *Comptes Rendus Hebdomadaires Des Seances De L Academie Des Sciences* **1964**, 259 (16), 2725-&.

18. Perry, N. B.; Blunt, J. W.; Munro, M. H. G.; Pannell, L. K., Mycalamide-a, an Antiviral Compound from a New-Zealand Sponge of the Genus Mycale. *Journal of the American Chemical Society* **1988**, *110* (14), 4850-4851.
19. Perry, N. B.; Blunt, J. W.; Munro, M. H. G.; Thompson, A. M., Antiviral and Antitumor Agents from a New-Zealand Sponge, Mycale Sp .2. Structures and Solution Conformations of Mycalamide-a and Mycalamide-B. *Journal of Organic Chemistry* **1990**, *55* (1), 223-227.
20. Minale, L.; Riccio, R.; Sodano, G., Avarol, a Novel Sesquiterpenoid Hydroquinone with a Rearranged Drimane Skeleton from Sponge Disidea-Avara. *Tetrahedron Letters* **1974**, (38), 3401-3404.
21. Ford, P. W.; Gustafson, K. R.; McKee, T. C.; Shigematsu, N.; Maurizi, L. K.; Pannell, L. K.; Williams, D. E.; de Silva, E. D.; Lassota, P.; Allen, T. M.; Van Soest, R.; Andersen, R. J.; Boyd, M. R., Papuamides A-D, HIV-inhibitory and cytotoxic depsipeptides from the sponges Theonella mirabilis and Theonella swinhoei collected in Papua New Guinea. *Journal of the American Chemical Society* **1999**, *121* (25), 5899-5909.
22. Rashid, M. A.; Gustafson, K. R.; Cartner, A. K.; Shigematsu, N.; Pannell, L. K.; Boyd, M. R., Microspinosamide, a new HIV-inhibitory cyclic depsipeptide from the marine sponge Sidonops microspinoso. *Journal of Natural Products* **2001**, *64* (1), 117-121.
23. Sarin, P. S.; Sun, D.; Thornton, A.; Muller, W. E. G., Inhibition of Replication of the Etiologic Agent of Acquired-Immune-Deficiency-Syndrome (Human T-Lymphotropic Retrovirus Lymphadenopathy-Associated Virus) by Avarol and Avarone. *J Natl Cancer I* **1987**, *78* (4), 663-666.
24. Coutinho, A. F.; Chanas, B.; Souza, T. M. L. E.; Frugrulhetti, I. C. P. P.; Epifanio, R. D., Anti HSV-1 alkaloids from a feeding deterrent marine sponge of the genus Aaptos. *Heterocycles* **2002**, *57* (7), 1265-+.
25. Cutignano, A.; Bifulco, G.; Bruno, I.; Casapullo, A.; Gomez-Paloma, L.; Riccio, R., Dragmacidin F: A new antiviral bromoindole alkaloid from the mediterranean sponge Halicortex sp. *Tetrahedron* **2000**, *56* (23), 3743-3748.
26. Sakai, R.; Higa, T., Manzamine-a, a Novel Antitumor Alkaloid from a Sponge. *Journal of the American Chemical Society* **1986**, *108* (20), 6404-6405.
27. (a) Sagar, S.; Kaur, M.; Minneman, K. P., Antiviral lead compounds from marine sponges. *Mar Drugs* **2010**, *8* (10), 2619-38; (b) Singh, I. P.; Bharate, S. B.; Bhutani, K. K., Anti-HIV natural products. *Current Science* **2005**, *89* (2), 269-290.

CHAPTER 1: Bioprospecting of a Central Red Sea Sponge Library

1.1 Abstract

Marine sponges represent an important source of natural products with potent biological activities and unique structural characteristics. Several sponge-derived compounds have been successfully converted into approved medications with various therapeutic applications. The bioactive potential of marine sponges of the Central Red Sea has not been studied in great detail due to the inaccessibility of the Saudi Arabian coast. This study aimed to assess the antiviral potential of a collection of 15 distinct sponges species collected in coral reefs in the Central Red Sea off the Saudi Arabian coast. We used a cytological profiling approach by image-based High-Content Screening (HCS) with a set of 10 cellular markers. The pre-fractionated organic sponge extracts were evaluated for an antiviral potential based on their ability to show phenotypic similarity to any of the 600 reference compounds with known structures and assigned biological activities. Our approach provided two candidate fractions that showed a close matching of cytological profiles with several reference compounds. Fraction 2 of *Amphimedon chloros* clustered with two reference compounds that are hypothesized to show activity against viral proteases whereas cytological profiles of Fraction 1 of *Stylissa carteri* showed phenotypic similarity to reference compounds with various mechanisms-of-activity against the human immunodeficiency virus 1 (HIV-1). These two fractions were selected as prospective candidates for further antiviral testing for activity on the West Nile Virus NS3 protease as well as replication of HIV-1, respectively. In summary, our work demonstrates the versatility and power of cytological profiling for bioprospecting of unknown biological resources and for the selection of candidates for further studies on specific biological targets.

1.2 Introduction

Coral Reefs in the Central Red Sea off the coast of Saudi Arabia constitute a unique and understudied environment that provides the promise of new bioactive molecules with unexplored pharmacophores. The Red Sea exhibits a very warm, saline, and semi-isolated environment where organisms have adapted to thrive despite challenging conditions. This has consequences not only to eukaryotic reef organisms, but also on the composition, identity, and function of the associated bacterial assemblages, where the bacteria associated with sponges have also been shown to produce bioactive molecules in the form of secondary metabolites^{1 2} This study taps into the chemical potential of Central Red Sea reef sponges as a natural reserve for novel antiviral pharmacophores.

To date much of the work performed on the topic of marine natural products in the Red Sea has originated from sampling in the northern Red Sea on the account of accessibility. Bioprospecting of a sponge library from the central Red Sea offers a unique sampling environment that is highly different from the northern Red Sea because of the contrasting gradients of temperature and salinity found along the north-to-south axis of the Red Sea. The northern Red Sea is characterized by increased salinity (41psu vs. 36 psu.) and decreased surface temperature (24°C vs. 30°C) in comparison to the southern Red Sea, which is fed by the Indian Ocean through the Gulf of Aden ³. A connectivity study of *Stylissa carteri* by microsatellite analysis showed that populations of this sponge in the Red Sea experience a break in connectivity at 16.85°N ⁴. Our sampling points are at approximately 22°N this suggests that our central Red Sea collection is genetically distinct from sponges from the same genus that originate in the Indian Ocean; however, southerly enough to experience quite distinct environmental conditions compared to their genetically more similar counterparts in the north.

Natural products have been reported in the literature for the following sponge species collected from the northern Red Sea: *Aaptos aaptos* ⁵, *Biemna fortis* ⁶, *Callyspongia fistularis* ⁷, *Diacarnus erythraeanus* ⁸, *Dysidea herbacea* ⁹, *Dysidea avara* ¹⁰, *Erylus* sp. ⁵, *Haliclona* ¹¹, *Hyrtios erecta* ¹², *Latrunculia magnifica* ¹³, *Mycale euplectellioide* ¹⁴, *Negombata magnifica* ¹⁵, *Petrosia* sp. ¹⁶, *Psammaplysilla purpurea* ¹⁷, *Pseudoceratina Arabica* ¹⁸, *Siphonochalina siphonella* ^{9, 19}, *suberea mollis* ^{18a, 20}, *Xestospongia exigua* and *Theonella swinhoei* ²¹. The sponge collection assembled in this study represents many previously uninvestigated sponges from the Red Sea, having little overlap with species reported from the northern Red Sea including: *Amphimedon chloros*, *Aplysinnella rhax* or *dysidea rhax*, *Clathria* sp., *Crella* aff. *Papillata*, *Crella cyathophora*, *Dactylea*, *Dragmacidon "Ectyoplysia" coccineum*, *Haliclona (Reniera) fascigera*, *Hyrtios erectus*, *Iotrochota*, *Leucetta*, *Stylissa carteri*, *Theonella swinhoei*, *Xestospongia testudinaria*, Order: Verongida, Family: Respailiidae.

1.2.1 High Content Screening using pre-fractionated Marine extracts

The focus of High Content Screening (HCS) has followed an evolution from single compounds with single markers to single compounds with multiple markers to the screening of mixtures using multiple markers. Marine invertebrate-derived extracts present several challenges with regard to screening because a high chemical diversity is often present in crude extracts and the resulting interactions among molecules can mask the bioactivity of the individual constituents²². A pre-fractionated solid phase extraction of the marine material is used to desalt the sample and resolve the chemical diversity of the fraction. The pre-fractionated mixtures of unknown composition can then be evaluated by the phenotype they elicit in cells and how they cluster with compounds from a reference library. This has allowed for the identification of a novel group of iron siderophores by

Schulze et al. 2013²², which are structurally dissimilar to the DNA binding agents to which they clustered but are capable of a similar mechanism of action. Iron siderophores are able to interfere with DNA synthesis by sequestering iron in tumor cells and inhibiting the ribonucleotide reductase, the enzyme responsible for catalyzing the formation of deoxyribonucleotides from ribonucleotides. This novel family of iron siderophores, the microferrioxamines A-D, exhibit a cytological profile which suggests their ability to impose a G1/S arrest similar to the iron siderophore, desferrioxamine, a known antitumor agent.

1.2.2 High Content Screening for the identification of novel Antivirals

Due to the fact that viruses are non-living and require the host's cellular machinery to replicate, antiviral drug discovery is not as straightforward as identifying a compound with anticancer potential. However, historically the identification of the nucleoside inspired DNA synthesis inhibitors in anticancer screens led to the first antiviral, Ixouridine, to be approved in 1962. This compound has a remarkable similarity to the naturally occurring spongouridine from the sponge *Tethya crypta*, whose synthetic analog Ara-C was approved in 1969 for the purpose of inhibiting DNA synthesis associated with leukemia, lymphomas and generalized herpes infections. These foundational discoveries paved the way for techniques that explored ways to inhibit DNA synthesis, such as the technique of Sanger sequencing developed in 1977, where modified nucleotides lacking the 3'OH group of the five carbon base, terminate synthesis. Years later in 1987, the same mechanism of action observed for nucleoside analogs was used to inhibit the reverse transcriptase of HIV, with that came the approval of the drug AZT. Viral proteins are not found in living cells if there was never a previous infection of the cell; however, as discussed above compounds that have been developed for the treatment of cancers and other diseases harbor pharmacophores with the potential to inhibit diseases other than for what they have been

previously approved. De Clercq et al 2015²³ recounts the role serendipity has played in the discovery of antiviral drugs. He cites the discovery of seramin that was a known antitypanosomal agent, which emerged as a reverse transcriptase inhibitor before AZT and the 2',3' dideoxynucleosides used in Sanger sequencing.

Another approach aside from directly targeting viral proteins is to target host cellular proteins in order to decrease viral pathogenesis. Martinez et al. 2015²⁴ cites the use of new assays and predictive tools as the reason for the re-emergence of efforts focused on identifying broad-spectrum antivirals with the capacity to block host processes that facilitate viral pathogenesis. This approach has met skepticism in the past because of the propensity to cause toxicity to the host cell. However, HCA offers the ability to assess toxicity using a detailed assessment of whole-cell morphology, nuclear architecture and DNA content, cell-cycle characteristics, cytoskeletal re-arrangement, mitochondrial distribution and physiology, parameters of the endoplasmic reticulum, and lysosomal vesicles as well as plasma membrane rearrangement. Additionally, the approach of using a reference library composed of drug-like compounds to which the fractions of interest are clustered allows for a prioritization of previously unevaluated extract compounds that are drug-like. These prioritized extracts are then investigated for their ability to assert a mechanism of action that maybe able to inhibit viral pathogenesis either by inhibiting host factors or by directly inhibiting viral proteins.

The approach used here employs an image-based High Content Analysis (HCA) in order to characterize the cytological activity of pre-fractionated sponge fraction mixtures. The mixtures of unknown composition are clustered to the LOPAC1280 library (Sigma Aldrich) based on the phenotypic fingerprint, which they share with compounds of the

reference library. This comprehensive approach allows for the detailed understanding of the biological activities of these extract mixtures of unknown composition on a human cell line. The assay includes markers for all the major organelles as well as the important mediators of the major cellular regulatory pathways, i.e. NFkB, p53, and Caspase 9. Identifying and ameliorating toxicity at an early stage, as well as observing changes in cell morphology and cell attrition, and other cellular effects helps to ensure that the compound will not lead to any downstream side effects and can save both cost and time in drug development ^{22, 25}.

1.3 Materials and Methods

1.3.1 Red Sea Sponge Specimen collection

Sponges were collected using gardening sheers from four reef locations, which include Inner Fsar/Outer Fsar (22°14'37.61"N; 39°00'28.03"E), Inner Al Fahal/Outer Al Fahal (22°17'40.51"N; 38°57'55.13"E), Rose Reef (22°00'22.50"N; 38°00'53.839"E) and Shib Nsar (22°20.502"N; 38° 51.245"E) using SCUBA (Table 1.1). The specimens were washed with 1% Phosphate Buffered Saline (PBS) then wrapped in foil and placed on ice then stored at -80°C until processing (Table 1.1).

1.3.2 Red Sea Sponge Specimen Identification

Frozen sponges were thawed in 70% ethanol and sliced perpendicular to the outer ectoderm into thin sections and placed on microscope slide. The slide was placed on a heating block on low and a coverslip was placed on the slide to help flatten the specimen while drying. When completely dry a few drops of Dulbecco's Canadian balsam mounting media were used to adhere coverslips to the microscope slide. This was allowed to dry for

24hrs. Specimen were visualized at 40X using the Leica CTR 7000HS and imaged with the Hamamatsu EM-CCD Digital Camera C9100 (Figure 1.2).

1.3.3 Compilation of a Red Sea Sponge Screening Library

A pre-fractionated chemical extract library of Red Sea sponges was generated using a standardized processing of the biological extracts (Figure 1.1), which is imperative for successful discovery of bioactives. This is because marine invertebrate-derived extracts present several challenges with regard to screening. First, they contain large quantities of inorganic salts that can interfere with all downstream applications²⁶. Second, a high chemical diversity is often present in crude extracts and the resulting interactions among molecules can mask the bioactivity of the individual constituents²². A pre-fractionated solid phase extraction (SPE)-based approach was used to remove inorganic salts; this was followed by an elution with solvents of different polarities in order to reduce the chemical diversity of the fraction. More specifically HP20SS (highly porous styrenic, small) absorbent beads that are small in size (75-150 μm) with a proportionately large pore size were used. This gives the finer chromatographic separation that is recommended for the fractionation of small biomolecules when aiming for the isolation of successful drug candidates, which have in general characteristically small size of around 100-500 Daltons. Specifically, 4-10 grams of sponge specimen were extracted with 15 ml of methanol then dried to 150mg of Diaion HP20SS beads then loaded into a 25 ml flash cartridge with a 2.02 cm diameter frit (Sorbent Technologies) then desalted with deionized water (FW1, FW2) and then eluted in the following series of solvents with different polarities: 25%IPA/H₂O, 50%IPA/H₂O, 75%IPA/H₂O, 100%MeOH ²⁷ then dried using an evaporating centrifuge and redissolved in Methanol (Figure 1.1).

1.3.4 High Content Screening of a Red Sea Sponge Library

41 samples, comprised of 17 sponge species (Table 1.1), were screened using an image-based High Content Analysis system. To begin the screening HeLa cells were plated at a density of 2,000 cells per well in 384-well plates (Corning). The cells were maintained in 25 μ l of cell culture medium for 24 hours. Cells were treated in quadruplicate with 6.25 μ l of the unknown sponge mixture. After a 24 hour incubation, 11 cellular targets were assessed using four different cell-staining protocols (panels 1-4) (Table 1.2). To commence staining, cells were fixed with 4% formaldehyde for 20 minutes. For permeabilization, blocking, and washing steps, HCS-optimized reagents were used (Cellomics HCS reagents Wash Buffer (WB), Wash Buffer II (WBII), Blocking Buffer (BB) and Permeabilization Buffer (PB), Thermo Fisher Scientific, Waltham, MA, USA).

Panel 1: Fixed cells were permeabilized for 15 minutes and blocked for 15 min. 12.5 μ l of the primary staining solution containing 3.6 μ l/ml phalloidin-FITC (Sigma Aldrich) and 1.3 μ l/ml of beta-tubulin antibody (Thermo Fischer Scientific) were added per well for 1 hour. After two washing steps with BB, 12.5 μ l of the secondary staining solution was added (1:500 GAM-DyLight 550, Thermo Fischer Scientific, in BB) for 1 hour. Subsequently, cells were washed 3 times with WB and nuclei were stained with 0.1 μ l/ml of Hoechst33342 (Thermo Fisher Scientific).

Panel 2: Cells were incubated with stains for the ER (1 μ l/ml, ER-Tracker Blue-White DPX, Life Technologies) and lysosomes (0.2 μ l/ml, LysoTracker Red DND-99, Life Technologies) in pre-warmed cell culture medium for 30 minutes under standard conditions. After fixation, cells were washed twice with WB and incubated with a solution of

a labelled wheat germ agglutinin (5 µl/ml, Wheat Germ Agglutinin, Alexa Fluor® 488 Conjugate, Life Technologies) for 10 minutes.

Panel 3: Cells were incubated with a solution of mitochondrial dye (0.17µl/ml, MitoTracker® Orange CMTMRos, Life Technologies) in cell culture medium for 30 minutes under standard cell culture conditions. After fixation, cells were permeabilized, washed twice with WB, and incubated with the primary staining solution, including the antibody for NFκB (Thermo Fisher Scientific) for 1 hour. After removal of the primary antibody solution, cells were incubated with WBII for 15 min, washed twice with WB, and incubated with the secondary staining solution (1:500 GAR-DyLight 550, Thermo Fischer Scientific, in WB) for one hour. Subsequently, cells were incubated with WBII for 10 minutes and stained with a solution of Hoechst33342 (0.1 µl/ml, Thermo Fisher Scientific) afterwards for another 10 minutes.

Panel 4: After fixation, cells were permeabilized for 17 minutes, washed twice with WB, and blocked for 30 minutes. After removal of BB, cells were incubated with the primary antibody solution (5.5µl/ml of p53 antibody and 1.5µl/ml of caspase 9 antibody, both Thermo Fisher Scientific, in blocking buffer) for 1 hour. After two washing steps with WBII and one washing step with WB, the secondary staining solution (1:500 GAR-DyLight 488 and 1:500 GAM-DyLight 550, both Thermo Fischer Scientific, in WB) was added for 1 hour. After removal of the staining solution, cells were washed once with WBII and stained with Hoechst33342 for 10 minutes.

For High-Content Analysis, the CellomicsArrayScan VTI (Thermo Fisher Scientific) platform equipped with a 10x objective (Zeiss Plan Neofluar, NA 0.3 was used. Images were analyzed using the Compartmental Analysis Bio Application (Cellomics, Thermo Fisher

Scientific). At least 500 valid objects were analyzed per well. Cell cycle analysis and analysis of cell loss were accomplished by using the Cell Cycle Bio Application (Cellomics, Thermo Fisher Scientific) using a minimum of 2000 valid objects.

Data analysis. Raw data from the automated image analysis for each cytological feature are reported in relation to the corresponding values from control wells. The control values are set to 1. All cytological features of a given fraction or reference compound were combined to result in a cytological profile with 102 factors generated from 10 cells target estimates. The 102 factors were subjected to hierarchical clustering using complete linkage clustering of a spearman correlation using Multi Experiment Viewer²⁸ (MeV v4.9, Dana-Farber Cancer Institute, Boston, MA,USA).

1.4 Results

1.4.1 Sponge Taxonomy

The pre-fractionated Red Sea sponge library consisted of biological replicates of the sponges presented in Table 1.1 and 1.2. Fourteen of the 15 sponges fell into the class Demospongiae, the largest class in the phylum Porifera; whereas, one sponge, *Leucetta*, belonged to the class Calcarea. Most sponges were collected at different reef locations to ensure that the observed bioactivity was not site-specific but sponge-specific. Since the central Red Sea is less accessible than the northern Red Sea (off the coast of Egypt, Jordan, Israel) information on the species identification of the sponge fauna is sparse in the literature. Sponge genera such as *Haliclona*, *Hyrtios* and *Stylissa* are among the more easily identifiable sponges, whereas the remainder of the sponge collection required microscopic analysis of their spicules in order to assign a binomial nomenclature to the sponge (Figure 1.2).

The central Red Sea off the coast of Saudi Arabia is a region that has yet to be represented in the World Porifera Database (<http://www.marinespecies.org/porifera/>) (as of December 2014). However, other regions of the Red Sea such as the Sudanese Exclusive Economic Zone are represented. From this it is possible to see that *Hyrtios erectus* (Keller, 1889) has been identified in the central Red Sea as well as a specimen of *Clathria* (*Clathria*) *arbuscula* (Row, 1911). *Dragmacidon* "*Ectyoplasia*" *coccineum* (Row, 1911) was identified at the Suez Canal (Egypt) as well as *Haliclona* sp. (*Haliclona*) (Grant, 1836) and *Theonella swinhoei* (Gray, 1868) near Eilat (Israel). *Amphimedon chloros* (Keller, 1889) was found near Israel. *Crella* aff. *Papillata* (Levi, 1958) was reported in the Southern Red Sea. *Stylissa carteri* (Dendy, 1889) can be found in the Eritrean Exclusive Economic Zone distribution report. *Xestospongia testudinaria* (Lamarck, 1895) has been identified around the Aldabra Islands (Seychelles). *Iotrochota* (Ridley 1884) has been identified in the Christmas Island Exclusive Economic Zone and *Leucetta* (Dendy, 1913) was found around the Seychelles economic zone. Sponges identified as *Aplysinella rhax* (de Laeбенfels, 1954, Micronesia; Marshall Islands), *Dactylea* sp. (Carter, 1885), *Leucetta* (Haeckel, E., 1972), as well as sponges belonging to the Order Verongida and Family Respiliidae have yet to be reported in the Red Sea.

Spicule identification was performed for the sponges that were not easily identified. 20X magnification of *Amphimedon chloros* shows a fine branching matrix, which gives the genus its typical sponge quality. *Aplysinella rhax* has a lack of spicules but instead has conules. *Clathria* sp. has many fine spicules surrounded by canals of tissue. *Crella* aff. *papillata* not only has long fine oxea but also has small "c"-shaped sigma microscleres. *Dactylea* is composed of a fibrous matrix. *Dragmacidon coccineum* specimens are very red with long strongyle megascleres. *Leucetta* is the only representative of the class Calcarea in

our collection with triaxons made of calcium carbonate. *Theonella swinhoei* spicules have the same 3-point star configuration as *Leucetta* but are instead made of more fragile spongin fibers. *Xestopongia testudinaria* is a mesh of sponging tylostyle megascleres and the sponge of the family Raspailidae consists of the characteristic bundle of fibers with spiny acanthostyles that stick out perpendicular to the bundle.

1.4.2 High Content Screening identifies antiviral candidates

Image-based high content analysis was performed using 10 cellular markers (Nucleus, Actin, Tubulin, Mitochondrial, Cell membrane, Endoplasmic Reticulum, Lysosome, NFkB, p53 and Caspase 9) on HeLa cells and evaluated using 102 parameters (Table 1.2). The cells were exposed to a single concentration of each pre-fractionated mixture of the sponge extract fraction library. Concurrent screening of the single compound reference library (Sigma Aldrich) provides a reference standard to which the cytological profiles of the unknown test mixtures are clustered. This allows for inferences to be made concerning the mechanism of action of the compound present in the tested pre-fractionated mixture. From this analysis we were able to identify two sponge species, *Amphimedon chloros* and *Stylissa carteri* with clustering profiles of interest (Figure 1.3).

With hierarchical clustering using Spearman distance and complete linkage, all biological replicates of *Amphimedon chloros* fraction 2 cluster with the following reference compounds: 4-Chlorobenzo[f]isoquinoline (CBIQ), an alkaloid; Corticosterone, a steroid hormone; and more distantly to Gossypol, a natural phenol derived from the cotton plant; Quazinsonine, an alkaloid; Quercetin dehydrate, a natural flavonoid found in plants; and TG003, a benzothiazole. CBIQ, Corticosterone and the biological replicates of Fraction 2 share a pronounced enhancement of NFkB expression relative to the control, which

suggests an interference with the cell cycle (Figure 1.4). Gossypol, Quazinone, Quercetin dehydrate, TG003, and the biological replicates of Fraction 2 share a decrease of the actin and tubulin signal and as well as a less intense staining of the ER relative to the control. The *A.chloros* fraction also shares a decrease in lysosomal staining with Gossypol (Figure 1.3 B).

The profile for Fraction 1 of *Stylissa carteri* is more stochastic with a reference compound interrupting the clustering of the fraction 1 biological replicates. Biological replicates, samples C14 and D5 of *Stylissa carteri* fraction 1 cluster to beta-Lapachone, an ortho-naphthoquinone, and biological replicates C26 and C5 of *Stylissa carteri* Fraction 1 cluster to 3-bromo-7-nitroindazole, a indazole-type alkaloid; AC-93253 iodide, a type of indoline; Chelerythrine chloride, an plant-derived isoquinoline alkaloid, and cyclosporin A, a small cyclic protein (Figure 1.5) The biological replicate C14 originates from the same collection point as C26; however, this collection point is different for sample D5 and C5, demonstrating that this is not a composition bias resulting from different environmental input (Figure 1.3 A). Rather, this is most likely attributed to the different final concentrations of the substituents within the mixtures. These results gave us two avenues for further antiviral bioprospecting from our Red Sea sponge library.

1.5 Discussion

Ten years ago, the first HCS studies screened single compounds and looked for a uni-directional outcome using one cytological marker ²⁹ this progressed to the use of multiple cytological markers in order to characterize one mechanism of action ²⁵. These approaches assume the “molecular similarity principle,” in that structurally similar molecules are likely to show similar biological properties ²⁵ and is illustrated by a close clustering of the single compounds. A seminal publication by Schulze et al 2013²²

demonstrated and discussed the advantages and pitfalls of using marine natural product mixtures on an image-based high content cytological screening platform. The ingenuity of the publication lies in their ability to resolve the bioactivity of mixtures by using a single-molecule reference library of 480 small molecules. This was done by evaluating 250 cellular features acquired by staining various organelles (nucleus, actin, tubulin), and using markers for DNA replication and mitosis quantification. This allowed for mixtures of unknown composition to be clustered to compounds with a known oncological relevance and further allowed them to dereplicate the compounds in their test samples from compounds already present in the reference library so that they did not expend efforts on previously characterized compounds. However, they also discovered a novel class of iron siderophores, which were structurally distinct from the compounds with which they clustered. This demonstrates that HCS also allows for the identification of novel compounds that are structurally dissimilar from the reference compound but capable of a similar mechanism of action. In the publication the authors ultimately concluded that cytological profiling is able to generate a mechanism-of-action hypothesis, which requires further targeted assays in order to define the precise molecular target responsible for the observed phenotype.

In an effort to take this concept one step further, a similar foundation was set by screening more than 600 compounds of the LOPAC 1280 as a reference library together with a screening of a pre-fractionated library of organic Red Sea sponge extracts. Similar to Schulze et al 2013, the sponge library provided mixtures for which a phenotypic profile or “fingerprint” was generated using 102 cellular features. The cellular features were obtained by staining seven organelles (nucleus, actin, tubulin, mitochondria, endoplasmic reticulum, lysosome, and the cell membranes) in addition to three major regulatory proteins (NFkB, Caspase 9, and p53) (Table 1.2). Then by a similar clustering method where the pre-

fractionated sponge extract library is grouped with the single molecule reference library, the antiviral potential of the sponge fractions was assessed. The close clustering of a cytological profile resulting from a sponge fraction to a reference compound with proposed antiviral activity allowed us to prioritize antiviral leads by assuming a shared mechanism-of-action or compound structure.

Two major factors to consider when screening mixtures are concentration and the number of bioactive compounds in each fraction. When using a mixture of molecules such as an extract fraction prepared by Solid Phase Extraction (SPE) it is only possible to extrapolate plated concentrations from starting material weights. It is difficult to comment on the absolute concentrations of the compounds within the sample until the compound is purified and no longer a mixture. If the concentration is too low, the compound may not cluster properly with the reference compound. If it is too high, it might be cytotoxic to the cell. Another issue arises with the presence of two or more bioactive compounds within the same test mixture. This can result in the compounds generating a cross signal where neither fraction will cluster with the correct reference compounds ²² or it can result in the test mixtures clustering only among other test mixtures of unknown composition. The latter scenario can give an inflated estimate as of the number of novel compounds and biological targets represented in the mixtures. After considering these two factors, the need to test at multiple concentrations is obviated by focusing on sponge fractions whose biological replicates show a close clustering to reference compounds. Using this qualifier it is possible to prioritize the SPE Fraction 2 of *Amphimedon chloros* and SPE Fraction 1 of *Stylissa carteri* as mixtures of interest for further evaluation (Figure 1.3). Additionally, the clustering of these selected fractions to certain reference molecules sparked our imagination to explore them as antivirals effective against the West Nile Virus, Nonstructural Protein 3 (WNV NS3)

protease and Human Immunodeficiency Virus-1 (HIV-1), respectively, and further describe their precise molecular targets.

This pursuit is on account of *A. chloros* Fraction 2 clustering to the reference compounds, Gossypol and Quercetin dehydrate which have been proposed Dengue Virus NS2B/NS3 protease inhibitors as evidenced by molecular docking studies³⁰. Quercetin dehydrate (Figure 1.4 E) is a flavonoid common to plants that is known to modulate oxidative stress and inflammatory response by reducing tumor necrosis factor- α (TNF- α) and interleukin-1 β (IL-1 β)³¹. Gossypol (Figure 1.4 C) has been shown to inhibit replication of the HIV-1 virus as well as inhibition of the protein kinase C³². The Dengue Virus NS3 protease/ NS2B cofactor and the WNV NS3/NS2B protease are closely related NS3 proteases; both in the flavivirus family, and a biochemical assay is commercially available for WNV testing. This laid the framework for the further investigation of *A. chloros* Fraction 2 components and their potential as an NS3 protease inhibitor. Along the lines of host cell effectors able to alleviate viral pathogenicity *A. chloros* Fraction 2 also clusters with 4-Chlorobenzo[f]isoquinoline (CBIQ), an alkaloid; Corticosterone, a steroid hormone; and more distantly to Gossypol, a natural phenol derived from the cotton plant; Quazinsonine, an alkaloid; Quercetin dehydrate, a natural flavonoid found in plants; and TG003, a benzothiazole.

CBIQ (Figure 4A) is a known activator of the cystic fibrosis transmembrane conductance regulator (CFTR), which is mutated in three-fourths of cystic fibrosis patients. CBIQ also activates the intermediate-conductance calcium-sensitive K⁺ channel (KCNN4), which promotes anion flux by hyperpolarizing epithelial cells. HCV has been shown to benefit when the function of another K⁺ channel, Kv2.1, is inhibited by the Nonstructural

protein 5A (NS5A) and is unable to induce apoptosis in response to cellular oxidative stress. When the K⁺ channel is constitutively activated it would induce apoptosis of the affected cell reversing the host cell modulation imposed by the virus³³

In the case of corticosterone (Figure 1.4 B), a corticosteroid, there is the possibility that like other corticosteroids a reduction in virally induced inflammation will occur³⁴. Along the same lines, Quazinone (Figure 1.4 D) is a phosphodiesterase III (PDE III) inhibitor, clinically used as a cardiotonic and vasodilator. Phosphodiesterase III is found in lymphocytes, and shares selectivity for cAMP with phosphodiesterase IV (PDE IV). The ability to inhibit PDE IV has been shown to increase intracellular cAMP levels, which in turn reduces the production of virally relevant cytokine, TNF- α ³⁵. An inhibition of PDE III may do the same to a lesser extent. Finally, TG003 (Figure 1.4 F) is an ATP-competitive Cdc2-like kinase (Clk) inhibitor of Clk1, Clk2, and Clk4. These kinases have been implicated in the alternative splicing and RNA processing of HIV-1³⁶

Similarly, The biological replicates of *S. carteri* samples C14 and D5 Fraction 1, cluster to beta-Lapachone, and more distantly to samples C26 and C5, which cluster to 3-bromo-7-nitroindazole, AC-93253, Chelerythrine chloride, and cyclosporin A. Specific to our aim of identifying antivirals, beta-lapachone (Figure 1.5 A) has been shown to inhibit the HIV-1 long terminal repeat (LTR) with an IC₅₀ of 0.3 μ M in cells stimulated by TNF- α ³⁷. In house screening on an HIV-1 cell-based assay revealed 3-bromo-7-nitroindazole (Figure 5B) as capable of inhibiting HIV-1 replication by 30%, where the compound was originally noted for its inhibition of bovine nitric oxide synthase 1 (NOS3) and rat nitric oxide synthase 1 (NOS1) enzyme activity. AC-93253 iodide (Figure 5C) is reported as an inhibitor of sirtuin 2 (SIRT2) and to a lesser extent SIRT1, both NAD-dependent deacetylases^{1a}. SIRT1

is reported to regulate HIV transcription by the deacetylation of the HIV Tat protein³⁸. Chelerythrine (Figure 1.5 D), which is a potent inhibitor of protein kinase C (PKC)³⁹ where PKC is reported to aid in the phosphorylation of various viral proteins^{40 41}. Furthermore, the pharmacological derivatives of cyclosporine A (Figure 1.5 E) are suggested to have the ability to inhibit HIV-1 reverse transcription by an interference with calcineurin, disallowing it to dephosphorylate NF- κ B and express IL-2 to promote viral reverse transcription. Additionally, cyclophilin A, the cellular ligand of cyclosporine A is necessary for HIV-1 replication as it binds to the HIV-1 capsid protein, thus treatment with cyclosporine A results in virions that are not infectious⁴².

The HCA of a pre-fractionated sponge library and their clustering to compounds of a well-characterized reference library allowed for predictions of the structure class and/or mechanism-of-action to be expected for the compounds in the pre-fractionated sponge mixtures. A further antiviral bioprospecting of the two sponges, *A. chloros* and *S. carteri*, is explored in the following two chapters using a biochemical assay and a combination of a cell-based assay and biochemical assay, respectively.

1.6 Figures and Tables

Red Sea Extract Library: Fractionation Process

Red Sea Sponge was ground
in liquid Nitrogen and
placed in Methanol then
dried to HP20SS for Solid
Phase Extraction (SPE).



Four step elution:
dH2O wash (FW1)
25% IPA/H2O (F1),
50% IPA/H2O (F2),
75% IPA/H2O (F3),
100% MeOH (F4)



Solvent is Centrifugally
Evaporated from sample



Fractions are
redissolved in Methanol

Figure 1. 1: Red Sea extract fractionation process. Sponges are collected from the coral reefs of KAUST. A crude methanol extract is dried to HP20SS beads. Solid phase extraction is carried out using a four-step elution, the samples are then evaporated and redissolved in methanol ready for screening or for analysis using analytical techniques.

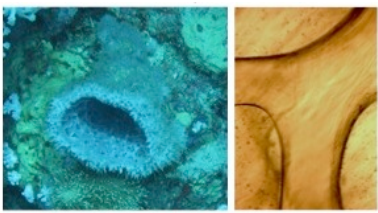
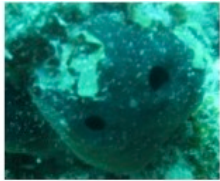
Amphimedon chloros	Aplysinella rhax or dysidea rhax	Clathria sp.
		
Crella aff. papillata	Dactylea sp.	Dragmacidon "Ectyoplysia" coccineum
		
Haliclona (Reniera) fascigera	Hyrtios erectus	Iotrochota sp.
		
Leucetta	Stylissa carteri	Theonella swinhoei
		
Xestospongia testudinaria	Order: Verongida	Family: Raspailidae
		

Figure 1. 2: Images of sponges species represented in the Red Sea sponge library. Images on the left are of the whole sponge. Images on the right are 20X magnifications of the less easily identifiable specimen. Well-known sponges did not require spicule ID.

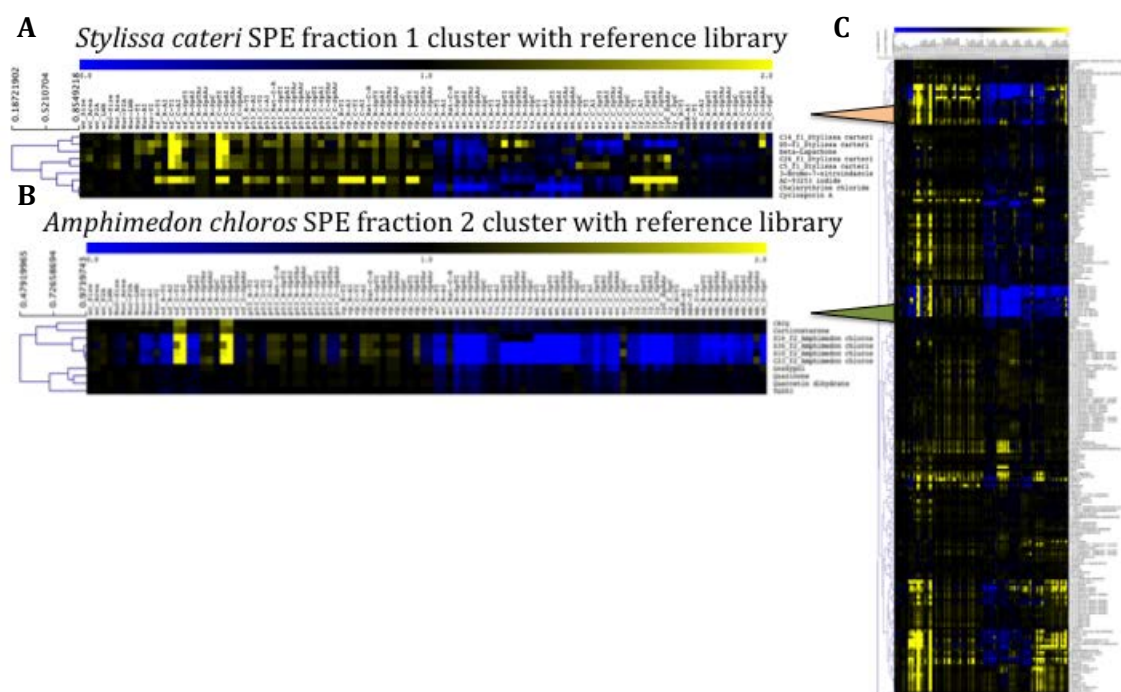


Figure 1. 3: Sponge samples and the LOPAC library were clustered according to Spearman distance with complete linkage and displayed as a heat map. (A) Cluster containing fractions containing *Stylisha cateri* SPE fractions 1 and beta-Lapachone, 3-bromo-7-nitroindazole, AC-93253 iodide, chelerythrine chloride, and cyclosporin A. (B) *Amphimedon chloros* SPE fraction 2 cluster with CBIQ, Corticosterone, Gossypol, Quazinson, Quercetin dehydrate, TG003 (C) reference compounds of the LOPAC library.

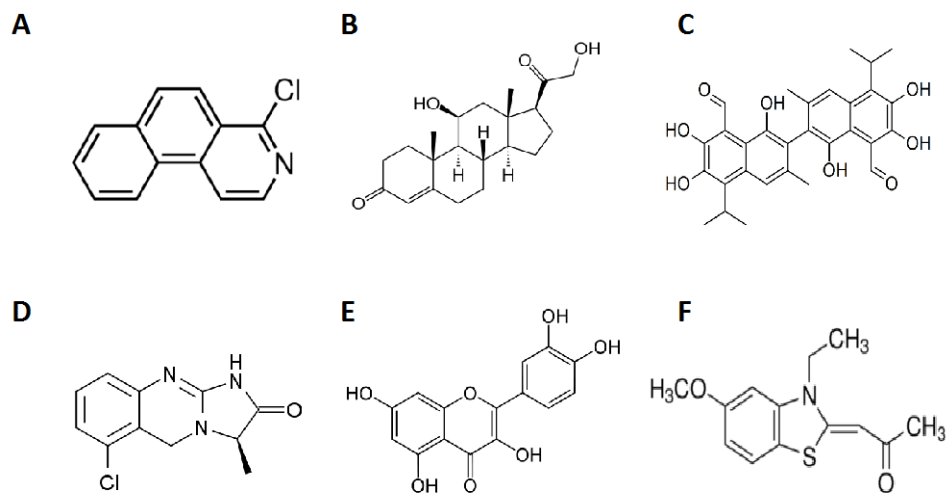


Figure 1. 4: Compounds which cluster with *A. chloros* fraction 2. (A) CBIQ, (B) Corticosterone, (C) Gossypol, (D) Quaziquone, (E) Quercetin dehydrate, (F) TG003. (Structure images from PubChem database.)

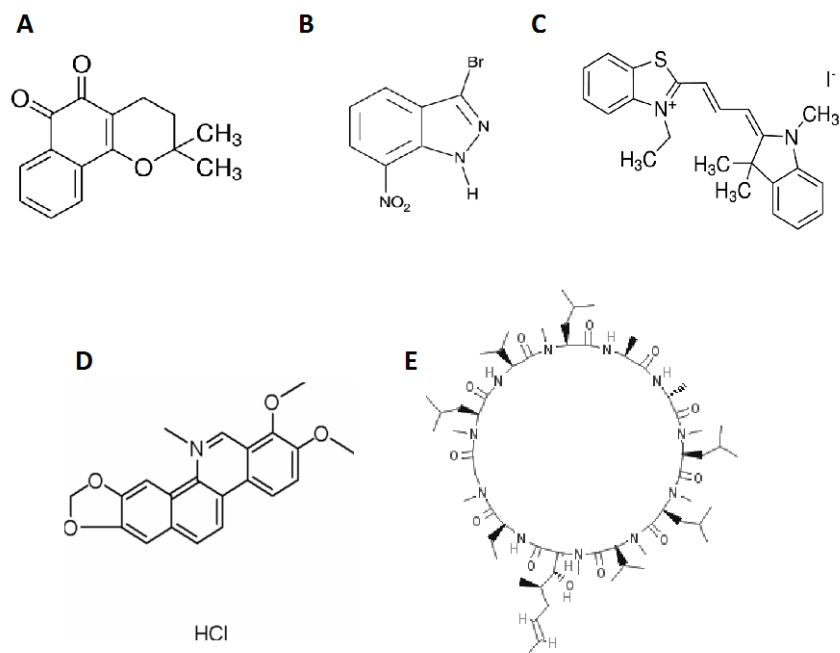


Figure 1. 5: Compounds which cluster with *S. carteri* fraction 1. **(A)** Beta-Lapachone **(B)**, 3-bromo-7-nitroindazole **(C)**, AC-93243 **(D)**, Chelerythrine chloride **(E)**, Cyclosporin A. (Structure images from PubChem database.)

Table 1. 1: Inventory of the Red Sea Sponge library includes the Call ID or sample number, available SPE fraction, the associated species name and point of collection.

Call ID	Fraction	Species name	Collection point
C16	f1,f3,f4	<i>Amphimedon chloros</i>	Inner Fsar,
C23	f1,f2,f3,f4	<i>Amphimedon chloros</i>	Inner Fsar,
S10	f1,f2,f3,f4	<i>Amphimedon chloros</i>	Inner Fsar, outer
S16	f1,f2,f3,f4	<i>Amphimedon chloros</i>	Inner Fsar, outer
S36	f1,f2,f3,f4	<i>Amphimedon chloros</i>	Inner Fsar, outer
C3	f1,f3,f4	<i>Aplysinnella rhax or dysidea rhax</i>	Shib Nsar inner
D2	f1,f3,f4	<i>Clathria</i> sp.	Al Fahal inner
D9	f1,f2,f3,f4	<i>Crella</i> aff. <i>papillata</i>	Al Fahal inner
B11	f2,f3,f4	<i>Crella cyathophora</i>	Rose reef
C11	f1,f2,f3,f4	<i>Crella cyathophora</i>	Inner Fsar
B1	f1, f2	<i>Dactylea</i> sp.	Rose reef
B14	f2, f4	<i>Dactylea</i> sp.	Rose reef
B8	f2,f3,f4	<i>Dactylea</i> sp.	Rose reef
C17	f1,f2,f3,f4	<i>Dragmacidon "Ectyoplysia" coccineum</i>	Outer inner Fsar
C25	f1,f2,f3,f4	<i>Dragmacidon "Ectyoplysia" coccineum</i>	Inner Fsar outer
D7	f1,f2,f3,f4	<i>Dragmacidon "Ectyoplysia" coccineum</i>	Al Fahal inner
B-Purple	f3,f4	<i>Haliclona (Reniera) fascigera</i>	Rose reef
C18	f1,f2,f3,f4	<i>Haliclona (Reniera) fascigera</i>	Outer inner Fsar
C20	f1,f3,f4	<i>Haliclona (Reniera) fascigera</i>	Inner Fsar, outer
CS1	f2,f3,f4	<i>Haliclona (Reniera) fascigera</i>	Rose reef
CS2	f2,f3,f4	<i>Haliclona (Reniera) fascigera</i>	Rose reef
CS3	f2,f3,f4	<i>Haliclona (Reniera) fascigera</i>	Rose reef
BE1	f1,f2,f3,f4	<i>Hyrtios erectus</i>	Rose reef

BE2	f1,f2,f3,f4	<i>Hyrtios erectus</i>	Rose reef
BE3	f1,f2,f3,f4	<i>Hyrtios erectus</i>	Rose reef
BE4	f1,f2,f3,f4	<i>Hyrtios erectus</i>	Rose reef
BE5	f1,f2,f3,f4	<i>Hyrtios erectus</i>	Rose reef
C2	f1,f3,f4	<i>Hyrtios erectus</i>	Shib Nzar inner
C24	f1,f3,f4	<i>Hyrtios erectus</i>	Inner Fsar,
S41	f1,f2,f3,f4	<i>Hyrtios erectus</i>	Inner Fsar, outer
D10	f4	<i>Iotrochota</i> sp.	Al Fahal inner
C4	f1,f3,f4	<i>Leucetta</i> sp.	Shib Nzar
C1	f4	<i>Stylissa carteri</i>	Inner Fsar,
C14	f1,f2,f3,f4	<i>Stylissa carteri</i>	Inner Fsar,
C26	fw1,f1,f2,f3,f4	<i>Stylissa carteri</i>	Inner Fsar, outer
C5	f1,f3,f4	<i>Stylissa carteri</i>	Shib Nzar inner
D5	f1,f2,f3,f4	<i>Stylissa carteri</i>	Al Fahal inner
C13	f1,f2,f3,f4	<i>Theonella swinhoei</i>	Inner Fsar
C21	f1,f2,f3,f4	<i>Xestospongia testudinaria</i>	Inner Fsar,
BG	f3,f4	Order: <i>Verongida</i>	Rose reef
C27	f1,f2,f3,f4	Family: <i>Raspailidae</i>	Inner Fsar,

Table 1. 2: Cellular stains used for High Content Screening (HCS) and parameters measure

Cellular feature	Fluorescent Stain	Examples of parameters measured
Actin	Rhodamine-labeled phalloidin	Cytoplasm total intensity, Cytoplasm average intensity, Ratio of nucleus to cytoplasm intensity, Nucleus spot total intensity, Cytoplasm spot average intensity, Cytoplasm spot total area, Cytoplasm spot average area, Cytoplasm spot nucleus
Tubulin	FITC-conjugated mouse anti- α -tubulin antibody	Cytoplasm total intensity, Cytoplasm average intensity, Cytoplasm spot total intensity, Cytoplasm spot average intensity, Cytoplasm spot total area, Cytoplasm spot average area, Cytoplasm spot nucleus
Nucleus	Hoechst stain	Nucleus size, Nucleus area, nucleus P2A, Nucleus LWR, Nucleus total intensity, Nucleus average intensity, Nucleus variation intensity
ER	ER-Tracker Blue-White DPX	Nucleus total intensity, Nucleus average intensity, Nucleus spot total intensity, Nucleus spot average intensity, Nucleus spot total area, Nucleus spot average average area, Nucleus spot nucleus
Lysosome	LysoTracker Red DND-99	Same as ER above.
Mitochondrial	MitoTracker® Orange CMTMRos	Same as ER above.
NFkB	Antibody and secondary stain GAR-DyLight 550	Cytoplasm total intensity, Cytoplasm average intensity, Nucleus total intensity, Nucleus average intensity, Cytoplasm spot total intensity, Cytoplasm spot average intensity, Cytoplasm spot total area, Cytoplasm spot average area, Cytoplasm spot nucleus, Nucleus spot total intensity, Nucleus spot average intensity, Nucleus spot total area, Nucleus spot average average area, Nucleus spot nucleus

p53	Antibody and secondary stain GAR-DyLight 488	Cytoplasm total intensity, Cytoplasm average intensity, Nucleus total intensity, Nucleus average intensity, Ratio of nucleus to cytoplasm intensity, Cytoplasm spot total intensity, Cytoplasm spot average intensity, Cytoplasm spot total area, Cytoplasm spot average area, Cytoplasm spot nucleus, Nucleus spot total intensity, Nucleus spot average intensity, Nucleus spot total area, Nucleus spot average average area , Nucleus spot nucleus
Caspase 9	Antibody and secondary stain GAR-DyLight 550	Same as p53 above
Cell membrane	WGA-AlexaFluor488	Same as NFkB above

1.7 References

1. (a) Zhang, Y. J.; Au, Q. Y.; Zhang, M. H.; Barber, J. R.; Ng, S. C.; Zhang, B., Identification of a small molecule SIRT2 inhibitor with selective tumor cytotoxicity. *Biochem Bioph Res Co* **2009**, *386* (4), 729-733; (b) Berdy, J., Bioactive microbial metabolites. *J Antibiot (Tokyo)* **2005**, *58* (1), 1-26.
2. Zhang, L.; An, R.; Wang, J.; Sun, N.; Zhang, S.; Hu, J.; Kuai, J., Exploring novel bioactive compounds from marine microbes. *Curr Opin Microbiol* **2005**, *8* (3), 276-81.
3. Ngugi, D. K.; Antunes, A.; Brune, A.; Stingl, U., Biogeography of pelagic bacterioplankton across an antagonistic temperature-salinity gradient in the Red Sea. *Mol Ecol* **2012**, *21* (2), 388-405.
4. Giles, E. C.; Saenz-Agudelo, P.; Berumen, M. L.; Ravasi, T., Novel polymorphic microsatellite markers developed for a common reef sponge, *Stylissa carteri*. *Marine Biodiversity* **2013**, *43* (3), 237-241.
5. Rudi, A.; Kashman, Y., Aaptosine - a New Cytotoxic 5,8-Diazabenz[*Cd*]Azulene Alkaloid from the Red-Sea Sponge *Aaptos Aaptos*. *Tetrahedron Lett* **1993**, *34* (29), 4683-4684.
6. Delseth, C.; Kashman, Y.; Djerassi, C., Minor and Trace Sterols in Marine-Invertebrates .14. Ergosta-5,7,9(11),22-Tetraen-3-Beta-Ol and Its 24-Zeta-Ethyl Homolog, 2 New Marine Sterols from the Red-Sea Sponge *Biemna-Fortis*. *Helvetica Chimica Acta* **1979**, *62* (6), 2037-2045.
7. Youssef, D. T. A.; van Soest, R. W. M.; Fusetani, N., Callyspongamide A, a new cytotoxic polyacetylenic amide from the Red Sea sponge *Callyspongia fistularis*. *Journal of Natural Products* **2003**, *66* (6), 861-862.
8. Youssef, D. T. A.; Yoshida, W. Y.; Kelly, M.; Scheuer, P. J., Cytotoxic cyclic norterpene peroxides from a Red Sea sponge *Diacarnus erythraenus*. *Journal of Natural Products* **2001**, *64* (10), 1332-1335.
9. Carmely, S.; Gebreyesus, T.; Kashman, Y.; Skelton, B. W.; White, A. H.; Yosief, T., Dysidamide, a Novel Metabolite from a Red-Sea Sponge *Dysidea-Herbacea*. *Australian Journal of Chemistry* **1990**, *43* (11), 1881-1888.
10. Hamed, A. N. E. S.; Watjen, W.; Schmitz, R.; Chovolou, Y.; Edrada-Ebel, R.; Youssef, D. T. A.; Kamel, M. S.; Proksch, P., A New Bioactive Sesquiterpenoid Quinone from the Mediterranean Sea Marine Sponge *Dysidea avara*. *Natural Product Communications* **2013**, *8* (3), 289-292.
11. Alarif, W. M.; Abdel-Lateff, A.; Al-Lihaibi, S. S.; Ayyad, S. E. N.; Badria, F. A., A New Cytotoxic Brominated Acetylenic Hydrocarbon from the Marine Sponge *Haliclona* sp with a Selective Effect against Human Breast Cancer. *Zeitschrift Fur Naturforschung Section C-a Journal of Biosciences* **2013**, *68* (1-2), 70-75.

12. Youssef, D. T. A., Hyrtioerectines A-C, cytotoxic alkaloids from the Red Sea sponge *Hyrtios erectus*. *Journal of Natural Products* **2005**, 68 (9), 1416-1419.
13. Neeman, I.; Fishelson, L.; Kashman, Y., Isolation of a New Toxin from Sponge *Latrunculia-Magnifica* in Gulf of Aquaba (Red-Sea). *Marine Biology* **1975**, 30 (4), 293-296.
14. Mohamed, G. A.; Abd-Elrazek, A. E. E.; Hassanean, H. A.; Alahdal, A. M.; Almohammadi, A.; Youssef, D. T. A., New fatty acids from the Red Sea sponge *Mycale euplectelioides*. *Natural Product Research* **2014**, 28 (14), 1082-1090.
15. Khalifa, S.; Ahmed, S.; Mesbah, M.; Youssef, D.; Hamann, M., Quantitative determination of latrunculins A and B in the Red Sea sponge *Negombata magnifica* by high performance liquid chromatography. *Journal of Chromatography B-Analytical Technologies in the Biomedical and Life Sciences* **2006**, 832 (1), 47-51.
16. Abdel-Lateff, A.; Alarif, W. M.; Asfour, H. Z.; Ayyad, S. E. N.; Khedr, A.; Badria, F. A.; Alihaibi, S. S., Cytotoxic effects of three new metabolites from Red Sea marine sponge, *Petrosia* sp. *Environmental Toxicology and Pharmacology* **2014**, 37 (3), 928-935.
17. Rotem, M.; Carmely, S.; Kashman, Y.; Loya, Y., 2 New Antibiotics from the Red-Sea Sponge *Psammaphysilla-Purpurea* - Total C-13-Nmr Line Assignment of *Psammaphysin-a* and *Psammaphysin-B* and *Aerothionin*. *Tetrahedron* **1983**, 39 (4), 667-676.
18. (a) Shaala, L. A.; Bamane, F. H.; Badr, J. M.; Youssef, D. T., Brominated arginine-derived alkaloids from the red sea sponge *Suberea mollis*. *J Nat Prod* **2011**, 74 (6), 1517-20; (b) Badr, J. M.; Shaala, L. A.; Abou-Shoer, M. I.; Tawfik, M. K.; Habib, A. A., Bioactive brominated metabolites from the Red Sea sponge *Pseudoceratina arabica*. *J Nat Prod* **2008**, 71 (8), 1472-4.
19. (a) Angawi, R. F.; Saqer, E.; Abdel-Lateff, A.; Badria, F. A.; Ayyad, S. E. N., Cytotoxic neviotane triterpene-type from the red sea sponge *Siphonochalina siphonella*. *Pharmacognosy Magazine* **2014**, 10 (38), 334-341; (b) Kashman, Y.; Yosief, T.; Carmeli, S., New triterpenoids from the Red Sea sponge *Siphonochalina siphonella*. *Journal of Natural Products* **2001**, 64 (2), 175-180.
20. Abou-Shoer, M. I.; Shaala, L. A.; Youssef, D. T. A.; Badr, J. M.; Habib, A. A. M., Bioactive brominated metabolites from the Red Sea sponge *Suberea mollis*. *Journal of Natural Products* **2008**, 71 (8), 1464-1467.
21. Youssef, D. T.; Shaala, L. A.; Mohamed, G. A.; Badr, J. M.; Bamanie, F. H.; Ibrahim, S. R., Theonellamide G, a potent antifungal and cytotoxic bicyclic glycopeptide from the Red Sea marine sponge *Theonella swinhoei*. *Mar Drugs* **2014**, 12 (4), 1911-23.
22. Schulze, C. J.; Bray, W. M.; Woerhmann, M. H.; Stuart, J.; Lokey, R. S.; Linington, R. G., "Function-First" Lead Discovery: Mode of Action Profiling of Natural Product Libraries Using Image-Based Screening. *Chemistry & Biology* **2013**, 20 (2), 285-295.
23. De Clercq, D. J.; Risseuw, M. D.; Karalic, I.; De Smet, A. S.; Defever, D.; Tavernier, J.; Lievens, S.; Van Calenbergh, S., Alternative Reagents for Methotrexate as Immobilizing

Anchor Moieties in the Optimization of MASPIT: Synthesis and Biological Evaluation. *Chembiochem : a European journal of chemical biology* **2015**, *16* (5), 834-43.

24. Martinez, J. P.; Sasse, F.; Bronstrup, M.; Diez, J.; Meyerhans, A., Antiviral drug discovery: broad-spectrum drugs from nature. *Natural product reports* **2015**, *32* (1), 29-48.

25. Young, D. W.; Bender, A.; Hoyt, J.; McWhinnie, E.; Chirn, G. W.; Tao, C. Y.; Tallarico, J. A.; Labow, M.; Jenkins, J. L.; Mitchison, T. J.; Feng, Y., Integrating high-content screening and ligand-target prediction to identify mechanism of action. *Nature Chemical Biology* **2008**, *4* (1), 59-68.

26. Bugni, T. S.; Richards, B.; Bhoite, L.; Cimbor, D.; Harper, M. K.; Ireland, C. M., Marine natural product libraries for high-throughput screening and rapid drug discovery. *J Nat Prod* **2008**, *71* (6), 1095-8.

27. Bugni, T. S.; Harper, M. K.; McCulloch, M. W. B.; Reppart, J.; Ireland, C. M., Fractionated marine invertebrate extract libraries for drug discovery. *Molecules* **2008**, *13* (6), 1372-1383.

28. Howe, E. A.; Sinha, R.; Schlauch, D.; Quackenbush, J., RNA-Seq analysis in MeV. *Bioinformatics* **2011**, *27* (22), 3209-10.

29. Sumiya, E.; Shimogawa, H.; Sasaki, H.; Tsutsumi, M.; Yoshita, K.; Ojika, M.; Suenaga, K.; Uesugi, M., Cell-morphology profiling of a natural product library identifies bisbromoamide and miuraenamide A as actin filament stabilizers. *ACS Chem Biol* **2011**, *6* (5), 425-31.

30. (a) Qamar, T. U.; Mumtaz, A.; Ashfaq, U. A.; Azhar, S.; Fatima, T.; Hassan, M.; Hussain, S. S.; Akram, W.; Idrees, S., Computer Aided Screening of Phytochemicals from *Garcinia* against the Dengue NS2B/NS3 Protease. *Bioinformation* **2014**, *10* (3), 115-8; (b) Senthilvel, P.; Lavanya, P.; Kumar, K. M.; Swetha, R.; Anitha, P.; Bag, S.; Sarveswari, S.; Vijayakumar, V.; Ramaiah, S.; Anbarasu, A., Flavonoid from *Carica papaya* inhibits NS2B-NS3 protease and prevents Dengue 2 viral assembly. *Bioinformation* **2013**, *9* (18), 889-95.

31. Chang, Y. C.; Tsai, M. H.; Sheu, W. H.; Hsieh, S. C.; Chiang, A. N., The therapeutic potential and mechanisms of action of quercetin in relation to lipopolysaccharide-induced sepsis in vitro and in vivo. *PLoS One* **2013**, *8* (11), e80744.

32. Polsky, B.; Segal, S. J.; Baron, P. A.; Gold, J. W.; Ueno, H.; Armstrong, D., Inactivation of human immunodeficiency virus in vitro by gossypol. *Contraception* **1989**, *39* (6), 579-87.

33. Mankouri, J.; Dallas, M. L.; Hughes, M. E.; Griffin, S. D.; Macdonald, A.; Peers, C.; Harris, M., Suppression of a pro-apoptotic K⁺ channel as a mechanism for hepatitis C virus persistence. *Proc Natl Acad Sci U S A* **2009**, *106* (37), 15903-8.

34. Dobbs, C. M.; Vasquez, M.; Glaser, R.; Sheridan, J. F., Mechanisms of Stress-Induced Modulation of Viral Pathogenesis and Immunity. *J Neuroimmunol* **1993**, *48* (2), 151-160.

35. Navarro, J.; Punzon, C.; Jimenez, J. L.; Fernandez-Cruz, E.; Pizarro, A.; Fresno, M.; Munoz-Fernandez, A., Inhibition of phosphodiesterase type IV suppresses human immunodeficiency virus type 1 replication and cytokine production in primary T cells: Involvement of NF-kappa B and NFAT. *J Virol* **1998**, *72* (6), 4712-4720.
36. Araki, S.; Dairiki, R.; Nakayama, Y.; Murai, A.; Miyashita, R.; Iwatani, M.; Nomura, T.; Nakanishi, O., Inhibitors of CLK Protein Kinases Suppress Cell Growth and Induce Apoptosis by Modulating Pre-mRNA Splicing. *Plos One* **2015**, *10* (1).
37. Li, C. J.; Averboukh, L.; Pardee, A. B., Beta-Lapachone, a Novel DNA Topoisomerase-I Inhibitor with a Mode of Action Different from Camptothecin. *J Biol Chem* **1993**, *268* (30), 22463-22468.
38. Pagans, S.; Pedal, A.; North, B. J.; Kaehlcke, K.; Marshall, B. L.; Dorr, A.; Hetzer-Egger, C.; Henklein, P.; Frye, R.; McBurney, M. W.; Hruby, H.; Jung, M.; Verdin, E.; Ott, M., SIRT1 regulates HIV transcription via Tat deacetylation. *Plos Biol* **2005**, *3* (2), 210-220.
39. Herbert, J. M.; Augereau, J. M.; Gleye, J.; Maffrand, J. P., Chelerythrine Is a Potent and Specific Inhibitor of Protein-Kinase-C. *Biochem Bioph Res Co* **1990**, *172* (3), 993-999.
40. Liu, Y. P.; Tian, X.; Lu, X. L.; Yu, J. R., Expression of Bcl-2 was downregulated and PKC beta II was activated during the apoptosis induced by bufalin in human leukemia HL-60 cells. *Blood* **2002**, *100* (11), 217b-217b.
41. Contreras, X.; Mzoughi, O.; Gaston, F.; Peterlin, M. B.; Bahraoui, E., Protein kinase C-delta regulates HIV-1 replication at an early post-entry step in macrophages. *Retrovirology* **2012**, *9*, 37.
42. Moore, J. P.; Stevenson, M., New targets for inhibitors of HIV-1 replication. *Nat Rev Mol Cell Biol* **2000**, *1* (1), 40-9.

CHAPTER 2: Identification of a 3-alkyl pyridinium from the Red Sea sponge *Amphimedon chloros* as an inhibitor of the West Nile Virus NS3 protease in vitro.

2.1 Abstract

3-alkyl pyridinium compounds, commonly known as Halitoxins are a group of structurally diverse natural products and are commonly isolated from marine sponges. These molecules can be found as cyclic or linear compounds, as monomer or as polymer alkyl pyridiniums (poly-APS). They were first characterized in 1978 for their characteristic toxicity to fish and since then a number of various biological activities have been identified. However, to date no conformation of a 3-alkyl pyridinium has been reported to show antiviral activity. The aim of this study was to assess the potential of a pre-fractionated organic extract of the Red Sea sponge *Amphimedon chloros* to inhibit the West Nile Virus NS3 protease (WNV NS3). The bioactive compound in the extract was determined using LC-MS and ¹H and DOSY NMR. It was found that at 4.69 µg/ml the biological replicates of *A. chloros* show an inhibitory activity up to 60% upon the WNV NS3 protease in a biochemical assay. The activity elicited by the fraction is specific to the WNV NS3 protease and did not show inhibition of the HCV NS4A protease or Factor XA, a cellular serin protease. The compound was identified as a 3-alkyl pyridinium of Halitoxin by LC-MS and ¹H NMR analysis. With the aid of DOSY NMR and an algorithm that relates the diffusion coefficient of the molecule to molecular weight, we found the compound to be in the size range of 39kDa. The same compound showed 60% cell loss when plated at 230 µg/ml on the human HeLa cell line. This study provides the first account of a Halitoxin exhibiting antiviral activity with negligible cytotoxicity.

2.2 Introduction

A well-represented group of marine natural products with unique structures are the Halitoxins. These 3-alkyl pyridinium molecules have acquired a number of hyponyms since the first isolation of the molecule, Halitoxin, from the sponge *Haliclona* sp. ¹. The first compound from *Haliclona* was investigated for its characteristic ichthyotoxicity. Accounts of the Halitoxin family bioactivity since the first isolation include epidermal growth factor (EGF) receptor activation ², histone deacetylase inhibition ³, dorsal root ganglion (DRG) neuron activity ⁴, antifungal ⁵, antimycobacterial, and antimicrobial ⁶ activity as well as cytotoxicity ^{1,7}. The caveat to cytotoxicity is that 3-alkyl pyridiniums can be found as cyclic or linear compounds, as monomers or as polymer alkyl pyridiniums (poly-APS), where the cytotoxicity of the molecules is both size- and dose- dependent ⁸. Interestingly, macrocyclic compounds, in general, are noted for their flexibility, high potency, selectivity, solubility, lipophilicity, membrane permeability, oral bioavailability, and metabolic stability and function as chemotherapeutics, immunosuppressants, antifungals, antiparasitics, antibacterials, and antivirals ⁹. However, to date no conformation of a 3-alkyl pyridinium has been reported to show antiviral activity.

Many viruses have little representation in pharmacological screening efforts. One example is the West Nile Virus (WNV). The *Culex* mosquito transmits the virus, which manifests as the neglected tropical disease, West Nile Fever. Symptoms of the virus include: fever, headache, body aches, skin rash, swollen lymph glands and in extreme cases, encephalitis or meningitis. The virus is endemic mainly to Africa, the Middle East and around the Mediterranean Sea¹⁰ but remains a threat to other countries when the infected hosts, both mosquitos and humans, travel. WNV is a flavivirus and in the *Flaviviridae* family

with the Hepatitis C Virus (HCV). HCV currently has more than 34 prospective antivirals in various clinical phases whereas WNV has none.

The replication cycle of the WNV begins as the 45-50nm enveloped, icosahedral nucleocapsid binds to unknown receptors on the host cell (Figure 2.1, step 1). Receptor mediated endocytosis brings the virion into the cell (Figure 2.1, step 2). The positive single-stranded 11kb RNA genomes is uncoated (Figure 2.1, Step 3) and can be directly translated by the host machinery into single long polyproteins at the rough endoplasmic reticulum (ER) (Figure 2.1, Step 6). The polyprotein contains three structural proteins (capsid, pre-membrane, envelope) and seven non-structural (NS) proteins (NS1, NS2A, NS2B, NS3, NS4A, NS2B, NS5). The polyprotein must be cleaved by the NS3 protease in order to produce the individual proteins required for replication and particle maturation¹¹ (Figure 2.1, Step 7). The replication complex, which contains the NS5 RNA dependent RNA polymerase transcribes more viral RNA by generating a negative sense RNA strand to serve as a template for the polymerization of positive sense RNA (Figure 2.1, Step 4 and 5). A molecule that can inhibit the NS3 protease, will prohibit subsequent replication, packaging, and spread of the virus within the host organism. Viral proteases are good drug targets as exemplified by the nine clinically approved HIV protease inhibitors and two approved inhibitors of the HCV NS3 protease. As a result, the WNV NS3 protease is a promising target for screening efforts directed at inhibiting the West Nile Virus. The WNV NS3 protease is a serine protease with a marked homology to the four serotypes of Dengue Virus (DENV) NS3 protease, where all have been described to have an active site that is relatively flat and very exposed; two features that pose a problem for identifying inhibitors. As a result, the non-competitive binding site has also become a targeted domain. Ideally, an inhibitor that is effective at inhibiting the WNV may prove effective on the DENV.

In this study a sponge-derived natural product library was screened and led to the identification of a fraction from the Red Sea sponge, *Amphimedon chloros*, which displays the ability to inhibit the WNV NS 3 protease *in vitro*. This activity is attributed to the 3-alkyl pyridiniums present in the fraction, which in their simplest form consist of an alkyl group connected to carbon three of a pyridine ring. An investigation into the Halitoxin or 3-alkyl pyridinium class of compounds revealed a long-standing question of how to ascertain the relative size of these compounds. This question was addressed by employing the 2D NMR technique of DOSY. The technique in combination with an algorithm reported by Evans et al 2013¹² provides a way to determine the molecular weight of a compound by its rate of diffusion. Knowing the molecular weight of the compound isolated from *A.chloros* allowed for the direct comparison of the cytotoxicity of the Halitoxin to cytotoxicity reports for other Halitoxins of various sizes. Provided here is the first account of antiviral activity for the Halitoxin family of compounds.

2.3 Materials and Methods

2.3.1 *A. chloros* Sponge Collection

The *Amphimedon chloros* specimen were collected using gardening sheers from Inner Fsar reef (22°14'37.61"N; 39°00'28.03"E) off the coast of KAUST at 12 meters depth using SCUBA. The samples were briefly rinsed with 1% PBS, wrapped in foil and placed on ice, then frozen to -80°C until processing. Dr. Nicole deVoogd provided assistance in the identification of *Amphimedon chloros* by spicule examination.

2.3.2 *A. chloros* Sponge Extraction

80 grams of sponge specimen were extracted with 1 liter of methanol then dried to 10g of Diaion HP20SS beads then loaded into a column, desalted with deionized water

(FW1, FW2) and then eluted in the following series: 25%IPA/H₂O, 50%IPA/H₂O, 75%IPA/H₂O, 100%MeOH ¹³.

2.3.3 West Nile Virus NS3 Protease Inhibition Assay

The West Nile Virus NS3 protease inhibition assay was carried out using the commercial kit SensoLyte® 440 West Nile Virus Protease Assay Kit (AnaSep, San Jose, CA, USA) [58]. The protease is a truncated form of West Nile NS3 protease (residues 1-186) connected to it is NS2B cofactor (residues 49-96) by the linker sequence, GGGGSGGGG. Protease activity was assessed by its ability to cleave the fluorogenic peptide Pyr-RTKR-AMC, and the subsequent production of free AMC (7-amino-4-methylcoumarin) fluorophores. All extracts and controls were performed with three replicates in a 384-well plate format, each with a total reaction mixture of 33 µl. To begin, the test extracts and protease solution were incubated at 37 °C for 10 min before the addition of the pre-heated substrate. After substrate addition and gentle mixing the reaction was incubated at 37 °C for one hour. The fluorophore was detected with the use of a SpectraMax® Paradigm® Multi-mode Microplate Detection Platform (Molecular Devices, Sunnyvale, CA, USA) by scanning at 354 nm excitation wavelength and 442 nm emission wavelength.

2.3.4 HCV NS3 Protease Inhibition Assay

The HCV NS3/4A protease inhibition assay was carried out using the commercial kit SensoLyte® 520 HCV Protease Assay Kit (AnaSep, San Jose, CA, USA) [58]. The HCV NS3/4A protease is a 217 amino acid fusion protein (22.7 kDa) with NS4A co-factor fused to the N-terminus of NS3 protease domain. HCV NS3/4A protease activity was assessed by its ability to cleave the fluorogenic FRET peptide, and the subsequent unquenching by QXL 520 quencher of the 5-FAM fluorophore, which emits fluorescence. All extracts and controls

were performed with three replicates in a 384-well plate format, each with a total reaction mixture of 18 μ L. To begin, the test extracts and protease solution were incubated at room temperature for 10 min before the addition of the substrate. After substrate addition and gentle mixing the reaction was incubated at room temperature for one hour. The fluorophore was detected with the use of a SpectraMax® Paradigm® Multi-mode Microplate Detection Platform (Molecular Devices, Sunnyvale, CA, USA) by scanning at 490 nm excitation wavelength and 520 nm emission wavelength.

2.3.5 Thrombin serine protease inhibition assay

The Factor Xa/Thrombin inhibition assay was carried out using the commercial kit SensoLyte® 520 Factor Xa Assay Kit (AnaSep, San Jose, CA, USA) [58]. The Factor Xa peptide consists of.... Thrombin Xa activity was assessed by its ability to cleave the fluorogenic FRET peptide, and the subsequent unquenching by QXL 520 quencher of the 5-FAM fluorophore which emits fluorescence. All extracts and controls were performed with three replicates in a 384-well plate format, each with a total reaction mixture of 12.5 μ L. To begin, the test extracts and Thrombin/Factor Xa solution were incubated for five minutes then the substrate was added. After substrate addition and gentle mixing the reaction was incubated at room temperature for one hour. The fluorophore was detected with the use of a SpectraMax® Paradigm® Multi-mode Microplate Detection Platform (Molecular Devices, Sunnyvale, CA, USA) by scanning at 490 nm excitation wavelength and 520 nm emission wavelength.

2.3.6 Cytotoxicity/HCA of *A. chloros*

A serial dilution of *A. chloros* SPE fraction 2 (230 μ g/ml, 115 μ g/ml and 57.5 μ g/ml) was plated on HeLa cells cultured and stained in the same fashion as reported in Chapter 1.

2.3.7 LC-MS of *A. chloros* Bioactive compound

Liquid chromatography-mass spectrometry (LC-MS) was carried out on the Thermo LTQ Orbitrap instrument in positive mode using electrospray ionization. The 10 μ l of solid phase extracted (SPE) sponge material was separated using a ZORBAX Eclipse XDB-C18 LC Column, 4.6 mm, 150 mm, 5 μ m and the gradient displayed in Table 1.

2.3.8 NMR of *A. chloros* 3-alkyl pyridinium

12mg of the isolated 3-alkyl pyridinium compound was evaluated using 1H and 2D DOSY on a Bruker 600MHz with a 5 mm NMR Economy Sample Tube (Wilmad-LabGlass). The DOSY experimental data was obtained using double stimulated echo gradient pulse pair and three spoil gradients pulse sequences (*dstegp3s*) in the standard Bruker pulse sequence library. The gradient shape was sinusoidal and its length (δ) was optimized at 2.3 ms ; its strength increased linearly, acquiring 32 steps of gradient levels. A gradient recovery delay of 1.5 ms was used and the diffusion time (\square) values was set to 300 ms (D20 of 300ms and a P30 of 2400 μ s at 298K.). Low and high gradient strengths were set at 5 and 95% of maximum, respectively. Each spectrum was recorded by collecting 128 transients with 10 second recycle delay. The experiment was run with CD₂OD as the solvent for 16 hrs, ns=128 for each of the 32 ramp cycles.

2.4 Results

2.4.1 *A. chloros* demonstrates inhibition of West Nile Virus NS3 Protease

Biological replicates of *A. chloros* SPE-fractionated organic extracts screened for activity against WNV NS3 protease revealed fraction 2 for all replicates (s36F2, c16F2, c23F2) to show a strong inhibition of NS3 activity at 37.5 μ g/ml (Figure 2A). Serial dilutions of the biological replicates of fraction 2 were performed showing a strong inhibition of NS3

protease activity to the lowest concentration of 4.69 $\mu\text{g/ml}$ with more than 60% inhibition (Figure 2.2 B). The same set of samples were screened for their ability to inhibit the HCV protease as well as Factor Xa associated with the serine protease, thrombin. All samples failed to show inhibition of either target.

2.4.2 High-Content Screening reveals cytotoxic of *A.chloros* treatment

With hierarchical clustering using Spearman distance and complete linkage, we showed in Chapter 1 that all biological replicates of *Amphimedon chloros* fraction 2 cluster with the LOPAC compounds CBIQ, Corticosterone and more distantly to Gossypol, Quazinone, Quercetin dehydrate and TG003. These compounds were tested on the WNV assay and showed no inhibition of the WNV NS protease. Cell counts of the HeLa cells cultures treated with the sponge test compounds show that the first dilution (230 $\mu\text{g/ml}$) used for generating HCA heatmap in Chapter 1 results in 60% cell loss. The following serial dilutions (115 $\mu\text{g/ml}$ and 57.5 $\mu\text{g/ml}$) approach 100% vitality (Figure 3). This can be compared to the 37.5 $\mu\text{g/ml}$ used in the WNV screen and shows us this concentration is expected to have cell vitality around 80%.

2.4.3 Analytical Chemistry reveals 3-alkyl pyridinium as bioactive compound

The MS² spectrum of the active SPE fraction 2 shows an abundance of a symmetrical compound with m/z 379.31 [M+H]⁺, composed for two smaller components at m/z 190.15 [M+H]⁺ (Figure 2.4). The ¹H NMR reported in the Supplemental material of Davies-Coleman and our ¹H spectra present the same signals. Their findings and ours, reported in brackets, are as follows: δ 8.95 [9.00], 8.84 [8.91], 8.45 [8.45], 8.01 [8.07] that are attributed to the 3-substituted pyridinium salt; δ at 4.60 [4.66] attributed to the methylene group on the quaternary nitrogen, which is coupled to a methylene signal at 2.20 [2.21], further coupled

to a methylene envelope at δ 1.41 [1.41]; and a signal at δ 2.87 [2.87] assigned to the methylene group bound to the C-3 position of the pyridinium ring, coupled to a methylene signal at δ 1.73 [1.73]. We also observe the presence of a peak at δ 1.31 in both spectra, but with great intensity in our sample, which we assume is associated with the methylene envelope at δ 1.41. We observe a solvent phase shift for the deuterated methanol- d4 at 3.31 ppm and 4.87 ppm as expected (Figure 2.5).

2.4.4 DOSY reveals the approximate size of the 3-alkyl pyridinium bioactive compound

Recently, DOSY experimentation has been used to analyze mixtures of small to medium sized molecules in order to determine the molecular weights of unknowns. Evans et al ¹² , took the approach one step further, keeping in mind that not all compounds are spheres moving through a continuum fluid. They were able to derive an expression to relate the diffusion coefficient to the molecular weight for a wide range of small molecules in a range of solvents:

$$D = \frac{k_B T}{6\pi\eta} \left(\frac{3a}{2} \right)^{-1} \left(\frac{1}{\rho} \right)^{-1} \left(\frac{1}{M} \right)^{-1/3}, \text{ where } a = \left(\frac{3}{4} \right)^{1/3} \left(\frac{MW_s}{MW} \right)^{1/3}$$

Their equation provides simplicity with a root mean square difference between experimental and estimated diffusion coefficients of only 15%. The 2D DOSY diffusion variable gradient was calculated for the most intense peak at δ 1.31, which is associated attributed to the methylene envelope of the halitoxin compound. From this we acquired the diffusion coefficient (D) of 1.34 E-10m²/s and using the algorithm from Evans et al., we

obtained the molecular weight estimate approximately 39 kDa for the halitoxin compound from its DOSY calculated rate of diffusion (Figure 2.6).

2.5 Discussion

Since the isolation of the first Halitoxin, a total of approximately 67 examples of 3-alkyl pyridium compounds have been reported from the species *Haliclona* ¹⁴ as well as from other sponge genera, including, *Theonella* ¹⁵, *Amphimedon* ¹⁶, *Callyspongia* ², *Cribochalina* ⁵, ¹⁷, *Echinochalina* ¹⁸, *Pachychalina* ¹⁹, *Niphates* ²⁰, and *Reniera* ²¹. Only one example has been isolated from a source outside of Porifera; this is from the mollusk *Haminoea orbignyana* ²².

3-alkyl pyridiniums in their simplest form consist of an alkyl group connected to carbon three of a pyridine ring. Halitoxins can be found as monomers with different alkyl chain lengths or as polymers of alkyl pyridiniums (poly-APS) connected in a head-to-tail or tail-to-tail arrangement or in a cyclic motif where the free tail of the alkyl chain connects to the nitrogen of another pyridine ring. The original compound, Halitoxin, was in essence a poly-APS, isolated on account of its toxicity to fish. Polymers in the size range of 500-1000 Daltons as well as the broad range from 1-25 kDa were found to have an ED₅₀ of 5-7 µg/ml when tested on the KB line of cancer cells- all compound with masses less than 500 Daltons were excluded and reported to be nontoxic ¹. Poly-APS are also known for their ability to act as surfactants and for their antifouling, antifungal and anti-algal activity. The cyclic variety of 3-alkyl pyridiniums are reported to have various bioactivities, such as the ability to inhibit histone deacetylase ³, activate epidermal growth factor (EGF) activity ² and exhibit a depolarizing effect on dorsal root ganglion (DRG) neurons ⁴, anticholinesterase²³ as well as harboring antimicrobial and antimycobacterial ²⁴ activity.

Various sizes of Poly-APS compounds have been evaluated for their ability to form pores in membranes, overall effect of cytotoxicity, and the ability of the cell to recover after exposure. As a result, their value as facilitators of drug delivery has been suggested, and a dose-dependence was found where an amount of less than 5.0 $\mu\text{g/ml}$ allowed for recoverability of the cell without cytotoxicity for high molecular weight compounds between 5.5 and 19kDa ⁸. It follows that the cytotoxicity of the compound may correlate to the size of the compound and the given dosage.

The fractionation used in the study presented here is the same solid phase extraction protocol presented in Bugni, Harper, McCulloch, Reppart and Ireland ¹³, where the crude extract of *Pseudoceratina purpurea* was dried onto Diaion HP20SS beads in order to fractionate the sample, similarly, they found a molecule at m/z 379.3123 (calcd for $\text{C}_{26}\text{H}_{39}\text{N}_2$, 379.3113) and m/z 190.1585 (calcd for $\text{C}_{13}\text{H}_{20}\text{N}$, 190.1596) that showed activity in a luciferase assay, and corresponds to our compound and its fragment. The compound was dismissed as a common hit in high throughput screening and the project was dropped on account of its classification as a Halitoxin, as class of compounds known for cytotoxicity.

The first characterization of this class of compounds was from a compound isolated from the sponge, *Callyspongia fibrosa*, by Davies-Coleman² in 1993. They report this compound to cause an activation of EGFR. The 3-alkyl pyridinium, which was identified from the Red Sea sponge *Amphimedon chloros*, appears to be the same compound as the one described in the study of 1992. This is because their LC-MS experimentation report similar peaks at m/z 379 as well as the m/z 190.1585 as was found in our experimentation (Figure 2.4 A). Furthermore, the ¹H NMR reported in the supplemental material of Davies-Coleman

and ^1H spectra presented here mirror the same signals (Figure 4B, C). Their findings and findings from this study, reported in brackets, are as follows: δ 8.95 [9.00], 8.84 [8.91], 8.45 [8.45], 8.01 [8.07] that are attributed to the 3-substituted pyridinium salt; δ at 4.60 [4.66] attributed to the methylene group on the quaternary nitrogen, which is coupled to a methylene signal at 2.20 [2.21], further coupled to a methylene envelope at δ 1.41 [1.40]; and a signal at δ 2.87 [2.87] assigned to the methylene group bound to the C-3 position of the pyridinium ring, coupled to a methylene signal at δ 1.73 [1.73]. We also observe the presence of a peak at δ 1.31 in both spectra, but with greater intensity in our sample, which we assume is also associated with a resonance of the broad methylene envelope at δ 1.41.

In Davies- Coleman et al. 1993² the authors attempted to synthesize the compound that they proposed. However, they were unable to generate the symmetrical cyclic compound with an m/z of 379, composed of two 3-alkyl pyridinium monomers at m/z 190.15. This led them to conclude that the compound they had isolated was giving an LC-MS fragmentation confounded by the ionization method and further concluded that their compound could be the fragment of a larger molecule. This issue reoccurred in other reports of the Halitoxins where activity was found but the absolute molecular size was unclear. It is certain that Halitoxins come in a variety of sizes from 500Da to 25kDa and as displayed in previous literature, Halitoxin cytotoxicity is dose-dependent and size dependent. The task then becomes accurately reporting on the size of the Halitoxin in order to assess its dosage.

In order to answer this question the 2D NMR technique of DOSY was used. This experiment evaluates the diffusion of purified samples as well as mixtures. It operates on the principle that molecules in liquids move and this translational motion is known as

diffusion Recently, DOSY experimentation has been used to analyze mixtures of small to medium sized molecules in order to determine the molecular weights of unknowns. Evans et al. 2013 ¹² , derived an expression to relate the diffusion coefficient to the molecular weight for a wide range of small molecules in a range of solvents. Using the DOSY technique and the algorithm from Evans et al. 2013 ¹², a diffusion coefficient of $1.34 \times 10^{-10} \text{ m}^2/\text{s}$ allowed for the molecular weight estimate of approximately 39 kDa for the bioactive Halitoxin (Figure 4D). This suggests that the LC-MS spectra that we found and what was reported by Davies-Coleman is showing only a fragment of the larger poly-APS compound- a compound 200 times larger than the 3-alkyl pyridinium monomer of m/z 190.15 and 100 times larger than the m/z 379 fragment..

From previous accounts of cytotoxicity for compounds in the broad size range of 0.5-25 kDa with a reported ED_{50} of 5-7 $\mu\text{g}/\text{ml}$ on the KB line of cancer cells, as well as accounts of cell recoverability after a 5 $\mu\text{g}/\text{ml}$ treatment with high molecular weight compounds between 5.5 and 19 kDa, we can make the assessment that the potency of our compound as an inhibitor of the WNV NS3 protease is not offset by an *in vivo* cytotoxicity. We have demonstrated that our compound has an inhibitory activity up to 60% upon the WNV NS3 protease at 4.69 $\mu\text{g}/\text{ml}$ (Figure 2.2 B). This inhibition is specific to the WNV NS3 protease as demonstrated by the lack of inhibitory activity of the fraction when tested on the thrombin and HCV serine proteases. The alkyl pyridinium fraction when plated on HeLa cells at 230 $\mu\text{g}/\text{ml}$ showed 50% cell loss (Figure 2.3). When manifestations of toxicity do arise, they are observed to adversely affect the actin and tubulin, the mitochondria and the ER, as well as the ability to cause a down-regulation of the cell-cycle associated protein NFkB in HeLa cells. As a result of our experimentation we propose that the poly-APS that we

have characterized as approximately 39 kDa, is a large Halitoxin, and the concentration at which inhibition is observed is low enough to avoid cytotoxicity to the host cell.

2.6 Figures and Tables

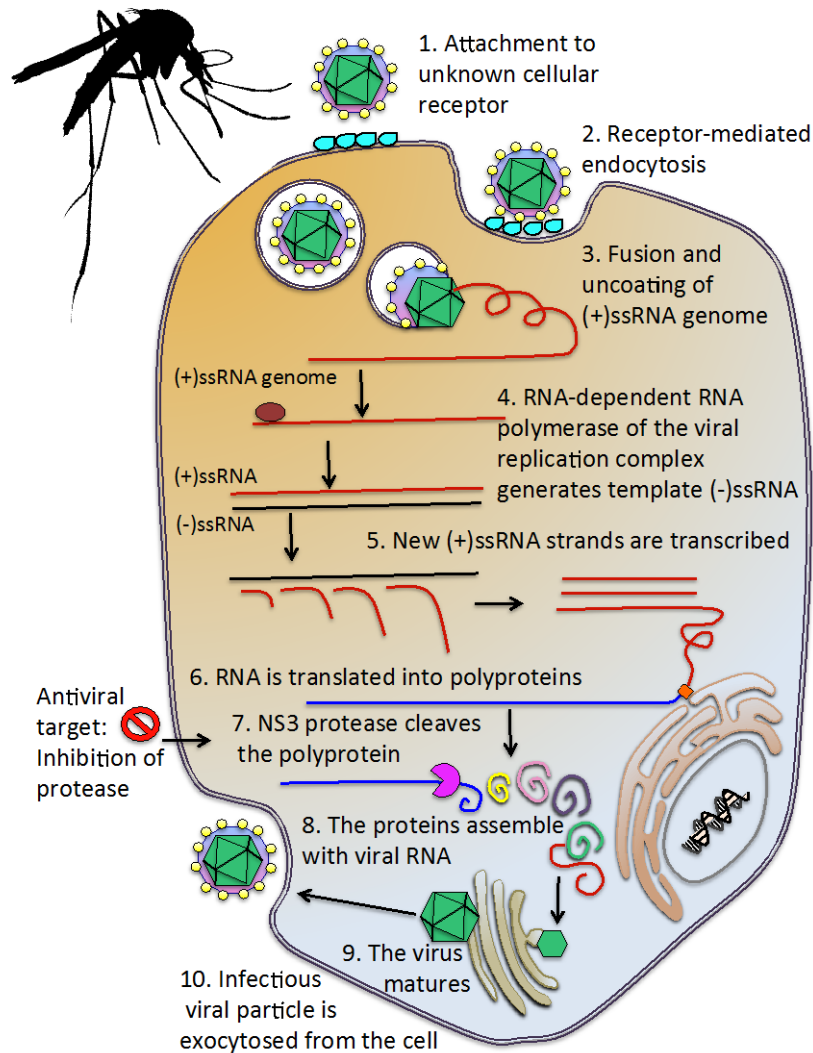


Figure 2. 1: Replication steps of the WNV depicting fusion and entry (Steps 1 and 2), uncoating and release (Step 3), translation of the polyprotein and packaging of a mature virus (Steps 4-10). This replication process post-translation can be stopped by inhibition of the WNV NS3 protease (demarcated by red stop sign).

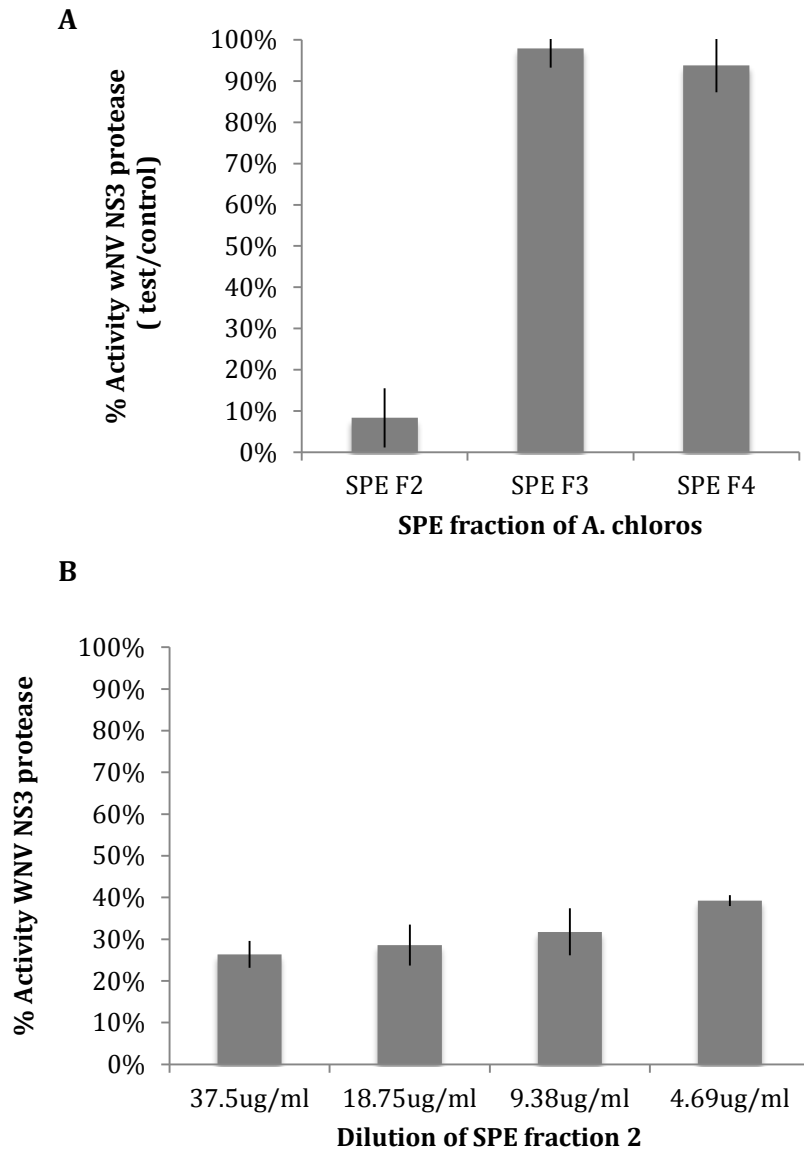


Figure 2. 2: Activity of *A. chloros* on the WNV NS3 protease. (A) Biological replicates (s10, s16, s36, and C16) of *A. chloros* SPE fraction 2, 3 and 4 (SPE F2,F3,F4) screened at approximately 37.5µg/ml for activity against WNV NS3 protease SPE F2 shows an inhibition of the protease. (B) Serial dilutions of two biological replicates of *A. chloros* SPE fraction 2

were screened against NS3 protease and maintain up to 60% inhibition of the protease at a concentration of 4.69 μ g/ml.

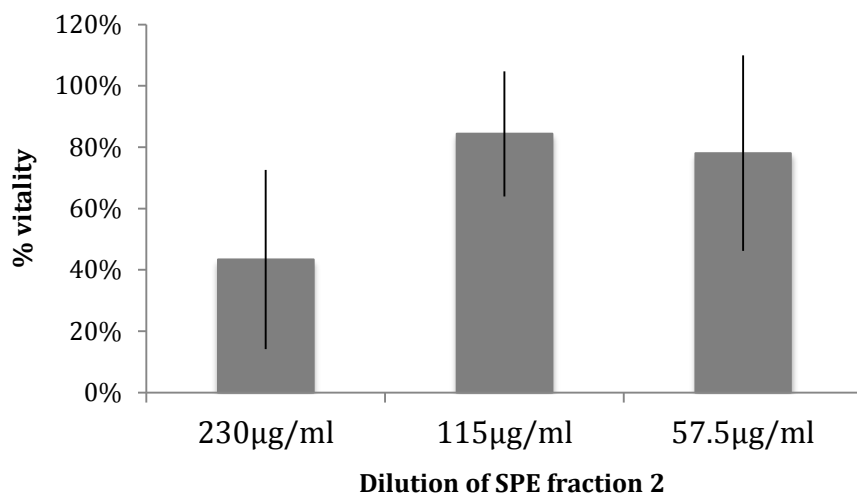
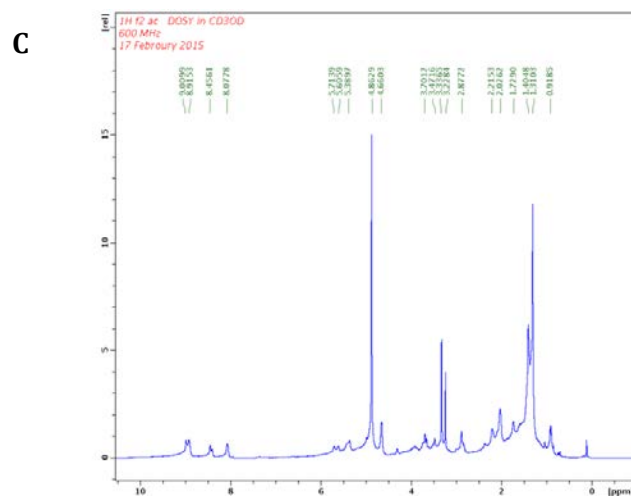
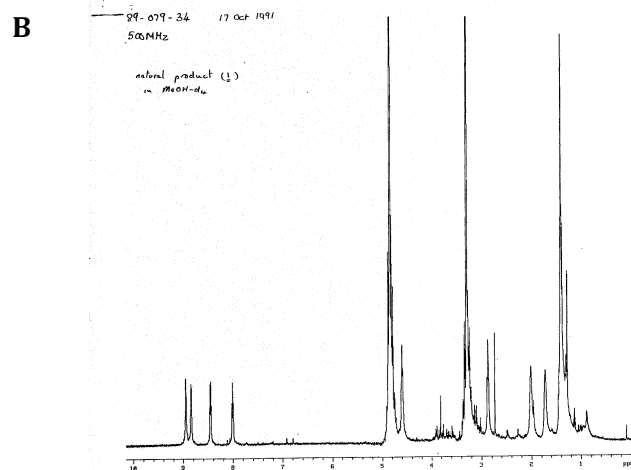
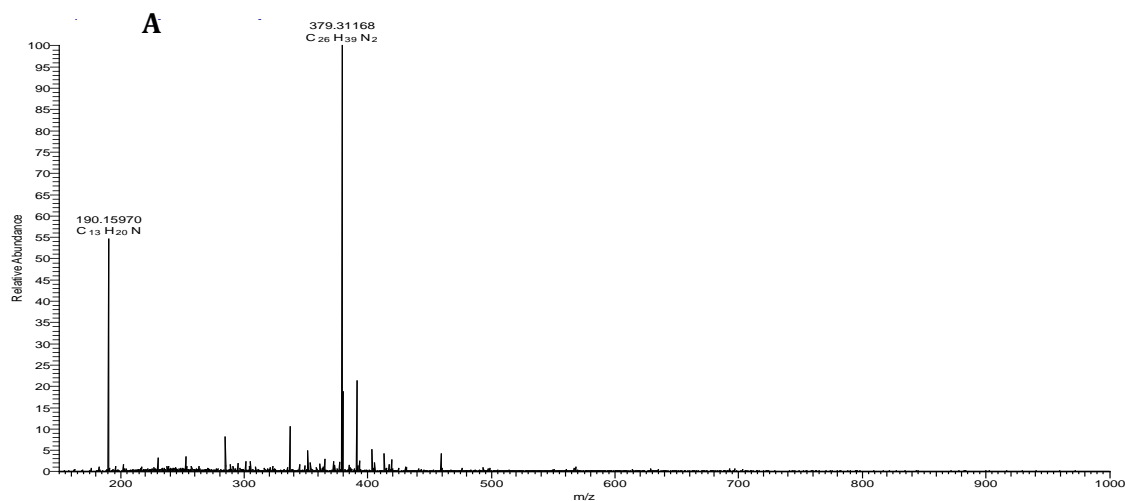


Figure 2. 3: Vitality of cells treated with HPLC fractions from the SPE fraction 2 (SPE F2) of *A. chloros*. Cell counts of the HeLa cells cultures treated with the test compound isolated from biological replicates (s10, s16, s36, and C16) of *A. chloros* show that the first dilution (230 μ g/ml) results in 60% cell death. The following serial dilutions (115 μ g/ml and 57.5 μ g/ml) approach 100% vitality. This can be compared to the 37.5 μ g/ml used in the WNV screen and shows us this concentration is expected to have cell vitality around 80%.



D

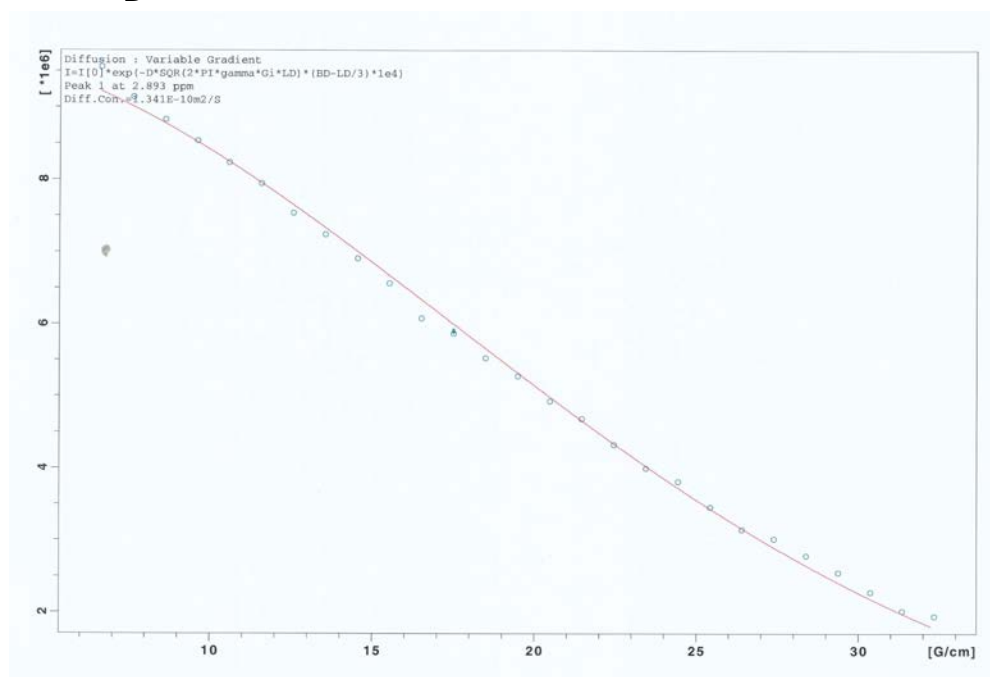


Figure 2. 4: Analytical chemistry of active SPE fraction 2 from *A. chloros* (A) LC-MS reveals the main substituent of the bioactive *A. chloros* SPE fraction 2 to be the parent m/z $[M+H]^+$ 379 and its daughter at m/z $[M+H]^+$ 190.15. (B, C) 1H NMR from Davies-Coleman publication and from this study. The 1H NMR reported in the Supplemental material of Davies-Coleman (B) and our 1H spectra (C) present the same signals. . Their findings and ours, reported in brackets, are as follows: δ 8.95 [9.00], 8.84 [8.91], 8.45 [8.45], 8.01 [8.07] that are attributed to the 3-substituted pyridinium salt; δ at 4.60 [4.66] attributed to the methylene group on the quaternary nitrogen, which is coupled to a methylene signal at 2.20 [2.21], further coupled to a methylene envelope at δ 1.41 [1.41]; and a signal at δ 2.87 [2.87] assigned to the methylene group bound to the C-3 position of the pyridinium ring, coupled to a methylene signal at δ 1.73 [1.73]. We also observe the presence of a peak at δ 1.31 in

both spectra, but with great intensity in our sample, which we assume is associated with the methylene envelope at δ 1.41. We observe a solvent phase shift for the deuterated methanol- d₄ at 3.31 ppm and 4.87 ppm as expected. (D) 2D DOSY diffusion variable gradient was calculated for the most intense peak at δ 1.31. The gradient is pictured above and provided the following coefficient of diffusion: 1.34 E-10m²/s, which was used to estimate the molecular weight of the compound using the Evans et al. 2013.

Time	% H2O	% MeOH	Formic acid in each solvent
0 min	90	10	0.10%
5 min	90	10	0.10%
40 min	10	90	0.10%
50min	10	90	0.10%
55min	90	10	0.10%
60min	90	10	0.10%

Table 2. 1: HPLC gradient used to separate the *A. chloros* SPE fraction 2.

2.7 References

1. Schmitz, F. J.; Hollenbeak, K. H.; Campbell, D. C., Marine Natural-Products - Halitoxin, Toxic Complex of Several Marine Sponges of Genus Haliclona. *Journal of Organic Chemistry* **1978**, *43* (20), 3916-3922.
2. Daviescoleman, M. T.; Faulkner, D. J.; Dubowchik, G. M.; Roth, G. P.; Polson, C.; Fairchild, C., A New Egf-Active Polymeric Pyridinium Alkaloid from the Sponge Callyspongia-Fibrosa. *Journal of Organic Chemistry* **1993**, *58* (22), 5925-5930.
3. Oku, N.; Nagai, K.; Shindoh, N.; Terada, Y.; van Soest, R. W. M.; Matsunaga, S.; Fusetani, N., Three new cyclostelletamines, which inhibit histone deacetylase, from a marine sponge of the genus Xestospongia. *Bioorganic & medicinal chemistry letters* **2004**, *14* (10), 2617-2620.
4. Scott, R. H.; Whyment, A. D.; Foster, A.; Gordon, K. H.; Milne, B. F.; Jaspars, M., Analysis of the structure and electrophysiological actions of halitoxins: 1,3 alkyl-pyridinium salts from Callyspongia ridleyi. *Journal of Membrane Biology* **2000**, *176* (2), 119-131.
5. Matsunaga, S.; Shinoda, K.; Fusetani, N., Bioactive Marine Metabolites .53. Cribrochalinamine Oxide-a and Oxide-B, Antifungal Beta-Substituted Pyridines with an Azomethine N-Oxide from a Marine Sponge Cribrochalina Sp. *Tetrahedron Lett* **1993**, *34* (37), 5953-5954.
6. de Oliveira, J. H. H. L.; Selegim, M. H. R.; Timm, C.; Grube, A.; Kock, M.; Nascimento, G. G. F.; Martins, A. C. T.; Silva, E. G. O.; de Souza, A. O.; Minarini, P. R. R.; Galetti, F. C. S.; Silva, C. L.; Hajdu, E.; Berlinck, R. G. S., Antimicrobial and antimycobacterial activity of cyclostelletamine alkaloids from sponge Pachychalina sp. *Marine Drugs* **2006**, *4* (1), 1-8.
7. Dasari, V. R. R. K.; Muthyala, M. K. K.; Nikku, M. Y.; Donthireddy, R. R., Novel Pyridinium compound from marine actinomycete, Amycolatopsis alba var. nov DVR D4 showing antimicrobial and cytotoxic activities in vitro. *Microbiological Research* **2012**, *167* (6), 346-351.
8. Tucker, S. J.; McClelland, D.; Jaspars, M.; Sepcic, K.; MacEwan, D. J.; Scott, R. H., The influence of alkyl pyridinium sponge toxins on membrane properties, cytotoxicity, transfection and protein expression in mammalian cells. *Biochimica Et Biophysica Acta-Biomembranes* **2003**, *1614* (2), 171-181.
9. Yu, X.; Sun, D., Macrocyclic drugs and synthetic methodologies toward macrocycles. *Molecules* **2013**, *18* (6), 6230-68.
10. Leyssen, P.; De Clercq, E.; Neyts, J., Perspectives for the treatment of infections with Flaviviridae. *Clinical microbiology reviews* **2000**, *13* (1), 67-82, table of contents.
11. Cregar-Hernandez, L.; Jiao, G. S.; Johnson, A. T.; Lehrer, A. T.; Wong, T. A.; Margosiak, S. A., Small molecule pan-dengue and West Nile virus NS3 protease inhibitors. *Antivir Chem Chemother* **2011**, *21* (5), 209-17.

12. Evans, R.; Deng, Z.; Rogerson, A. K.; McLachlan, A. S.; Richards, J. J.; Nilsson, M.; Morris, G. A., Quantitative interpretation of diffusion-ordered NMR spectra: can we rationalize small molecule diffusion coefficients? *Angew Chem Int Ed Engl* **2013**, *52* (11), 3199-202.
13. Bugni, T. S.; Harper, M. K.; McCulloch, M. W. B.; Reppart, J.; Ireland, C. M., Fractionated marine invertebrate extract libraries for drug discovery. *Molecules* **2008**, *13* (6), 1372-1383.
14. (a) Volk, C. A.; Kock, M., Viscosaline: new 3-alkyl pyridinium alkaloid from the Arctic sponge *Haliclona viscosa*. *Org Biomol Chem* **2004**, *2* (13), 1827-1830; (b) Teruya, T.; Kobayashi, K.; Suenaga, K.; Kigoshi, H., Cyclohaliclonamines A-E: Dimeric, trimeric, tetrameric, pentameric, and hexameric 3-alkyl pyridinium alkaloids from a marine sponge *Haliclona* sp. *Journal of natural products* **2006**, *69* (1), 135-137.
15. Kobayashi, J.; Murayama, T.; Ohizumi, Y., Theonelladins-a-D, Novel Antineoplastic Pyridine Alkaloids from the Okinawan Marine Sponge *Theonella-Swinhoei*. *Tetrahedron Letters* **1989**, *30* (36), 4833-4836.
16. (a) Albrizio, S.; Ciminiello, P.; Fattorusso, E.; Magno, S.; Pawlik, J. R., Amphitoxin, a New High-Molecular-Weight Antifeedant Pyridinium Salt from the Caribbean Sponge *Amphimedon Compressa*. *Journal of Natural Products-Lloydia* **1995**, *58* (5), 647-652; (b) Tsuda, M.; Hirano, K.; Kubota, T.; Kobayashi, J., Pyrinodemin A, a cytotoxic pyridine alkaloid with an isoxazolidine moiety from sponge *Amphimedon* sp. *Tetrahedron Letters* **1999**, *40* (26), 4819-4820; (c) Hirano, K.; Kubota, T.; Tsuda, M.; Mikami, Y.; Kobayashi, J., Pyrinodemins B-D, potent cytotoxic bis-pyridine alkaloids from marine sponge *Amphimedon* sp. *Chemical & Pharmaceutical Bulletin* **2000**, *48* (7), 974-977.
17. Kariya, Y.; Kubota, T.; Fromont, J.; Kobayashi, J., Pyrinadine A, a novel pyridine alkaloid with an azoxy moiety from sponge *Cribrorchalina* sp. *Tetrahedron Letters* **2006**, *47* (6), 997-998.
18. Jimenez, J. I.; Goetz, G.; Mau, C. M. S.; Yoshida, W. Y.; Scheuer, P. J.; Williamson, R. T.; Kelly, M., 'Upenamides: An unprecedented macrocyclic alkaloid from the Indonesian sponge *Echinorchalina* sp. *Journal of Organic Chemistry* **2000**, *65* (25), 8465-8469.
19. (a) de Oliveira, J. H.; Grube, A.; Kock, M.; Berlinck, R. G.; Macedo, M. L.; Ferreira, A. G.; Hajdu, E., Ingenamine G and cyclostelletamines G-I, K, and L from the new Brazilian species of marine sponge *Pachychalina* sp. *J Nat Prod* **2004**, *67* (10), 1685-9; (b) Laville, R.; Thomas, O. P.; Berrue, F.; Reyes, F.; Amade, P., Pachychalines A-C: Novel 3-alkylpyridinium salts from the marine sponge *Pachychalina* sp. *Eur J Org Chem* **2008**, (1), 121-125.
20. (a) Krauss, J.; Wetzel, I.; Bracher, F., A new approach towards ikimine A analogues. *Natural Product Research* **2004**, *18* (5), 397-401; (b) Kobayashi, J.; Murayama, T.; Kosuge, S.; Kanda, F.; Ishibashi, M.; Kobayashi, H.; Ohizumi, Y.; Ohta, T.; Nozoe, S.; Sasaki, T., Niphatesines a-D, New Antineoplastic Pyridine Alkaloids from the Okinawan Marine Sponge *Niphates* Sp. *Journal of the Chemical Society-Perkin Transactions 1* **1990**, (12), 3301-3303; (c) Kobayashi, J.; Zeng, C. M.; Ishibashi, M.; Shigemori, H.; Sasaki, T.; Mikami, Y., Niphatesines

E-H, New Pyridine Alkaloids from the Okinawan Marine Sponge *Niphates* Sp. *Journal of the Chemical Society-Perkin Transactions 1* **1992**, (11), 1291-1294.

21. Laville, R.; Genta-Jouve, G.; Urda, C.; Fernandez, R.; Thomas, O. P.; Reyes, F.; Amade, P., Njaoaminiums A, B, and C: Cyclic 3-Alkylpyridinium Salts from the Marine Sponge *Reniera* sp. *Molecules* **2009**, *14* (11), 4716-4724.

22. Cutignano, A.; Cimino, G.; Giordano, A.; D'Ippolito, G.; Fontana, A., Polyketide origin of 3-alkylpyridines in the marine mollusc *Haminoea orbignyana*. *Tetrahedron Lett* **2004**, *45* (12), 2627-2629.

23. Sepcic, K.; Batista, U.; Vacelet, J.; Macek, P.; Turk, T., Biological activities of aqueous extracts from marine sponges and cytotoxic effects of 3-alkylpyridinium polymers from *Reniera sarai*. *Comp Biochem Physiol C Pharmacol Toxicol Endocrinol* **1997**, *117* (1), 47-53.

24. Arai, M.; Ishida, S.; Setiawan, A.; Kobayashi, M., Haliclonacyclamines, tetracyclic alkylpiperidine alkaloids, as anti-dormant mycobacterial substances from a marine sponge of *Haliclona* sp. *Chem Pharm Bull (Tokyo)* **2009**, *57* (10), 1136-8.

25. Kobayashi, J.; Tsuda, M.; Kawasaki, N.; Matsumoto, K.; Adachi, T., Keramaphidin-B, a Novel Pentacyclic Alkaloid from a Marine Sponge *Amphimedon* Sp - a Plausible Biogenetic Precursor of Manzamine Alkaloids. *Tetrahedron Lett* **1994**, *35* (25), 4383-4386.

26. Kura, K.; Kubota, T.; Fromont, J.; Kobayashi, J., Pyrinodemins E and F, new 3-alkylpyridine alkaloids from sponge *Amphimedon* sp. *Bioorganic & medicinal chemistry letters* **2011**, *21* (1), 267-70.

27. Defant, A.; Mancini, I.; Raspor, L.; Guella, G.; Turk, T.; Sepcic, K., New Structural Insights into Saraines A, B, and C, Macrocyclic Alkaloids from the Mediterranean Sponge *Reniera* (*Haliclona*) *sarai*. *Eur J Org Chem* **2011**, (20-21), 3761-3767.

28. Tiraboschi, P.; Chito, E.; Sacco, L.; Sala, M.; Stefanini, S.; Defanti, C. A., Evaluating voting competence in persons with Alzheimer disease. *International journal of Alzheimer's disease* **2011**, *2011*, 983895.

29. Arai, M.; Ishida, S.; Settawan, A.; Kobayashi, M., Haliclonacyclamines, Tetracyclic Alkylpiperidine Alkaloids, as Anti-dormant Mycobacterial Substances from a Marine Sponge of *Haliclona* sp. *Chem Pharm Bull* **2009**, *57* (10), 1136-1138.

30. Damodaran, V.; Ryan, J. L.; Keyzers, R. A., Cyclic 3-alkyl pyridinium alkaloid monomers from a New Zealand *Haliclona* sp. marine sponge. *J Nat Prod* **2013**, *76* (10), 1997-2001.

CHAPTER 3: Alkaloids from *Stylissa carteri* present prospective scaffolds for the inhibition of the Human immunodeficiency Virus-1 (HIV-1)

3.1 Abstract

The Human Immunodeficiency Virus-1 (HIV-1) is a major global health concern with more than 35 million infected individuals. The development of the first approved antiretroviral drug, Azidothymidine (AZT, a nucleoside analog) was inspired by the naturally occurring sponge nucleoside Ara-C. Since then HIV-1 inhibitor classes have grown to include inhibitors of viral entry, membrane fusion, the integrase, and the viral protease in addition to the reverse transcriptase. Potential therapeutic targets have even extended to host factors in order to decrease the effects of viral pathogenesis. The sponge, *Stylissa carteri*, is globally distributed and has yielded a number of highly unique natural products. Aside from the antiviral activity reported for brominated derivatives of sceptrin on Herpes Simplex Virus-1 (HSV-1) and Vesicular Stomatitis Virus (VSV), antiviral activity has not been extensively reported for compounds from *S. carteri*. The primary objective of this study was to determine the inhibitory activity of a pre-fractionated extract of *S. carteri* on HIV-1 replication and to identify the chemical structure(s) of the underlying active compounds. LC-MS was used to identify the bioactive compounds from the active fractions. The single compounds, debromohymenialdisine, hymenialdisine and oroidin, were identified, obtained and screened for inhibition of viral replication and in a biochemical assay targeting the HIV-1 Reverse Transcriptase (HIV-1 RT). Debromohymenialdisine completely inhibits HIV-1 replication at 25 μ M, and exhibits a 50% inhibition of the virus at approximately 7 μ M. The chemically similar and brominated, hymenialdisine is slightly

more potent with 50% inhibition of the virus around 3 μM ; whereas, oroidin shows a 50% inhibition at 50 μM . Debromohymenialdisine is cytotoxic at concentrations greater than 13 μM ; however, hymenialdisine is significantly more cytotoxic starting at a concentration of 3 μM . Meanwhile, the brominated oroidin is not toxic for any of the concentrations assayed. When tested on a biochemical assay targeting the HIV RT oroidin is able to inhibit the activity of the enzyme up to 90% at 25 μM ; whereas, debromohymenialdisine and hymenialdisine were found to be inactive.

3.2 Introduction

In 2013, there was an estimated 35.3 (32.2–38.8) million people living with HIV. This demonstrates the need to scale up HIV treatment, while continuing efforts to screen for HIV and invest in prevention in order to avoid new HIV infections. The United Nations made the Millennium Development Goal 6, which set out to reach 15 million people living with HIV and provide them with antiretroviral treatment by this year. In December 2012, 9.7 million people in low- and middle- income countries were receiving antiretroviral therapy. Such therapies are estimated to be able to reduce the risk of HIV transmission by as much as 96%¹.

Current HIV-1 therapeutics fall under five categories, these include inhibitors of viral entry, membrane fusion, reverse transcriptase, integrase, and protease. Yet drug resistance persists despite treatment attempts to curb the disease using highly active antiretroviral therapy (HAART)- which combines antiretroviral drugs that encompass at least two different classes of the available drugs (<http://www.niaid.nih.gov>). For instance, a new aggressive form of HIV was identified in Cuba in February of this year², which progresses to AIDS in as few as three years and is composed of recombined fragments of

three HIV subtypes. This can result from one individual being infected by multiple HIV subtypes as well as an individual's failure to properly take medication.

The greatest number of drugs exists for the reverse transcriptase at 15 approved drugs followed by protease inhibitors at 8 approved drugs in comparison to the integrase, entry and fusion inhibitors at 3, 1 and 1, respectively (<http://www.fda.gov>). Most commonly, HAART treatment selects from a combination of reverse transcriptase and protease inhibitors and less commonly includes a fusion inhibitor. Aside from the previously stated enzymatic targets encoded for by the HIV-1 *gag* and *pol* genes, the targeting of other genes encoded by the “accessory” genes, *vif*, *vpr*, *vpu* and *nef*, as well as regulatory *tat* and *rev* of the HIV genome would also serve to reduce the pathogenesis of HIV³ (Figure 1). Today, the effectiveness of HIV therapy relies on the discovery and approval of novel therapeutics in order to combat the various viral phases.

3.2.1 Human immunodeficiency virus -1 replication

HIV-1 infection is initiated by fusion of the 120 nm HIV virion by its Envelope (Env) glycoprotein to the target host cell bearing a CD4 receptor (eg. Tcells, macrophages, etc.) and one of two co-receptors (CCR5 or CXCR4)(Figure 3.2, step 1). Two copies of the single-stranded RNA genome along with the virally encoded enzymes, reverse transcriptase, integrase, polymerase, and ribonuclease, enter the host cell (Figure 3.2, step 2). The single-stranded viral RNA is reverse transcribed to double-stranded viral DNA (Figure 3.2, step 3). The viral DNA translocates to the nucleus and is integrated into the host genome by the integrase (Figure 3.2, step 4) where new viral RNA copies are transcribed. After a certain threshold of Tat proteins are translated, this viral regulatory protein aids in drastically enhancing viral transcription. The spliced viral mRNAs easily export to the cytoplasm;

whereas, the second regulatory protein, Rev, capable of nuclear import and export, aids in the exportation of the incompletely spliced mRNAs of the viral structural proteins. The nascent viral RNAs are used as new viral genomes or become translated to generate viral enzymes and proteins necessary for viral packaging and pathogenesis (Figure 3.2, step 5). The RNAs encoded for by the *gag*, *pol*, and *env* genes generate the structural proteins such as the capsid, the reverse transcriptase, integrase, protease, and the envelope surface glycoprotein. Additionally, the *vif*, *vpr*, *vpu* and *nef* genes code for proteins with the ability to aid in the infection of human immune cell lines, arrest of the cell cycle in G2 phase, release of virions from infected cells and promotion of apoptosis for increased virus infection, respectively. The newly formed viruses bud from the host cell membrane (Figure 3.2, step 6) and the virus matures (Figure 3.2, step 7).

3.2.2 Known compounds from *Stylissa carteri*

The chemical repertoire of *Stylissa carteri* is well characterized with nearly 100 compounds reported in the literature. This sponge is known to produce a number of pharmacologically active brominated pyrrole-2-aminoimidazole (B-P-2-AI) alkaloids. These B-P-2-AI have been isolated from marine sponge families including Agelasidae, Axindellidae, Hymeniacidonidae, and Dictyonellidae. Many of the B-P-2-AI alkaloids are assumed to be derivatives of the building block oroidin⁴ (Figure 3.3). An account of antiviral activity has been reported for hymenialdisine where it has been found to bind Nuclear Factor- κ B (NF κ B) and disallows it from engaging the transcription of the HIV long terminal repeat (LTR) *in vitro*. Furthermore, sceptrin and its derivatives, debromosceptrin, dibromosceptrin, and oxysceptrin have been previously reported to inhibit Herpes Simplex Virus-1 (HSV-1) and Vesicular Stomatitis Virus (VSV)⁵.

3.2.3 Brominated marine natural products

Halogenated secondary metabolites are abundant in the marine environment. Bromine is found in the oceans at 65mg/L, a concentration far less than that of chlorine at 19,000 mg/L; however, marine eukaryotes commonly oxidize bromide for incorporation into organic compounds equal to their use of chlorine. The brominated compound of hymenialdisine bears a striking resemblance to the meridianins compounds first isolated from the Ascidian *Aplidium meridianum*, which have been described as potent inhibitors of various protein kinases. The ability to inhibit cyclin-dependent kinases (CDKs) is attractive for the treatment of cancer as well as neurodegenerative diseases. The brominated variolins have been isolated from the Antarctic sponge *Kirkpatrickia variolosa* and have rare skeleton that has shown activity against capable HSV1 infection. The motifs from the brominated meridianins and variolins were combined to generate the meriolin analogs. These hybrids display potent inhibitory activity towards CDK2 and CDK9. X-ray crystallography revealed that they bind to the ATP binding site of the kinase⁶.

3.2.4 Reduction of viral pathogenesis by host regulation

A review by Martinez et al 2015⁷ reports on the re-emergence of an approach to viral inhibition, which is achieved by targeting host factors instead of directly targeting viral proteins. In the context of HIV-1 this could be achieved by countering the host modulation invoked by the accessory genes, *vif*, *vpr*, *vpu* and *nef* or inhibiting the host genes which aid in the transcriptional activity of Tat and the nuclear export of Rev. For the sponge *S. carteri* in relation to HIV-1, the compound hymenialdisine (HD) has been reported in a direct association with the HIV LTR, as mentioned above. HD has also been shown to compete with ATP for binding to a number of cyclin-dependent kinases (CDK), including CDK2, as well as other kinases⁸ CDK2 is a kinase with a known role in phosphorylating the Tat protein of

HIV-1 responsible for HIV-1 transcription⁹. This is a binding activity that is perhaps not unlike the binding activity reported for the brominated meriolin analogs with CDK2. The ability of HD to inhibit CDK2 is one way to decrease viral pathogenesis by a modulation of a host factor. HD and its, debrominated form, debromohymenialdisine (DBH) are reported as able to abrogate the G2-checkpoint and therefore have the potential to relieve the Vpr and Tat-induced cell cycle arrest that support HIV pathogenesis. These lines of evidence suggest that *S.carteri* may harbor a number of compounds effective in inhibiting HIV-1 pathogenesis aside from HD and DBH because the metabolites of the sponge share common features as a result of being derived from the same building block of oroidin.

3.2.5 Pharmacophores from a Red Sea Sponge

In 1987, the first antiretroviral medicine, AZT, was approved for the treatment of HIV and was inspired by a natural product produced by a sponge ¹⁰. AZT is a nucleoside analog and bares a striking resemblance to pharmaceutically relevant hymenialdisine. However, in the past 15 years of clinical trials only five novel natural product scaffolds out of the 52 known pharmacophores have been explored where only one of the 133 naturally derived compounds in clinical trials for the period of 2008-2013 is an antiviral ¹¹ - not for the treatment of HIV/AIDS. This reveals that there is a need for new antiviral pharmacophores and their derivatives in clinical trials. In our evaluation of a Red Sea sponge library we used a cell-based HIV full replication assay (EASY-HIT¹²) and identified an extract fraction with the ability to inhibit HIV.

As a first step in this investigation an image-based High-Content (HCA) cytological profiling tool was employed in order to identify and characterize the detailed cytological effects of the active fraction and suggest its potential antiviral activity (see chapter 1). This

was followed by screening on the EASY-HIT system, a technology that uses LC5-RIC cells, a HIV-1 permissive HeLa-derived cell line with a stable fluorescent reporter gene activated by HIV Tat and Rev proteins (Figure 4)¹². This allowed for the identification of an extract fraction from *Stylissa carteri* with activity, which was further HPLC fractionated and retested on the EASY-HIT system.

Liquid chromatography-mass spectrometry (LC-MS) analysis of the active fractions revealed known compounds with unknown HIV activity as well as unknown compounds. Subsequently, the known compounds, hymenialdisine (HD) and debromohymenialdisine (DBH), and oroidin, were found to be responsible for the observed anti-HIV activity, which was not known before our study. Our experimentation led us to conclude that oroidin is capable of HIV-1 reverse transcriptase inhibition; where as HD and DBH have a more general mechanism of action that inhibits HIV pathogenesis. This presents a cabal effect from *Stylissa carteri* in its bioactive capability to inhibit HIV-1 replication.

The observation of this cabal comes at an opportune time as the “omics age” translates to marine biology, where the ability to sequence genomes, transcriptomes and metabolomes has led to the emergence of “lab rat” species of aquatic organisms. *Stylissa carteri* is on its way to becoming as one such model in the world of sponges as it is globally distributed, its genome currently being compiled (Ravasi in review), and has a number of studies expounding upon its bacterial composition¹³ and metatranscriptome¹⁴.

3.3 Materials and Methods

3.3.1 S. carteri Specimen collection and sample fractionation

Sponges were collected using gardening sheers from four coral reef locations, which include Inner Fsar/Outer Fsar, Inner Al Fahal/Outer Al Fahal, Rose Reef and Shib Nsar using SCUBA at approximately 12 meters depth (Chapter 1, Table 1.1). The specimens were washed with 1% Phosphate Buffered Saline (PBS) then wrapped in foil and placed on ice then stored at -80°C until processing. 4-10 grams of sponge specimen were extracted with 15 ml of methanol then dried to 150mg of Diaion HP20SS beads then loaded into a column, desalted with deionized water (FW1, FW2) and then eluted in the following series: 25%IPA/H₂O, 50%IPA/H₂O, 75%IPA/H₂O, 100%MeOH ¹⁵.

3.3.2 Human Immunodeficiency Virus, full Virus Screening

LC5-RIC cells were seeded into 96-well plates using only the 60 inner wells to avoid variations in the culture conditions in the outer wells. Cells were seeded at a density of 100 cells per well 24 hours prior to infection. SPE fractions for the biological replicates C26, C14 and D5, were tested in a serial dilution with a maximum of 3% methanol or approximately 75µg/ml for *S. carteri* fraction 1 mixture. For the HPLC fractions, SPEF1 HPLC fractions 1-11, were tested on the EASY-HIT assay for biological replicates C26, C14 and D5 at approximately half the concentration of the SPE parent fraction.

Test compound treatment was followed the addition of 20 ul of HIV inoculum (108RNA copies/ml inoculum for KE37.1-derived HIV-1IIIB or 28.8 ng of p24 for HIV-1LAI derived from HEK 293T cells) to each well. Virus treated plates were incubated for 48 hour then the plates were assayed for cellular reporter expression. A control for 100% infection, where HIV inoculum was added to LC5-RIC cells incubated with compound-free medium was included as well as a control for background expression where LC5-RIC cells were cultured in conditioned medium from KE37.1 (i.e., uninfected) cells. The total fluorescent

signal intensity of each culture was read in order to assess reporter expression. This was done with a fluorescence microplate reader (Fluoroskan Ascent; ThermoFisher, Schwerte, Germany) at a 544 nm excitation filter wavelength and a 590nm emission filter wavelength.

3.3.3 MTT assay

The colorimetric assay, MTT, was used in order to assess the viability and activity of LC5-RIC cells exposed to the unknown sponge mixtures, SPE fraction 1 and HPLC fractions 1-11, for three biological replicates. This cell vitality assay provides a visualization of the process where mitochondrial enzymes reduce the yellow MTT to purple formazan. After reading the HIV reporter expression, cultures were incubated with 100 μ l of MTT solution (0.5 mg of MTT; Sigma, Taufkirchen, Germany) in 100 μ l of culture medium for 2 hours. MTT solution was removed and 100 μ l of lysis solution (10% [wt/vol] SDS and 0.6% [vol/vol] acetic acid in dimethyl sulfoxide [DMSO]) was added. The formazan concentrations of the test compounds and the uninfected control cultures were determined by an ELISA plate reader (SmartSpec Plus; Bio-Rad, Muenchen, Germany) and scanned with a test wavelength of 570 nm and a reference wavelength of 630 nm.

3.3.4 Human Immunodeficiency Virus, Reverse transcriptase biochemical test

The HIV-1 reverse transcriptase inhibition assay was carried out using the commercial kit EnzChek® Reverse Transcriptase Assay (Invitrogen, San Jose, CA, USA). The reverse transcriptase is a heterodimer with the p66 and the p51 subunits with RNase H activity located in the last 15KDa of the p66 HIV Reverse transcriptase (Calbiochem, Merck-Millipore). Polymerase activity was assessed by its ability to produce RNA-DNA heteroduplexes from a mixture of a long poly(A) template, an oligo-dT primer and dTTP which is then detected by PicoGreen® dsDNA quantitation reagent. All extracts and controls

were performed with three replicates in a 384-well plate format, each with a total reaction mixture of 50µL. To begin, the poly(A) template was annealed to the oligo dT primer for one hour, then diluted 200 fold in polymerization buffer. 1.2ul of reverse transcriptase was added per 300 reactions. This mixture was kept on ice and aliquoted to each well with test compounds. The reaction was incubated at room temperature for one hour, then 2ul of 50nM EDTA was added to stop the reaction. The RNA-DNA heteroduplex was labeled with PicoGreen and incubated for 5 minutes then detected with the use of a SpectraMax® Paradigm® Multi-mode Microplate Detection Platform (Molecular Devices, Sunnyvale, CA, USA) by scanning at 480 nm excitation wavelength and 520 nm emission wavelength.

3.3.5 Analytical Chemistry of bioactive *S. carteri* fractions

HPLC fractionation was peak-based and was carried out with 50ul of material and a flow rate of 0.400ml/min using a ZORBAX Eclipse XDB-C18 LC Column, 4.6 mm, 150 mm, 5 µm and the gradient reported in Table 1. LC-MS on the Thermo LTQ Orbitrap was carried out with 10ul of material and a flow rate of 0.800 ml/min using a ZORBAX Eclipse XDB-C18 LC Column, 4.6 mm, 150 mm, 5 µm and the gradient reported in Table 3.2.

3.3.6 Principle component analysis of molecular descriptors

A PCA was first run in R studio with all 144 available descriptors, which were calculated in Bioclipse for the twenty-five 3D SDF files acquired from PubChem. The vectors mapping was viewed and overlapping descriptors were removed to reveal 45 molecular descriptors that best described the data. These descriptors are listed in Table 3.3.

3.3.7 In silico modeling

Computer-aided molecular modeling of the candidate Reverse Transcriptase inhibitor, oroidin (PubChem CID: 6312649) and the HIV-1 RT protein (PDB:1S1U) was

performed in AutoDockTools 1.5.6 and Autodock Vina¹⁶. The modeling used a grid (center x -0.237, center y -34, center z -26 ; size x-60, size y 68, size z-70). The binding affinity values are reported in Table 3.4.

3.4 Results

3.4.1 Activity of *S. carteri* SPE fraction 1 on HIV-1 replication

Three biological replicates were tested at six concentrations starting at 3% on the EASY-HIT assay. The highest concentration is 75µg/ml. *Stylissa carteri* SPE fraction 1 shows a strong inhibition at all concentrations (Figure 5A). The same 3 biological replicates were evaluated for their cytotoxicity which is % vitality using the MTT test. *Stylissa carteri* SPE fraction 1 shows a high degree of cytotoxicity on HeLa cells at all concentrations (Figure 3.5 B).

3.4.2 Activity of *S. carteri* HPLC fractions on HIV-1 replication

SPE fraction 1 was separated into 11 HPLC fractions and the averaged biological replicates of C14, C26 and D5 for SPEF1HPLC fractions 1,2,5,6,7 show activity on the EASY-HIT assay (Figure 3.6 A) and their cytotoxicity was evaluated by MTT revealing fractions 2 and 6 as fractions of interest where inhibitory activity is strongest and cell vitality maintains ~50% (Figure 3.6 B).

3.4.3 Activity of *S. carteri* HPLC fractions 2 and 6 on HIV-1 RT activity in vitro

HPLC fractions 2 and 6 (originating from SPE fractions 1) were screened for their ability to inhibit the HIV-1 reverse transcriptase in a dilution series. The dilution concentrations were 37.5 µg/ml, 18.75 µg/ml, 9.375µg/ml, and 4.688 µg/ml (Figure 3.7 A). HPLC fraction 2 showed inhibition of the HIV RT while HPLC fraction 6 does not.

Additionally, HPLC fractions 1,3, and 4 were screened for their ability to inhibit the HIV-1 reverse transcriptase in a dilution series. HPLC fraction 1 (similar to HPLC fraction 2) showed inhibition of the HIV RT while HPLC fraction 3 and 4 do not (Figure 3.7 B).

3.4.4 High Content Screening of *S.carteri* SPE fractions

The biological replicates of the SPE Fraction 1 (C5, C14, C26, D5) cluster with the LOPAC library reference compounds using spearman method with complete linkage. SPE fractions 1, of C26 and C5 showed close matching with 3-bromo-7-nitroindazole (a potent inhibitor of all nitric oxide synthase isoforms), chelerythrine chloride (PKC inhibitor), cyclosporine A (powerful immunosuppressant, also inhibits Tcell receptor transduction pathway by inhibiting calcineurin, and inhibits NO synthesis), and AC-93253 iodide (potent, cell permeable, subtype selective RAR (RAR α) agonist) whereas, SPE fraction 1 of C14 and D5 clustered with beta-lapachone, which has chemopreventive properties. The selected LOPAC compounds were screened for anti-HIV RT activity in the biochemical assay and showed no inhibition; whereas, 3-bromo-7-nitroindazole showed 30% inhibition of HIV-1 replication in the EASY-HIT assay (Figure 3.8 A). The cell counts for all cultures treated with the HPLC fraction biological replicates (C14, C26, D5) were assessed in order to determine the vitality of the cells after treatment. This cell vitality is comparable to the % vitality obtained after treatment of the LC-RIC cells in the EASY-HIT assay (Figure 3.8 B). This proves that we are evaluating a similar concentration and that there is consistency across screening platforms..

3.4.5 Analytical Chemistry of active HPLC fractions

LC-MS chromatograms for HPLC fractions of interest H2 (red) and H6 (black) were overlaid for comparison. HPLC fraction 2 and fraction 6 have many peaks in common

(Figure 9A). These peaks show the presence of debromohymenialdisine ($C_{11}H_{11}N_5O_2$, m/z 246), 2- Debromohymenin ($C_{11}H_{13}BrN_5O$, m/z 312), hymenialdisine ($C_{11}H_{10}BrN_5O_2$, m/z 324), 3-bromohymenialdisine ($C_{11}H_9Br_2N_5O_2$, m/z 403), oroidin ($C_{11}H_{11}Br_2N_5O$, m/z 389) in both HPLC 2 and 6 (Figure 3.9 B)

3.4.6 Principal Component Analysis of Molecular Descriptors for LOPAC reference compound, Sponge constituents, and approved HIV-1 Reverse Transcriptase drugs

A principle component analysis was performed on data aggregated from the High Content Analysis (LOPAC, pink), EASY-HIT, RT biochemical test and LC-MS data (*Stylissa*, red) and known HIV RT inhibitors (NaRTI, yellow; NNRTI, blue; NtRTI, green; RHRTI, black). This resulted in a plot of 25 PubChem 3D SDF files defined by 45 molecular descriptors. The principle component 1 (PC1) explains 21% of the variation in the dataset, whereas, PC2 explains 19%. A PCA plot using 147 molecular descriptors (not show here) reveals the same overall clustering with a higher proportion of variance explained by PC1 at 44%, followed by PC2 at 13%. This similarity despite the reduction of molecular descriptors suggests the trend is conserved and the analysis is robust. The analysis shows that the candidate compounds from *Stylissa*, 3-bromohymenialdisine, oroidin, 10Z-hymenialdisine and debromohymenialdisine cluster more closely with known reverse transcriptase inhibitors according to their molecular properties than they do with their closest associated hits in the LOPAC library. It also suggests that oroidin, 3-bromohymenialdisine and hymenialdisine are more structurally similar to known Non-nucleoside reverse transcriptase inhibitors (NNRTI), rilpivirine and lersivirine, than they are to known Nucleoside analog or Nucleotide reverse transcriptase inhibitors (NaRTI, NtRTI). Whereas, debromohymenialdisine is more similar in structure to a NaRTI (Figure 3.11). This

pharmaceutical bioinformatics assessment of our compounds of interest helps us to predict HIV RT activity for our sponge-derived compounds.

3.4.7 Activity of single molecules on full-virus model HIV-1 replication

The single compounds of debromohymenialdisine (Figure 3.10 A), hymenialdisine (Figure 3.10 B), and oroidin (Figure 3.10 C) were purchased and tested on the EASY-HIT platform at 50 μ M, 25 μ M, 12.5 μ M, 6.25 μ M, and 3.125 μ M. Debromohymenialdisine completely inhibits HIV-1 replication at 25 μ M, revealing a 50% inhibition of the virus at approximately 7 μ M. The chemically similar and brominated, hymenialdisine is slightly more potent with 50% inhibition of the virus around 3 μ M; whereas, oroidin shows a 50% inhibition at 50 μ M (Figure 3.12A). Debromohymenialdisine is cytotoxic at concentrations greater than 13 μ M; however, hymenialdisine is significantly more cytotoxic starting at a concentration of 3 μ M perhaps on account of the positioning of the bromine atom. Meanwhile, the brominated oroidin is not toxic for any of the concentrations assayed (Figure 3.12 B).

3.4.8 Activity of single molecules on HIV-1 reverse transcriptase assay

Serial dilutions of the single compounds debromohymenialdisine, hymenialdisine, and oroidin were screened for activity on a biochemical HIV-1 reverse transcriptase assay. This revealed oroidin as capable of inhibiting the activity of the enzyme up to 90% at 25 μ M; whereas, debromohymenialdisine and hymenialdisine were not active (Figure 3.13).

3.4.9 In Silico modeling of Oroidin on HIV-1 Reverse Transcriptase

Oroidin (green), when modeled in Autodock against HIV RT (PDB:1S1U) binds into the hinge at the “palm” and the “thumb” of the p66 subunit (white, the p51 subunit is in lilac). This is the hydrophobic pocket. Nine mode of binding were computed, binding mode

#7 of oroidin in the HIV-1 RT was evaluated with a binding affinity of -7.1 kcal/mol (Table 3.4). Oroidin interacts with residues Lys101 (pink), Val 179 (blue), Tyr 181 (red), Tyr 188 (purple), and W229 (orange). These are all residues of interest for an RT inhibitor¹⁷ (Figure 3.14).

3.5 Discussion

In 1951 a nucleoside containing an arabinose sugar, spongouridine was isolated from the Caribbean sponge *Tethya crypta*¹⁸. The antiviral activity of its synthetic analog, Ara-A was later described¹⁹. It was found capable of inhibiting viral DNA polymerases, the synthesis of herpes and the varicella zoster viruses. These spongonucleotides, which use an arabinose sugar instead of a deoxyribose or ribose sugar, inspired researchers to substitute the sugar rather than the base moiety, in order to yield greater bioactive versatility in their analogs¹⁰. The downstream result was the development of Azothymidine (AZT) with an “azido” group, at the 3’ carbon of the five-carbon sugar, capable of disrupting DNA polymerization. AZT is an effective HIV-1 reverse transcriptase inhibitor and was approved in 1987 as the first of its kind.

Today, there are two categories of HIV reverse transcriptase (RT) drugs. These are the Nucleoside/Nucleotide Reverse Transcriptase Inhibitors (NRTIs) and Non-nucleoside Reverse Transcriptase Inhibitors (NNRTIs). The virus uses the RT to generate double-stranded DNA from the single-stranded RNA viral genome. The eight approved NRTIs are drugs which mimic the nucleotide building blocks used during DNA synthesis; however, these mimetics lack the 3-OH group of the five carbon sugar found in the naturally occurring deoxyribonucleotides/nucleosides and thus terminate the building of the phosphate backbone²⁰. The seven NNRTIs, on the other hand, inhibit the RT by binding to a

hydrophobic pocket located at the hinge where the thumb of the polymerase meets the palm of the polymerase. The binding of the NNRTI to this pocket creates a conformational change in the protein and renders it inactive. Both types of RT inhibitors are used in HAART therapy along with antivirals targeting viral entry, fusion, the integrase, and the protease.

In this analysis of the anti-HIV activity of SPE fraction 1 of *Stylissa carteri* we observed an inhibition of HIV-1 replication in a cell-based full-infection assay. This inhibition by SPE fraction 1 occurs in phase 1 of the EASY-HIT assay, which shows that the candidates for affected processes encompass most HAART therapy targets, aside from the viral protease (Figure 3.5 A). A further testing of 11 HPLC fractions collected from SPE fraction 1 showed that HPLC fractions 1, 2, 6 and 7 have retained the anti-HIV activity of the parent SPE fraction (Figure 3.6 A). Further biochemical testing of the HPLC fractions 1,2,3,4 and 6 showed only fractions 1 and 2 to inhibit the HIV-1 Reverse Transcriptase (RT) *in vitro* (Figure 7 A, B). The LC-MS spectra for fractions 2 and 6 revealed an overlap of compounds common to the active and inactive fractions from the RT assay (Figure 3.9). This generates two hypotheses. One where the compounds shared between HPLC fractions 2 and 6 are capable of inhibiting HIV-1 replication in a general manner; however, among the compounds distinct to HPLC fraction 2 (as well as HPLC fraction 1) there exists a compound specifically targeting the RT. Alternatively, it is possible that the concentration of the active compound in HPLC fraction 2 was greater than that of HPLC 6, which would mean that the lack of activity in HPLC fraction 6 on the RT biochemical assay is a matter of the concentration being too low to show RT inhibition.

3.5.1 Previously described compounds from *S. carteri* as candidate inhibitors

The mechanism of inhibition from the compounds shared by the two HPLC fractions

has a number of possibilities. This is because there exists a cavalcade of proteins, not directly encoded by the nine viral genes, which favor viral replication by modulating host cell biology. The regulation of these genes is the dark matter of four less pharmacologically targeted HIV-1 proteins encoded by the genes *vif*, *vpr*, *vpu* and *nef*³ as well as *tat* and *rev*. Specifically the viral protein regulatory (Vpr) has been indicated in the transactivation of the HIV-1 long terminal repeat (LTR) *in vitro*, nuclear import of preintegration complexes (PICs), induction of cell cycle arrest in G2, and apoptosis in infected cells. Vpr is thought to facilitate infection of non-dividing tissue macrophages as well as inducing G2 cell-cycle arrest in dividing T cells²¹. Congruently, the HIV Trans-Activator of Transcription (Tat), known to drive viral replication, is shown to cause a 3-fold up-regulation of Checkpoint 1 (chk1), an important inducer of the G2 checkpoint causing cell-cycle arrest²². A G2 arrest is thought to pose a replicative advantage for the viral species, as the HIV-1 LTR is most active during this phase²³. A study with the objective of addressing the link between cell cycle arrest and apoptosis used caffeine as an inhibitor of the serine/threonine kinases Ataxia telangiectasia mutated (ATM) and ataxia telangiectasia and Rad3-related protein (ATR) and showed the relief of both cell cycle arrest and apoptosis induced by Vpr²⁴. Caffeine is one of the few compounds known to arrest G2-checkpoint activity, others include 2-aminopurine, and 6-dimethylaminopurine, staurosporine, 7-hydroxystaurosporine, SB-218078, and isogranulatimide²⁵.

After observing the chemical overlap present in HPLC fractions 2 and 6, both of which showed strong inhibition of HIV-1 replication with around 50% cell vitality in the EASY-HIT assay (Figure 3.6 B), the second hypothesis was pursued where the compounds common to the fractions were presumed good candidates for further antiviral screening. This resulted in the three marine-derived alkaloids, hymenialdisine (HD) (Figure 3.10 A),

debromohymenialdisine (DBH) (Figure 3.10 B), and oroidin as prospective candidates (Figure 3.10 C). The expected activity for HD was based on an a report by Breton et al 1997 where it was found to inhibit Interleukin-8 production in U937 cells by inhibition of Nuclear Factor- κ B (NF κ B). Additionally it is known that NF κ B binding to its consensus motif is critical for long terminal repeat (LTR)-mediated transcription of HIV ²⁶. HD as also been shown to compete with ATP for binding to a number of cyclin-dependent kinases^{8a}. One of which is CDK-2^{8b} a kinase that has a role in phosphorylating the Tat protein of HIV-1, which activates HIV-1 transcription. Inhibition of CDK-2 by hymenialdisine maybe an example of one way to inhibit the viral pathogenesis induced by Tat, which was achieved by inhibiting host cellular features.

In an experiment to characterize new heptacyclic peptides, oroidin was obtained as a by-product and both the peptides and the alkaloid were tested for HIV activity and were found inactive ²⁷. Additionally, they reported no cytotoxic effects for oroidin; however, they did report on a marginal anti-malarial activity with an IC₅₀ value of 1200 ng/ml and a 71% inhibition of *M. tuberculosis* at a concentration of 128 μ g/ml. We had no empirical evidence to generate a hypothesis for debromohymenialdisine aside from evidence from Curman et al. ²⁵, which reports debromohymenialdisine (DBH), as well as hymenialdisine, were able to abrogate the G2-checkpoint like caffeine. In their assessment, they found DHB capable of inhibiting the G2 checkpoint by a direct inhibition of Chk1 and Chk2 with an IC₅₀ of 8 μ M and an IC₅₀ of 25 μ M on MCF-7 cells. This suggests DBH may also be able to relieve the Vpr and Tat-induced cell cycle arrest that support HIV pathogenesis. All three compounds had been structurally elucidated ²⁸ and synthesized and were available for purchase from Enzo Life Sciences.

3.5.2 Debromohymenialdisine and Hymenialdisine demonstrate a broad inhibition of HIV-1 while Oroidin targets the HIV-1 Reverse Transcriptase

Testing of the candidate single molecules, debromohymenialdisine, hymenialdisine, and oroidin in the EASY-HIT assay and revealed debromohymenialdisine as capable of 70% HIV-1 inhibition at 13 μ M with cell viability between 90-100%. The lower cell survival rate displayed in cells treated with the same micromolar concentration of hymenialdisine- which differs from debromohymenialdisine by one bromine in the 4' position of pyrrole group- is perhaps due to the presence and positioning of the bromine. Contrary to a previous report of inactivity, a 50 μ M concentration of oroidin shows 50% inhibition of the HIV-1 virus; without displaying any cytotoxicity (Figure 3.12 A, B).

The single compounds were then screened on the HIV RT biochemical assay and the results show oroidin to be a prospective reverse transcriptase inhibitor displaying 90% inhibition of the reverse transcriptase at 12.5 μ M (Figure 3.13). This inhibition may account for the inhibition observed for the parent SPE fraction (Figure 3.5 A) and daughter HPLC fractions 1 and 2 (Figure 3.6 B). This would also support the alternative hypothesis where the RT activity is not distinct only to HPLC fraction 2 but that both fractions, HPLC 2 and 6, have the presence of oroidin, where it is more abundant in HPLC fraction 2. Furthermore, the only cell-based account of oroidin as an HIV inhibitor reports no activity for the compound and this may be a result of the concentration that was tested being too low. Our results show oroidin to be more effective at inhibiting the HIV RT *in vitro* than with the *in vivo* cell-based assay. This could be attributed to the need for improvement on the ADMET (Absorption, Distribution, Metabolism, Excretion, and Toxicity) value of absorption. Oroidin, may not be easily absorbed by the cell, which causes the double-brominated alkaloid to be less bioavailable but also less toxic. Meanwhile, the compounds, hymenialdisine and

debromohymenialdisine, could be competing with ATP for binding of CDKs as well as abrogating the G2 checkpoint cell-cycle arrest. The structures of the two compounds (Figure 3.10 A, B) resemble reconfigured nucleosides and their ability to outcompete ATP is very interesting. This recalls the first pharmaceutically relevant HIV antiviral, AZT, which was the analog of a nucleoside.

3.5.3 PCA helps to propose the binding of Oroidin

The multivariate statistical technique known as principle component analysis (PCA) uses molecular descriptors to illustrate the chemical space occupied by selected compounds. PCA is extensively used in the field of pharmaceutical bioinformatics in the application of statistical molecular design in order to reduce the number of compounds to be produced by combinatorial chemistry while maintaining the greatest amount of variation among the synthesis set. Along similar lines, PCA can be used to identify descriptors that best describe the data set whose values can be used for future computational quantitative structure activity relationships (QSAR). PCA has been used in the field of metabolomics in order to prioritize compounds for investigation ²⁹

PCA analysis using 3D SDF files obtained from the Pubchem database for three (AC-93253 iodide, 3-bromo-7-nitroindazole, chelerythrine chloride) of the five reference compounds which clustered with the *Stylissa* fraction in the High Content Analysis, the three procured *Stylissa*-derived compounds (HD, DBH, and oroidin) and 3-bromohymenialdisine, and all known HIV RT inhibitors (NaRTI, yellow; NNRTI, blue; NtRTI, green; RHRTI, black) were analyzed using this multivariate approach. From this analysis it is possible to conclude that debromohymenialdisine is more chemically similar to a nucleoside reverse transcriptase inhibitor (NRTI) than the other sponge-derived compounds. Whereas, oroidin,

hymenialdisine and 3-bromohymenialdisine are more chemically related to the non-nucleoside reverse transcriptase inhibitors (NNRTI) than they are to the LOPAC1280 reference compounds (Figure 3.11). With the knowledge that oroidin exhibits *in vitro* HIV RT inhibition the compound was modeled with the HIV-1 reverse transcriptase protein in order to speculate about its mode of binding (Figure 3.14).

3.5.4 *In Silico* modeling of Oroidin and the HIV-1 Reverse Transcriptase

In silico modeling of Oroidin, into the HIV RT (PDB:1S1U) shows a mode of binding that reflects the binding characteristics of approved NNRTIs. Oroidin binds into the palm of the p66 subunit, more specifically, it interacts with residues L101, V179, Y181, Y188, and W229- these are all residues of interest for an RT inhibitor ¹⁷(Figure 3.14). The binding of residues Y181 and Y188 cause the polymerase thumb to become rigid and unable to bind the RNA template, whereas, W229 is a highly conserved residue of the NNRTI-binding pocket. CP94707, an experimental imidazole containing compound, is able to disturb the residue W229 and releases the ‘primer grip’, which orients the template/primer of the viral RNA strand in the correct direction to receive the incoming dNTP^{30 31 17} Whereas, binding of the residue, Y188, was key to the success of first generation NNRTI inhibitors. Oroidin, a brominated pyrrole-imidazole alkaloid seems to have a similar binding activity as the approved NNRTIs and as well as an experimental compound lending to its strong *in vitro* binding of the HIV-1 reverse transcriptase.

3.5.5 Candidates show similarity to current marine alkaloid anti-HIV leads

In order to gauge where our sponge-derived compounds stand as lead molecules, we compared these values to a 2005 report by Singh et al 2005, which summarized all known anti-HIV natural products from both terrestrial and marine organisms. Table 1 of

Singh et al has been slightly modified to include only the alkaloid compounds with a reported IC_{50}/EC_{50} value. Additionally, four more sponge derived anti-HIV alkaloid compounds reported by Sagar et al 2010³² were added to our Table 5. Of the nineteen alkaloids reported as anti-HIV leads, 9 originate from marine sponges. While the ED_{50}/IC_{50} of the compounds range from 3 μ M to 40 μ M (one outlier at 0.91mM), the cytotoxicity of the compounds are poorly assessed. For instance the two compounds, Batzelladines A and B from the sponge *Batzella* sp., were tested *in vitro* and again in a cell based assay and they only report that the compounds were cytotoxic with no associated toxicity values. The two compounds Crambescidin 826 and Dehydrocrambine A from the sponge *Monanchora* sp. were also only testing in an *in vitro* assay. Dragmacidin F, being the weakest candidate, reports on an inhibition of syncytium formation however gives no report on cytotoxicity. The compounds Manadomanzamine A, B, and Xestomanzamine A from *Acanthostrongylophora* sp. did not report a specific activity and were only tested for cytotoxicity at a concentration lower than the ED_{50} , but was not cytotoxic. Trikendiol, from the sponge *Trikenrion loeve* has reported activity as an inhibitor of HIV-induced cytopathic effects with no reported cytotoxicity value. The phenomenon where “cytotoxicity” occurs a term without definition has been discussed in the Newmann et al 2008³³ review concerning natural products as drug leads when recounting the efforts of Novartis to attribute biological information to ‘privileged scaffolds’ in order to characterize them as effective ligands. Their efforts fell short on account of non-specific biological data. We accurately report on cytotoxicity and conclude that debromohymenialdisine compound with an ED_{50} of approximately 10 μ M and an LD_{50} of 35 μ M, would need modification to render it less toxic in order to be a better antiviral candidate. Oroidin, on the otherhand, has the least cytotoxicity among the marine alkaloids reported in Table 1; however, the concentration

required for inhibition in the cell-based assay at 50 μ M is high in comparison. Whereas, the active concentration of oroidin in the biochemical assay shows it to be a promising lead for further medicinal chemistry modification to improve its ability to be absorbed through cell membranes. Oroidin could have potential as a privileged scaffold as it shows to be an effective ligand of the HIV RT. In fact, of the 26 natural product-derived drugs (terrestrial and marine) launched from the years 2006-2013, only five are without any modification¹¹. This demonstrates the fine-tuning that occurs for most naturally derived compounds before becoming a drug.

3.6 Conclusion

Our endeavor to resolve the initial observed cytotoxicity of the SPE fraction 1 of *S. carteri* from HIV-1 activity illustrates the benefit of following through on a lead that is not an outright “hit”. There are two conventions when it comes to screening efforts aimed at natural products compound discovery, these have been described as an “isolate and then test” and “test and then isolate”³⁴. The “isolate then test” is often the method of chemists where novel compounds are fully elucidated and purified and even synthesized; whereas, from a biological standpoint it can be faster and easier to employ the “test then isolate” method in order to see what sticks and investigate. However, the nature of dealing with a diverse mixture can confound results and even produce false negatives where interesting compounds go uninvestigated.

In the case of *S. carteri*, its plethora of brominated metabolites would leave most cell-based assay with a cytotoxic readout and might deter the researcher from pursuing the fraction for antiviral activity. However, because we also employed an in depth cytological profile at an early stage in our screening pipeline we were able to determine a structural

similarity to other bioactive compounds, including a brominated compound (e.g. 3-bromo-7-nitroindazole), and extrapolate and attribute an anti-HIV activity worth pursuing to our fraction. The fact that debromohymenialdisine and hymenialdisine, and oroidin were first described in 1996, and that their synthesis has been resolved and carried out on moderately large scales, it is hard to believe that it was not until now, 19 years later that our screening efforts provide the first account of antiviral activity for the globally distributed sponge, *Stylissa cateri*. This reality stands as a testament to the need for screening natural products libraries for antiviral activity on a larger and broader scale than we have seen thus far, in a smart throughput manner, similar to what we have presented here.

3.7 Figures_and Tables

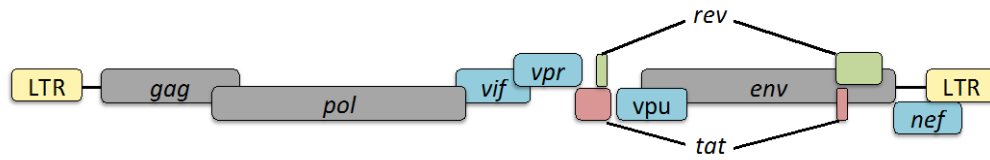


Figure 3. 1: The nine virally encoded genes of HIV-1: gag, pol, vif, vpr, rev, tat, nef, env and the Long Terminal Repeat (LTR). (Figure adapted from Gottfredsson et al. 199735.)

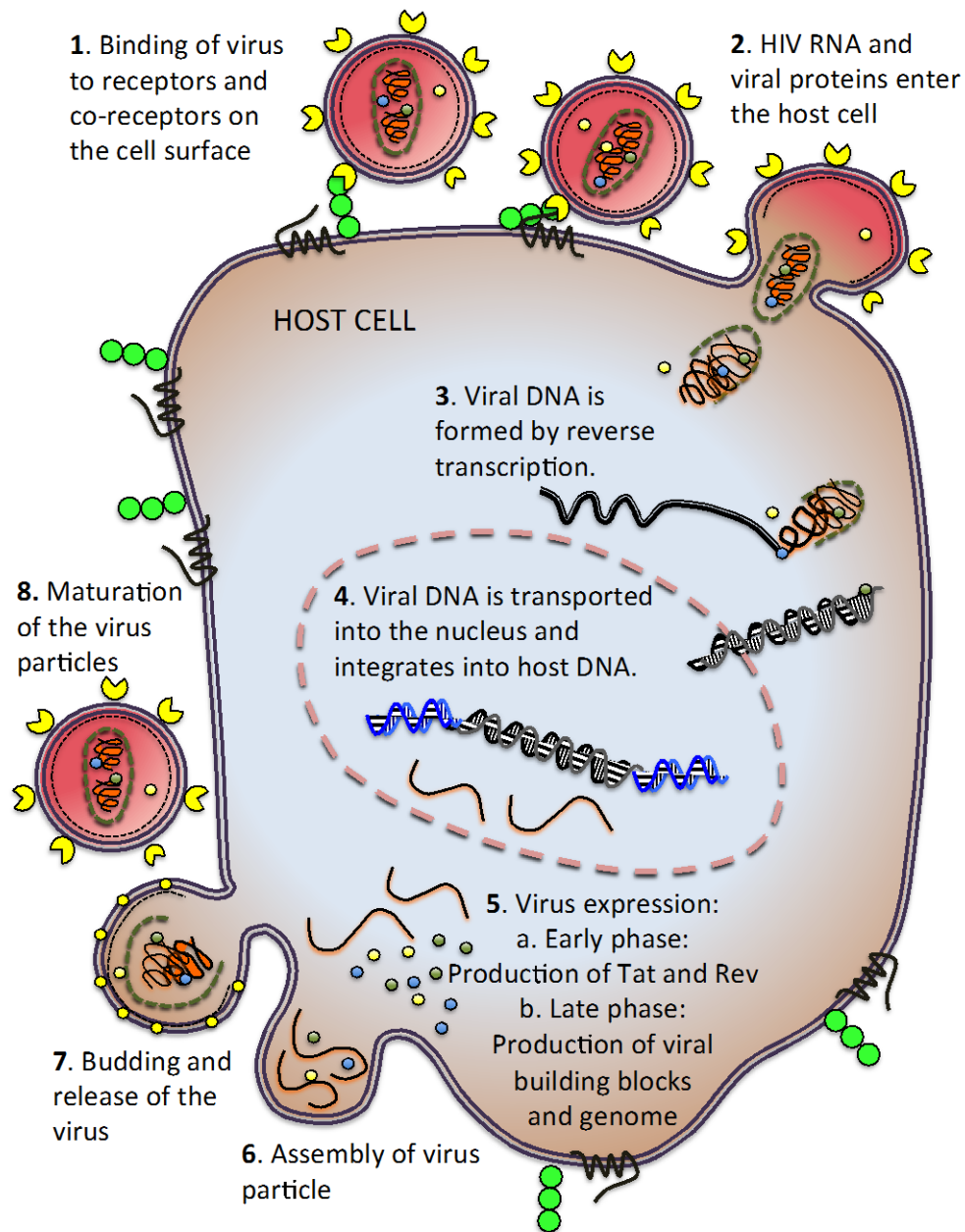


Figure 3. 2: The HIV replication cycle including 1. Fusion, 2. Virus entry, 3. Reverse transcription, 4. Integration, 5. Packaging, 6. Budding, and 7. Maturation. (Image redrawn from NIAID illustration)

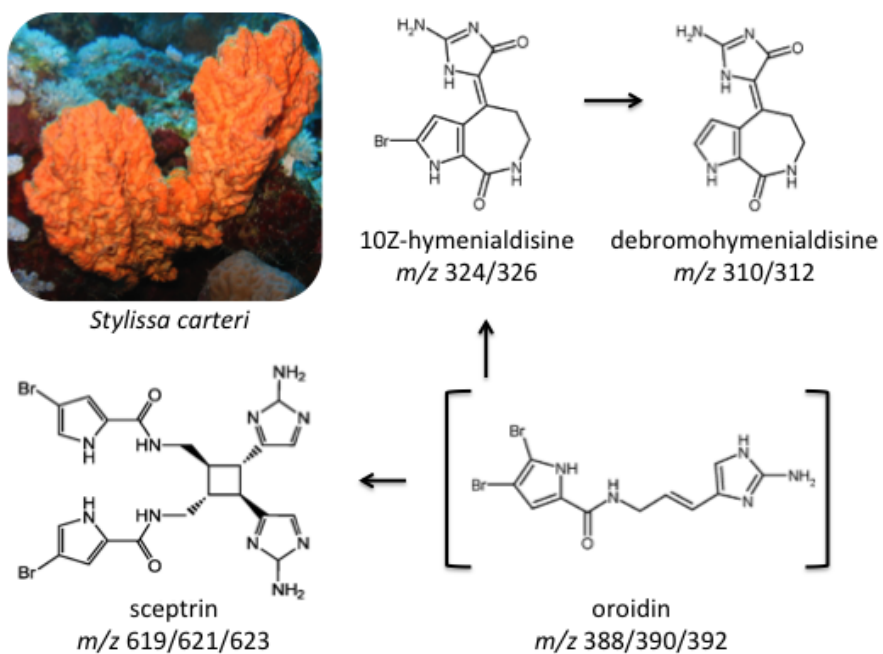


Figure 3. 3: Metabolites from *Stylissa carteri*, such as 10Z-hymenialdisine, debromohymenialdisine and sceptrin, with previously reported bioactivity are derivatives of the compound oroidin. (Figure adapted from Yarnold et al. 20124.)

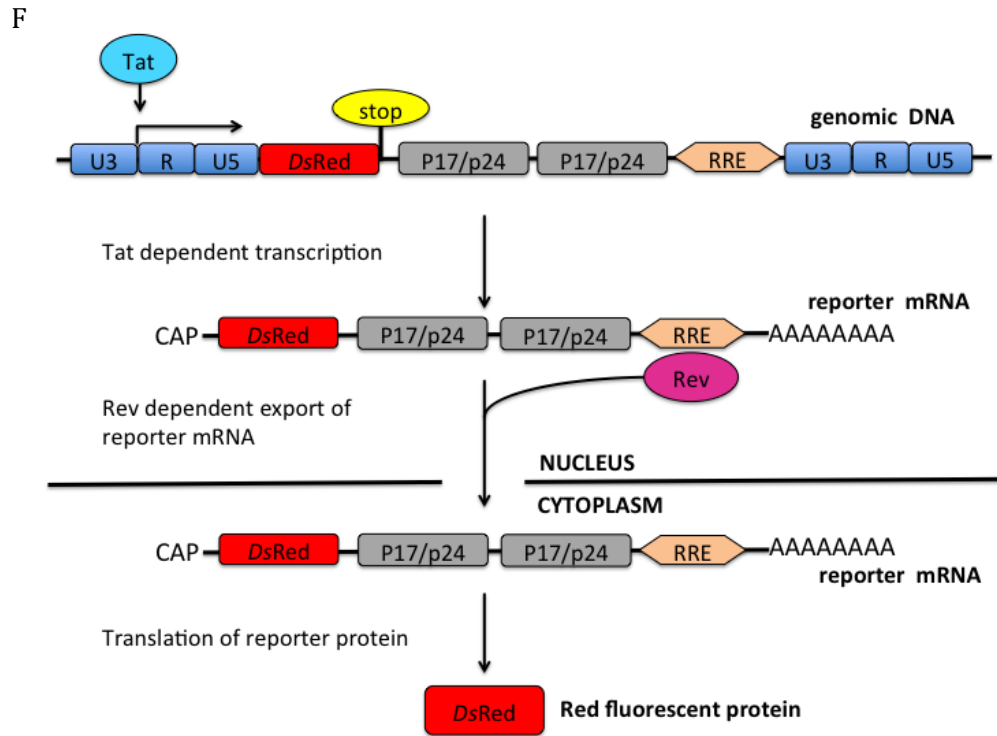


Figure 3. 4: Depiction of the EASY-HIT reporter scheme where the Tat protein drives transcription of the DsRed reporter harboring the p17/p24 elements of the HIV structural gag gene. The Rev protein binds to the Rev-responsive element (RRE) to translocate the DsRed containing (p17)/(p24) mRNA to the cytoplasm. The translation of the mRNA until the “stop” sequence results in only the expression of the red fluorescent protein. (Figure adapted from Kremb et al. 201012.)

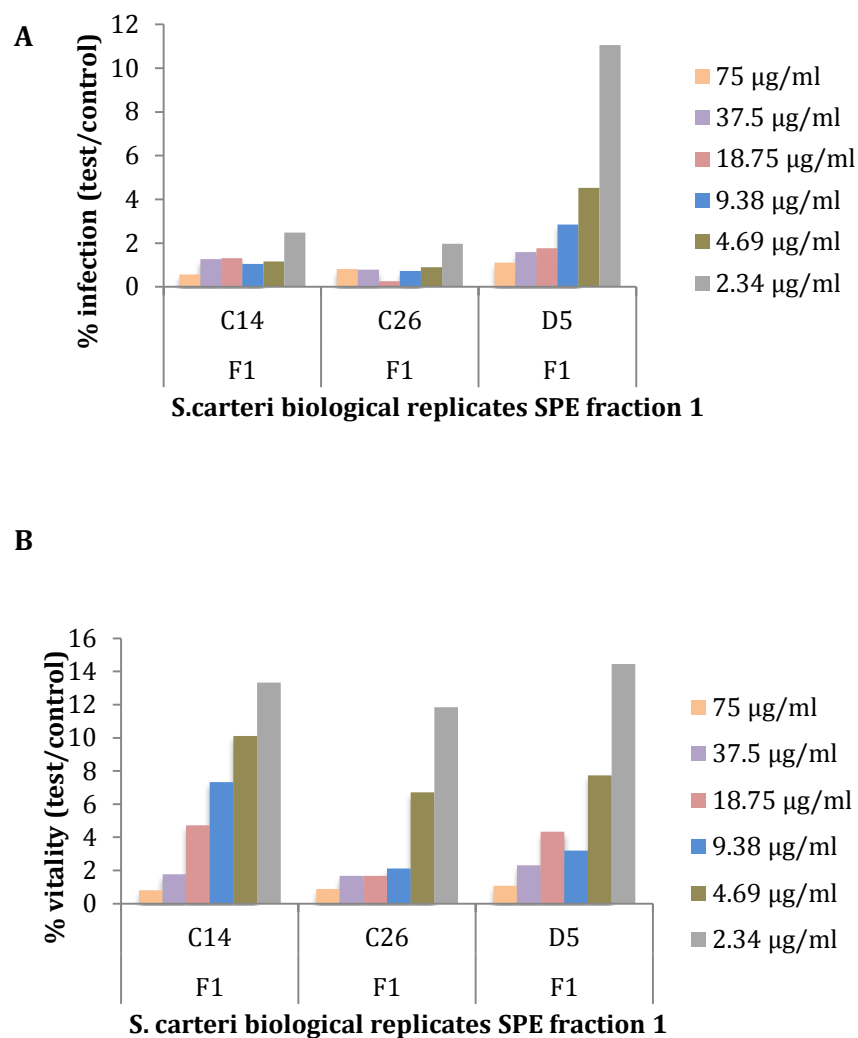


Figure 3. 5: % Infection and % Cell Vitality of EASY-HIT assay after *S. carteri* SPE fraction 1 treatment. (A) The percentage of HIV-1 infection for the 3 biological replicates (samples C14, C26 and D5) of *S. carteri* SPE fraction 1 tested at six concentrations on EASY-HIT. (B) The percentage cell vitality for 3 biological replicates (samples C14, C26 and D5) of *S. carteri* SPE fraction 1 tested at six concentrations and evaluated by MTT.

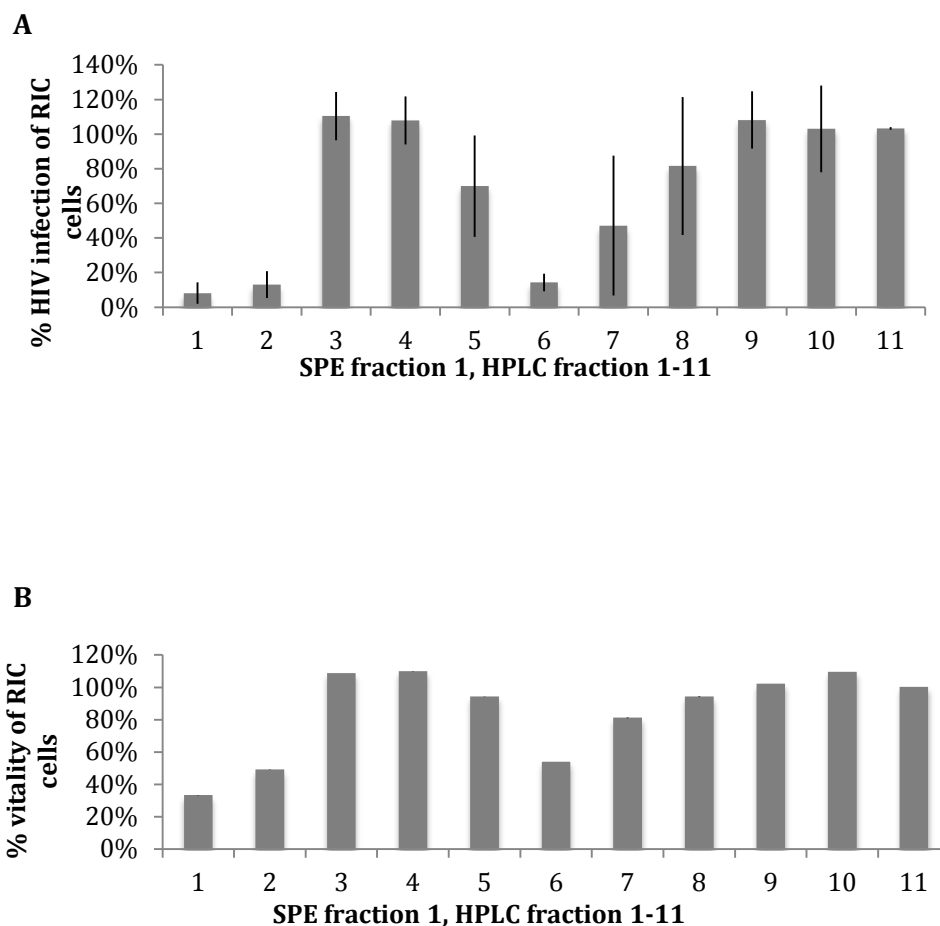


Figure 3. 6: % Infection and % Cell Vitality of EASY-HIT assay after *S. carteri* SPE fraction 1 HPLC fraction 1-11 treatment. (A) *S. carteri* SPE fraction 1 was separated into 11 HPLC fractions for the three biological replicates (samples C14, C26 and D5) and screened on the EASY-HIT assay. (B) Percentage of cell vitality after treatment with with SPE fraction 1, HPLC fractions 1-11 for the three biological replicates (samples C14, C26 and D5).

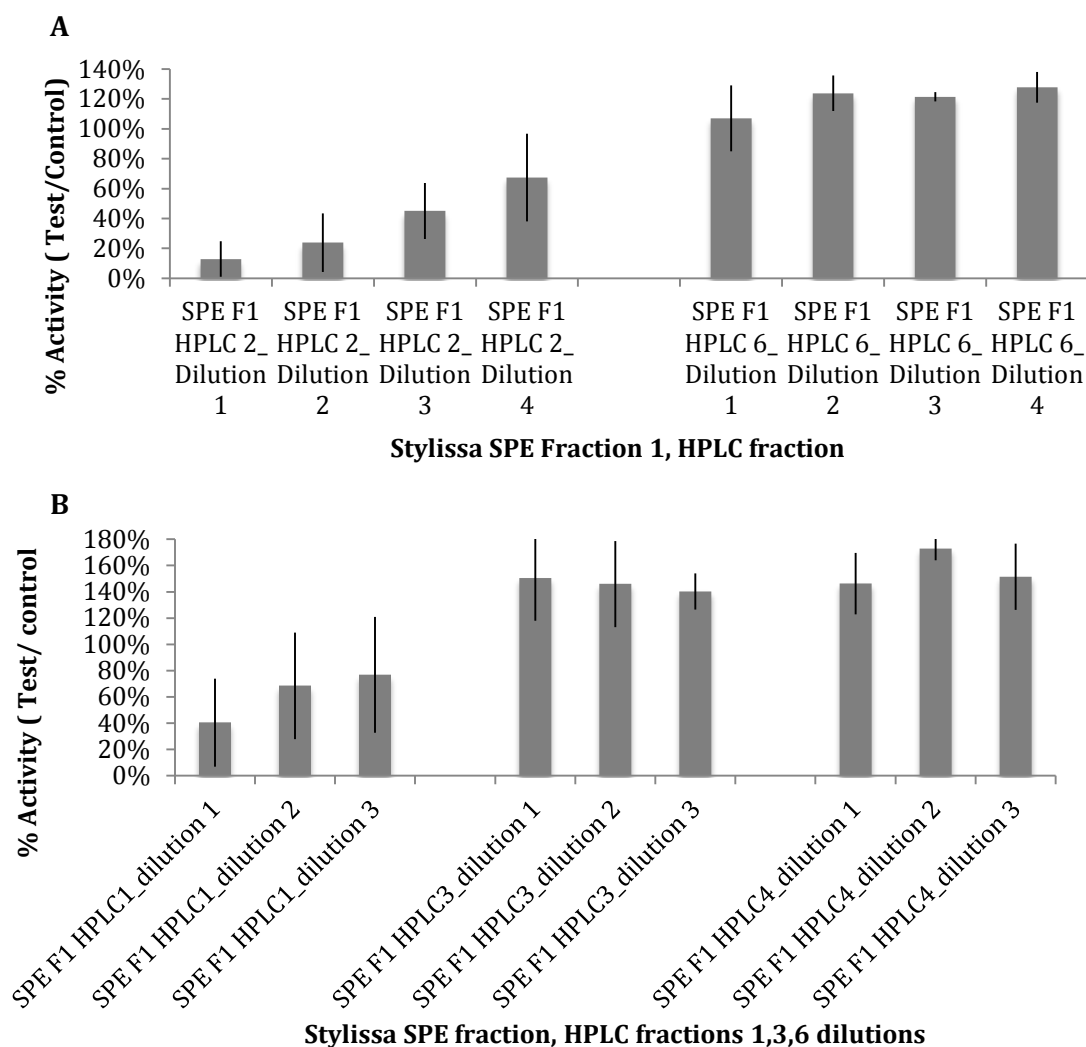


Figure 3. 7: % Activity of the HIV-1 Reverse transcriptase after treatment with *S.carteri* SPE fraction 1, HPLC fraction 1, 2, 3, 4, and 6 treatment (A) SPE fraction 1, HPLC fractions 2 and 6 for the three biological replicates (samples C14, C26 and D5) were screened for their ability to inhibit the HIV-1 reverse transcriptase in a dilution series. (B) SPE fraction 1, HPLC fractions 1,3, and 4 for the three biological replicates (samples C14, C26 and D5) were screened for their ability to inhibit the HIV-1 reverse transcriptase in a dilution series.

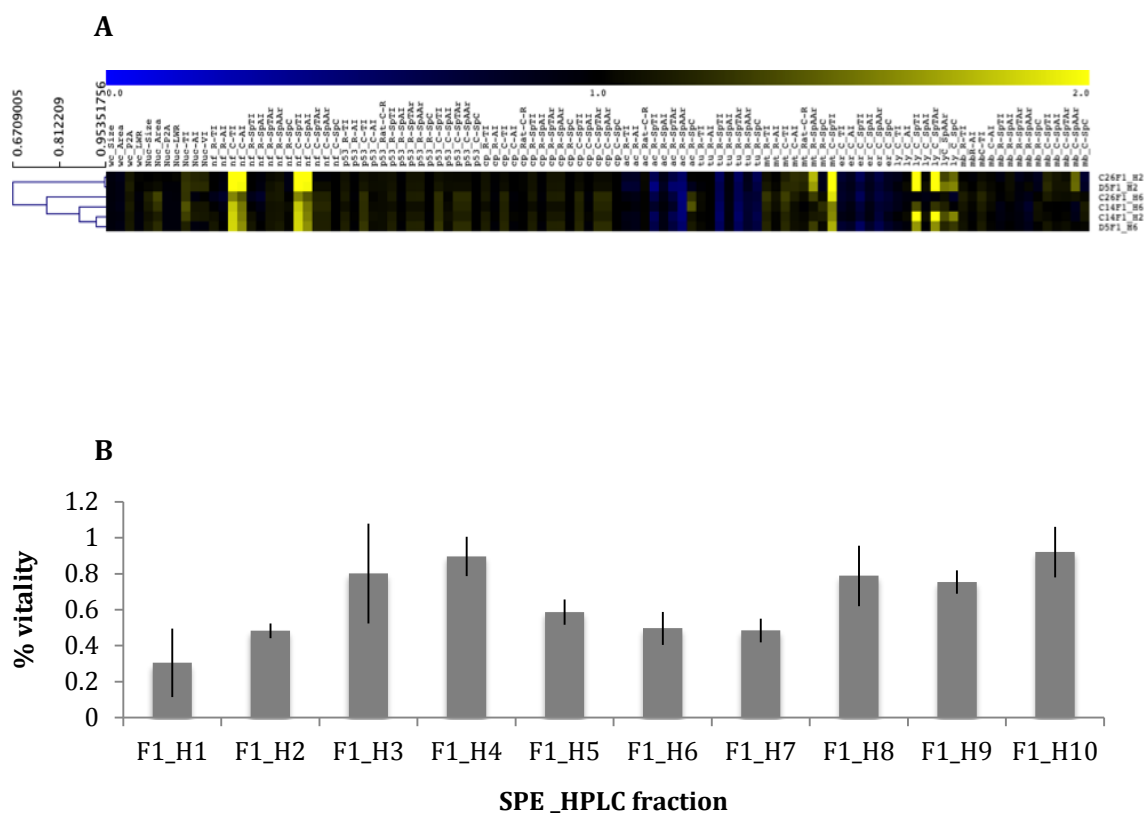


Figure 3. 8: HCS Heat map and cell counts for HPLC fractions 1-10. (A) Heat map of the biological replicates (C14, C26, D5) for HPLC fractions 2 and 6. (B) The cell counts for all cultures treated with the HPLC fraction biological replicates (C14, C26, D5) were assessed in order to determine the vitality of the cells after treatment. This cell vitality is comparable to the % vitality obtained after treatment of the LC-RIC cells in the EASY-HIT assay. This proves that we are evaluating a similar concentration and that there is consistency across screening platforms.

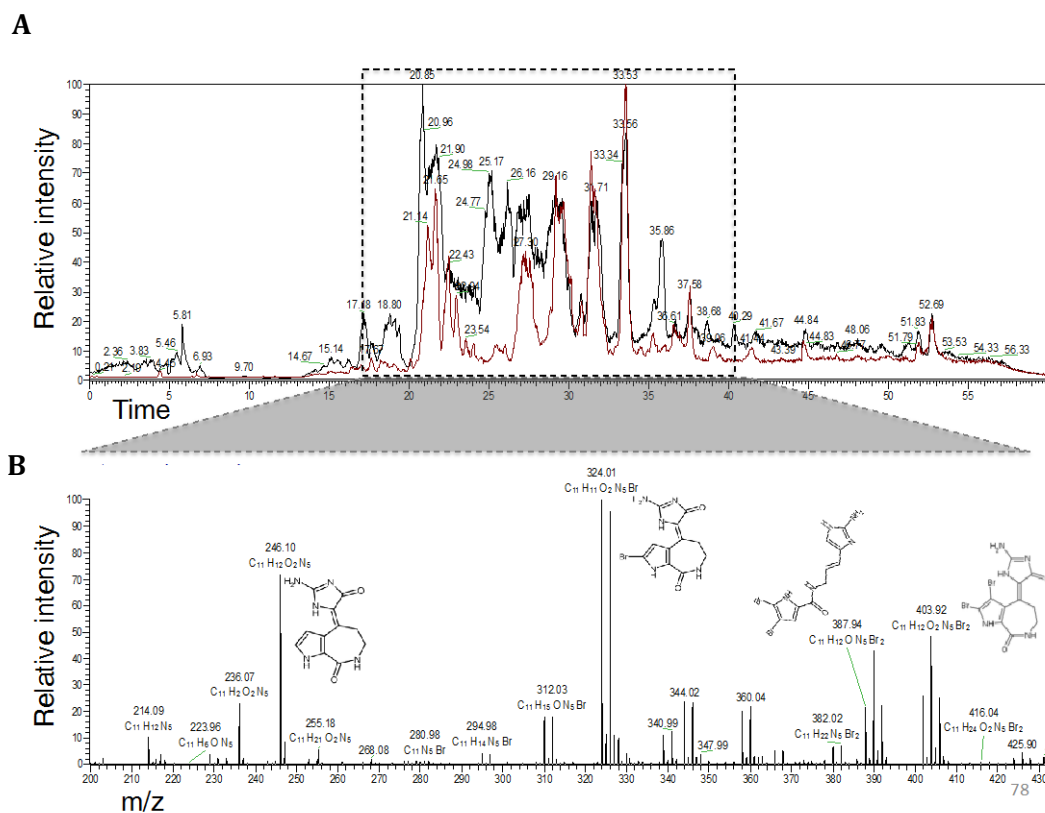


Figure 3. 9: LC-MS chromatogram and spectra for *S. carteri* SPE fraction 1, HPLC fraction 2 and 6 (A) Overlay of LC-MS chromatograms for HPLC fractions of interest H2 (red) and H6 (black). (B). Peak spectra shared between HPLC fractions H2 and H6. These peaks show the presence of debromohymenialdisine ($C_{11}H_{11}N_5O_2$, m/z $[M+H]^+$ 246), 2-Debromohymenin ($C_{11}H_{13}BrN_5O$, m/z $[M+H]^+$ 312), 10Z-hymenialdisine ($C_{11}H_{10}BrN_5O_2$, m/z $[M+H]^+$ 324), 3-bromohymenialdisine ($C_{11}H_9Br_2N_5O_2$, m/z $[M+H]^+$ 403), oroidin ($C_{11}H_{11}Br_2N_5O$, m/z $[M+H]^+$ 389) in both HPLC 2 and 6.

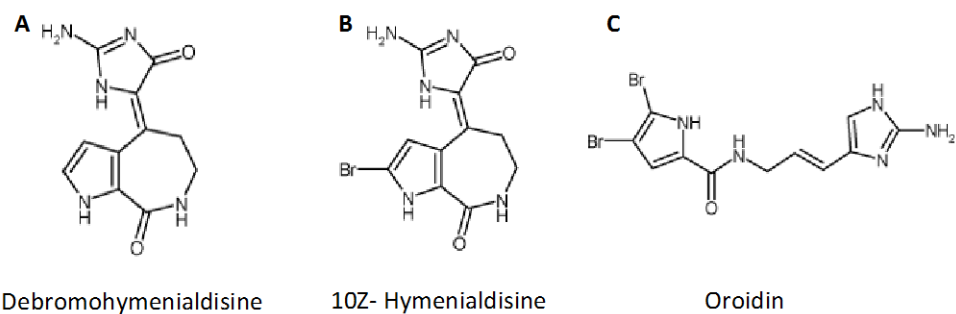


Figure 3. 10: Compound procured from Enzo Life Sciences. (A) Debromohymenialdisine, (B) 10Z- Hymenialdisine and (C) Oroidin.

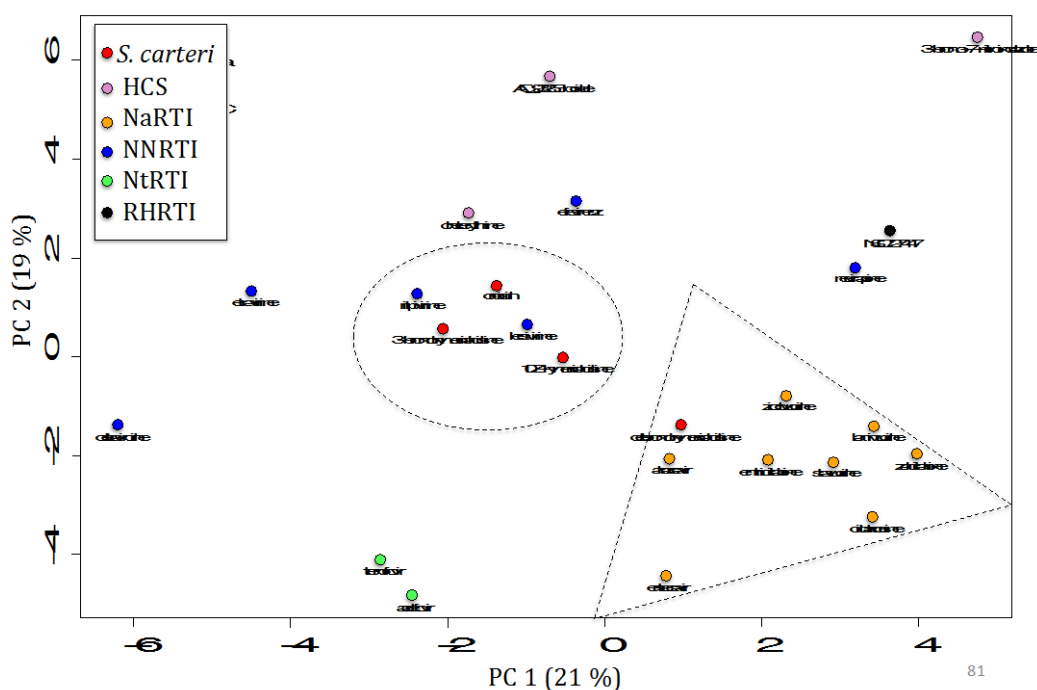


Figure 3. 11: Principle component analysis was performed on data aggregated from the High Content Analysis (LOPAC, pink), EASY-HIT, RT biochemical test and LC-MS data (Stylissa, red) and known HIV RT inhibitors (NaRTI, yellow; NNRTI, blue; NtRTI, green; RHRTI, black). The analysis was carried out using 45 molecular descriptors calculated for the twenty-five 3D SDF files from PubChem. The analysis shows that the candidate compounds from Stylissa, 3-bromohymenialdisine, oroidin, 10Z-hymenialdisine and debromohymenialdisine cluster more closely with known reverse transcriptase inhibitors according to their molecular properties than they do with their closest associated hits in the LOPAC library. Oroidin, 3-bromohymenialdisine and hymenialdisine are more structurally similar to known Non-nucleoside reverse transcriptase inhibitors (NNRTI), rilpivirine and lersivirine, than they are to known Nucleoside analog or Nucleotide reverse transcriptase inhibitors (NaRTI, NtRTI). Whereas, debromohymenialdisine is more similar in structure to a NaRTI.

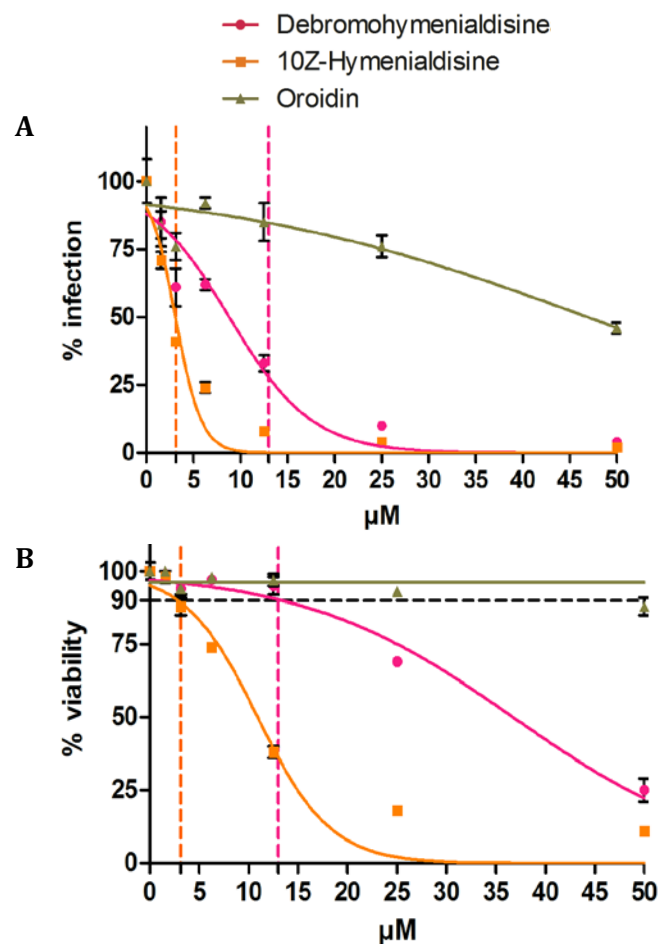


Figure 3. 12: % Infection and % Cell Viability of EASY-HIT assay after debromohymenialdisine, hymenialdisine, and oroidin treatment (A) The single compounds of debromohymenialdisine, hymenialdisine, and oroidin were purchase and tested on the EASY-HIT. Debromohymenialdisine completely inhibits HIV-1 replication at 25 μ M, revealing a 50% inhibition of the virus at approximately 7 μ M. Hymenialdisine is slightly more potent with 50% inhibition of the virus around 3 μ M; whereas, oroidin shows a 50% inhibition at 50 μ M. (B) The percentage of viability of the treated cells. Debromohymenialdisine is cytotoxic at concentrations greater than 13 μ M; however, hymenialdisine is significantly more cytotoxic starting at a concentration of 3 μ M. Oroidin is not toxic for any of the concentrations assayed.

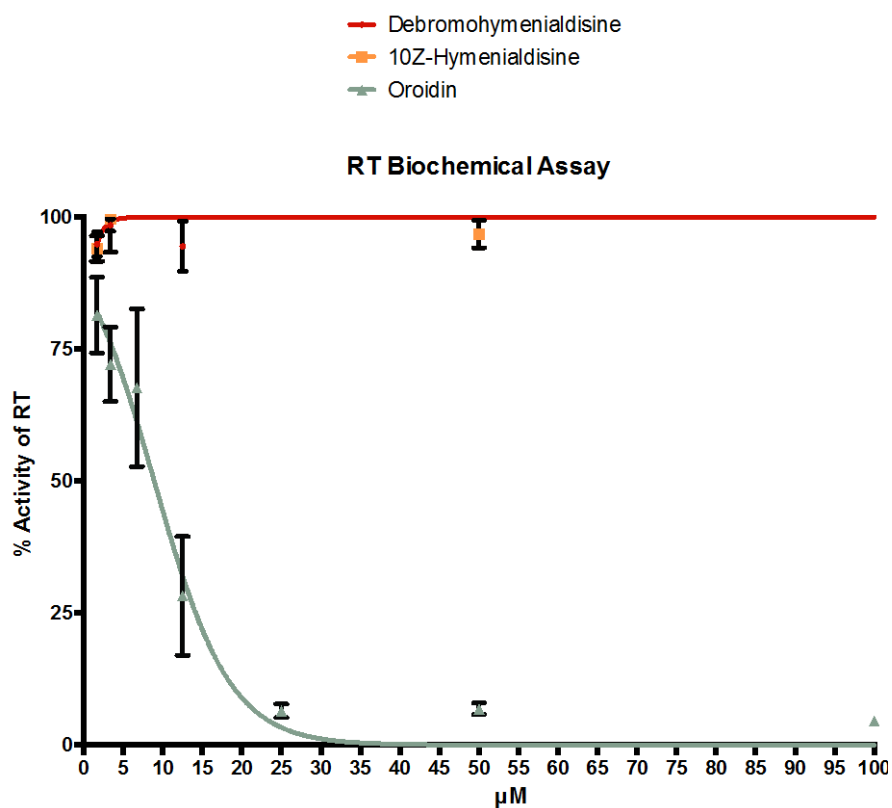


Figure 3. 13: Debromohymenialdisine, hymenialdisine, and oroidin screen on the biochemical HIV-1 reverse transcriptase assay. Serial dilutions of the single compounds debromohymenialdisine, hymenialdisine, and oroidin were screened for activity on a biochemical HIV-1 reverse transcriptase assay. This revealed oroidin as capable of inhibiting the activity of the enzyme up to 90% at 25 μM ; whereas, debromohymenialdisine and hymenialdisine were not active.

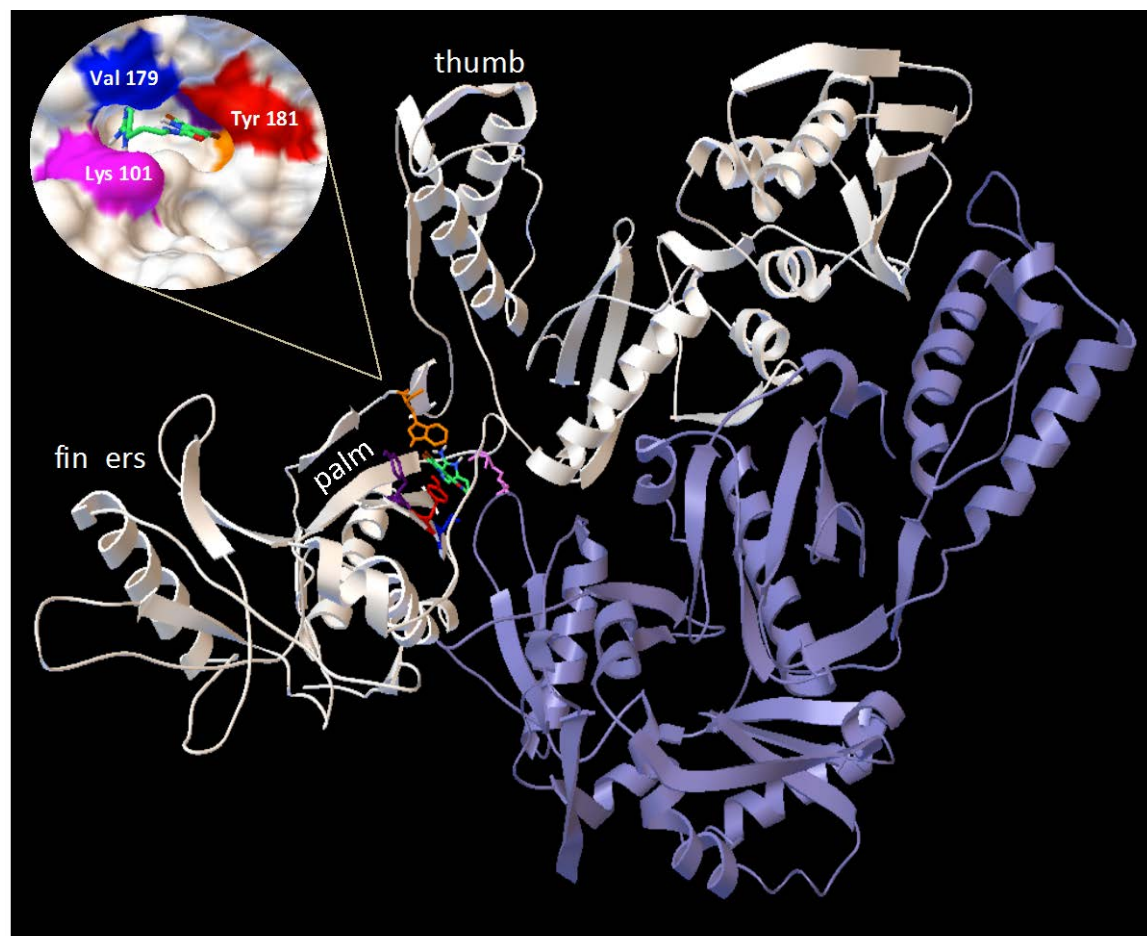


Figure 3. 14: In silico modeling of Oroidin with the HIV RT (PDB:1S1U) in Autodock vina. Oroidin binds into the hinge at the “palm” and the “thumb” of the p66 subunit (white, the p51 subunit is in lilac) where it interacts with residues Lys101 (pink), Val 179 (blue), Tyr 181 (red), Tyr 188 (purple), and W229 (orange).

Table 3. 1: HPLC gradient used to separate the *S. carteri* SPE fraction 1 into HPLC fractions 1-11.

Time	% H2O	% Acetonitrile
0 min	65	35
1 min	65	35
20 min	30	70
26 min	30	70
28 min	65	35
30 min	65	35

Table 3. 2: LC-MS gradient used to characterize the bioactive compounds of the *S. carteri* SPE fraction 1, HPLC fraction 2 and 6 (SPEF1_H2 and SPEF1_H6).

Time	% H2O	% MeOH	Formic acid in each solvent
0 min	90	10	0.10%
5 min	90	10	0.10%
40 min	10	90	0.10%
50min	10	90	0.10%
55min	90	10	0.10%
60min	90	10	0.10%

Table 3. 3: Molecular descriptors used for PCA analysis

ALogP	Atomic based prediction of lipophilicity
ALogP2	Atomic based prediction of lipophilicity
nAtomLC	number of atoms in largest chain
DPSA-2	difference in total charge weighted surface area
DPSA.3	difference in atomic charge weighted surface area
nHBAcc	Hydrogen Bond Acceptor Count Descriptor
nHBDon	Hydrogen Bond Donor Count Descriptor
PPSA-2	total charged weight positive surface area
PPSA-3	Atomic charged weight positive surface area
PNSA-1	sum of all partial negative surface area
FPSA-1	fractional charged partial positive surface areas
FPSA-2	Total fractional charged partial positive surface areas
FPSA-3	Atomic fractional charged partial positive surface areas
FNSA-1	fractional charged negative surface areas
RPCG	relative positive charge
RPCS	relative positive charge surface area

RNCS	relative negative charge surface area
TPSA	total polar surface area
RPSA	relative polar surface area
MOMI-Z	Moment of Inertia descriptor - Z- axis
MOMI-XY	Moment of Inertia descriptor - X,Y- axis
topoShape	topological shape index
Wlambda2.unity	Todeschini Grid-weighted holistic invariant molecular (GWHIM) descriptors
Wnu1.unity	Todeschini Grid-weighted holistic invariant molecular (GWHIM) descriptors
Wnu2.unity	Todeschini Grid-weighted holistic invariant molecular (GWHIM) descriptors
Weta1.unity	Todeschini Grid-weighted holistic invariant molecular (GWHIM) descriptors
Weta2.unity	Todeschini Grid-weighted holistic invariant molecular (GWHIM) descriptors
WD.unity	Todeschini Grid-weighted holistic invariant molecular (GWHIM) descriptors
C1SP2	Characterizes the carbon connectivity in terms of hybridization
C2SP2	Characterizes the carbon connectivity in terms of hybridization
C1SP3	Characterizes the carbon connectivity in terms of hybridization
SCH-5	Evaluates the Kier & Hall Chi chain indices of orders 3,4,5 and 6
SC-3	Evaluates the Kier & Hall Chi cluster indices of orders 3,4,5,6 and 7

Kier3	Descriptor that calculates Kier and Hall kappa molecular shape indices.
MDEC-33	Evaluate molecular distance edge descriptors for C, N and O
ATSc1	The Moreau-Broto autocorrelation descriptors using partial charges
ATSc3	The Moreau-Broto autocorrelation descriptors using partial charges
ATSc4	The Moreau-Broto autocorrelation descriptors using partial charges
ATSc5	The Moreau-Broto autocorrelation descriptors using partial charges
ATSm1	The Moreau-Broto autocorrelation descriptors using atomic weight
ATSm4	The Moreau-Broto autocorrelation descriptors using atomic weight
Petitjean Number	Descriptor that calculates the Petitjean Number of a molecule.
TopoPSA	Calculation of topological polar surface area based on fragment contributions
bpol	Descriptor that calculates the sum of the absolute value of the difference between atomic polarizabilities of all bonded atoms in the molecule (including implicit hydrogens)
C3SP2	Calculates the carbon connectivity in terms of hybridization

Table 3. 4: Binding affinity values for molecular modeling of oroidin and HIV-1 RT.

binding mode	affinity (kcal/mol)
1	-8.1
2	-7.8
3	-7.6
4	-7.5
5	-7.5
6	-7.3
7	-7.1
8	-7.1
9	-7

Table 3. 5: Anti-HIV alkaloids reported in the literature to date.

Natural Product	Source	Anti-HIV activity	Inhibition	Cytotoxicity	Reference
Alkaloids					
Batzelladines A	Sponge <i>Batzella</i> sp.	10 μ M	Binding to Tcells	complete cell death	Patil et al 1995
Batzelladines B	Sponge <i>Batzella</i> sp.	25 μ M	Binding to Tcells	complete cell death	Patil et al 1995
Buchapine	<i>Eodia roxburghiana</i>	0.94 μ M	cytopathic effects	29 μ M	McMormick et al 1996
Castanospermine	<i>Castanospermum australe</i>	> 10 μ g/ml	replication, glycosylation, syncytium formation	> 0.35 mg/ml	Karpas et al. 1988
Crambescidin 826	Sponge <i>Monanchora</i> sp.	1–3 μ M	cellular fusion	in vitro, no data	Chang et al 2003
Dehydrocrambine A	Sponge <i>Monanchora</i> sp.	~35 μ M	cellular fusion	in vitro, no data	Chang et al 2003
Dragmacidin F	Sponge <i>Halicortex</i> sp.	0.91 mM	syncytium formation	no value	Cutignano et al 2000
FK-3000	<i>Stephania cepharantha</i>	7.8 μ g/ml	HIV cytopathic effects	>15.6 μ g/ml	Ma et al 2002
Hypoglaucine B	<i>Tripterigium hypoglaucum</i>	0.1 μ g/ml	-	>100 μ g/ml	Duan et al 2000
3-(3-Methyl-2-butenyl)-4-[(3-methyl-2-butenyl) oxy]-2 (1H)-quinolinone	<i>Euodia roxburghiana</i>	1.64 μ M	HIV cytopathic effect	26.9 μ M	McMormick et al 1996
1-Methoxy canthinone	<i>Leitneria floridana</i>	0.26 μ g/ml	-	>100 μ g/ml	Xu et al 2000
Michellamine B	<i>Ancistrocladus korupensis</i>	1 μ M	Reverse Transcriptase, cellular fusion, syncytium formation	200 μ M	Manfredi et al 1991
Manadomanzamine A	Sponge <i>Acanthostrongylophora</i> sp.	7 μ g/ml (~27 μ M)	-	only tested at 4.8 μ g/ml	Peng et al 2003
Manadomanzamine B	Sponge <i>Acanthostrongylophora</i> sp.	16.5 μ g/ml (~11 μ M)	-	only tested at 4.8 μ g/ml	Peng et al 2003
Nitidine	<i>Toddalia asiatica</i>	14 μ M	Reverse Transcriptase,	in vitro, no data	Tan et al 1991
Trikendiol	Sponge <i>Trikentrion loeve</i>	2 μ g/ml (~3.4 μ M)	HIV cytopathic effects	no data	Loukaci et al 1994
Triptonine A	<i>Tripterigium hypoglaucum</i>	2.54 μ g/ml	-	>100 μ g/ml	Duan et al 2000
Triptonine B	<i>Tripterigium hypoglaucum</i>	< 0.1 μ g/ml	HIV cytopathic effects	>100 μ g/ml	Duan et al 2000
Xestomanzamine A	Sponge <i>Acanthostrongylophora</i> sp.	11.2 μ g/ml (~40 μ M)	-	only tested at 4.8 μ g/ml	Peng et al 2003

3.8 References

1. (UNAIDS), Global report: UNAIDS report on the global AIDS epidemic 2013. *UNAIDS/JC2502/1/E* **2013**.
2. Aleman, Y.; Vinken, L.; Kouri, V.; Perez, L.; Alvarez, A.; Abrahantes, Y.; Fonseca, C.; Perez, J.; Correa, C.; Soto, Y.; Schrooten, Y.; Vandamme, A. M.; Van Laethem, K., Performance of an in-house human immunodeficiency virus type 1 genotyping system for assessment of drug resistance in cuba. *PLoS One* **2015**, *10* (2), e0117176.
3. Andersen, J. L.; Le Rouzic, E.; Planelles, V., HIV-1 Vpr: Mechanisms of G(2) arrest and apoptosis. *Experimental and Molecular Pathology* **2008**, *85* (1), 2-10.
4. Yarnold, J. E.; Hamilton, B. R.; Welsh, D. T.; Pool, G. F.; Venter, D. J.; Carroll, A. R., High resolution spatial mapping of brominated pyrrole-2-aminoimidazole alkaloids distributions in the marine sponge *Stylissa flabellata* via MALDI-mass spectrometry imaging. *Mol Biosyst* **2012**, *8* (9), 2249-2259.
5. Keifer, P. A.; Schwartz, R. E.; Koker, M. E. S.; Hughes, R. G.; Rittschof, D.; Rinehart, K. L., Bioactive Bromopyrrole Metabolites from the Caribbean Sponge *Agelas-Conifera*. *J Org Chem* **1991**, *56* (9), 2965-2975.
6. Pauletti, P. M.; Cintra, L. S.; Braguine, C. G.; da Silva, A. A.; Silva, M. L. A. E.; Cunha, W. R.; Januario, A. H., Halogenated Indole Alkaloids from Marine Invertebrates. *Mar Drugs* **2010**, *8* (5), 1526-1549.
7. Martinez, J. P.; Sasse, F.; Bronstrup, M.; Diez, J.; Meyerhans, A., Antiviral drug discovery: broad-spectrum drugs from nature. *Nat Prod Rep* **2015**, *32* (1), 29-48.
8. (a) Meijer, L.; Thunnissen, A. M. W. H.; White, A. W.; Garnier, M.; Nikolic, M.; Tsai, L. H.; Walter, J.; Cleverley, K. E.; Salinas, P. C.; Wu, Y. Z.; Biernat, J.; Mandelkow, E. M.; Kim, S. H.; Pettit, G. R., Inhibition of cyclin-dependent kinases, GSK-3 beta and CK1 by hymenialdisine, a marine sponge constituent. *Chem Biol* **2000**, *7* (1), 51-63; (b) Wan, Y. Q.; Hur, W. Y.; Cho, C. Y.; Liu, Y.; Adrian, F. J.; Lozach, O.; Bach, S.; Mayer, T.; Fabbro, D.; Meijer, L.; Gray, N. S., Synthesis and target identification of hymenialdisine analogs. *Chem Biol* **2004**, *11* (2), 247-259.
9. Debebe, Z.; Ammosova, T.; Breuer, D.; Lovejoy, D. B.; Kalinowski, D. S.; Kumar, K.; Jerebtsova, M.; Ray, P.; Kashanchi, F.; Gordeuk, V. R.; Richardson, D. R.; Nekhai, S., Iron Chelators of the Di-2-pyridylketone Thiosemicarbazone and 2-Benzoylpyridine Thiosemicarbazone Series Inhibit HIV-1 Transcription: Identification of Novel Cellular Targets-Iron, Cyclin-Dependent Kinase (CDK) 2, and CDK9 (vol 79, pg 185, 2011). *Mol Pharmacol* **2011**, *80* (6), 1190-1190.
10. Newman, D. J.; Cragg, G. M.; Battershill, C. N., Therapeutic agents from the sea: biodiversity, chemo-evolutionary insight and advances to the end of Darwin's 200th year. *Diving and Hyperbaric Medicine* **2009**, *39* (4), 216-225.

11. Butler, M. S.; Robertson, A. A. B.; Cooper, M. A., Natural product and natural product derived drugs in clinical trials. *Nat Prod Rep* **2014**, *31* (11), 1612-1661.
12. Kremb, S.; Helfer, M.; Heller, W.; Hoffmann, D.; Wolff, H.; Kleinschmidt, A.; Cepok, S.; Hemmer, B.; Durner, J.; Brack-Werner, R., EASY-HIT: HIV Full-Replication Technology for Broad Discovery of Multiple Classes of HIV Inhibitors. *Antimicrob Agents Ch* **2010**, *54* (12), 5257-5268.
13. Lee, O. O.; Wang, Y.; Yang, J.; Lafi, F. F.; Al-Suwailem, A.; Qian, P. Y., Pyrosequencing reveals highly diverse and species-specific microbial communities in sponges from the Red Sea. *ISME J* **2011**, *5* (4), 650-64.
14. (a) Moitinho-Silva, L.; Bayer, K.; Cannistraci, C. V.; Giles, E. C.; Ryu, T.; Seridi, L.; Ravasi, T.; Hentschel, U., Specificity and transcriptional activity of microbiota associated with low and high microbial abundance sponges from the Red Sea. *Mol Ecol* **2014**, *23* (6), 1348-63; (b) Moitinho-Silva, L.; Seridi, L.; Ryu, T.; Voolstra, C. R.; Ravasi, T.; Hentschel, U., Revealing microbial functional activities in the Red Sea sponge *Stylissa carteri* by metatranscriptomics. *Environ Microbiol* **2014**, *16* (12), 3683-98.
15. Bugni, T. S.; Harper, M. K.; McCulloch, M. W. B.; Reppart, J.; Ireland, C. M., Fractionated marine invertebrate extract libraries for drug discovery. *Molecules* **2008**, *13* (6), 1372-1383.
16. Trott, O.; Olson, A. J., AutoDock Vina: improving the speed and accuracy of docking with a new scoring function, efficient optimization, and multithreading. *Journal of computational chemistry* **2010**, *31* (2), 455-61.
17. Esposito, F.; Corona, A.; Zinzula, L.; Kharlamova, T.; Tramontano, E., New Anthraquinone Derivatives as Inhibitors of the HIV-1 Reverse Transcriptase-Associated Ribonuclease H Function. *Chemotherapy* **2012**, *58* (4), 299-307.
18. Bergmann, W.; Feeney, R. J., Contributions to the Study of Marine Products .32. The Nucleosides of Sponges .1. *J Org Chem* **1951**, *16* (6), 981-987.
19. Degarilhe, M. P.; Derudder, J., Effet De Deux Nucleosides De Larabinose Sur La Multiplication Des Virus De Lherpes Et De La Vaccine En Culture Cellulaire. *Comptes Rendus Hebdomadaires Des Seances De L Academie Des Sciences* **1964**, *259* (16), 2725-&.
20. Junaid, M.; Lapins, M.; Eklund, M.; Spjuth, O.; Wikberg, J. E., Proteochemometric modeling of the susceptibility of mutated variants of the HIV-1 virus to reverse transcriptase inhibitors. *PLoS One* **2010**, *5* (12), e14353.
21. Eckstein, D. A.; Sherman, M. P.; Penn, M. L.; Chin, P. S.; De Noronha, C. M.; Greene, W. C.; Goldsmith, M. A., HIV-1 Vpr enhances viral burden by facilitating infection of tissue macrophages but not nondividing CD4+ T cells. *J Exp Med* **2001**, *194* (10), 1407-19.
22. Bettaccini, A. A.; Baj, A.; Accolla, R. S.; Basolo, F.; Toniolo, A. Q., Proliferative activity of extracellular HIV-1 Tat protein in human epithelial cells: expression profile of pathogenetically relevant genes. *BMC microbiology* **2005**, *5*, 20.

23. Goh, W. C.; Rogel, M. E.; Kinsey, C. M.; Michael, S. F.; Fultz, P. N.; Nowak, M. A.; Hahn, B. H.; Emerman, M., HIV-1 Vpr increases viral expression by manipulation of the cell cycle: a mechanism for selection of Vpr in vivo. *Nat Med* **1998**, *4* (1), 65-71.
24. Zhu, Y.; Gelbard, H. A.; Roshal, M.; Pursell, S.; Jamieson, B. D.; Planelles, V., Comparison of cell cycle arrest, transactivation, and apoptosis induced by the simian immunodeficiency virus SIVagm and human immunodeficiency virus type 1 vpr genes. *J Virol* **2001**, *75* (8), 3791-801.
25. Curman, D.; Cinel, B.; Williams, D. E.; Rundle, N.; Block, W. D.; Goodarzi, A. A.; Hutchins, J. R.; Clarke, P. R.; Zhou, B. B.; Lees-Miller, S. P.; Andersen, R. J.; Roberge, M., Inhibition of the G2 DNA damage checkpoint and of protein kinases Chk1 and Chk2 by the marine sponge alkaloid debromohymenialdisine. *J Biol Chem* **2001**, *276* (21), 17914-9.
26. Osborn, L.; Kunkel, S.; Nabel, G. J., Tumor necrosis factor alpha and interleukin 1 stimulate the human immunodeficiency virus enhancer by activation of the nuclear factor kappa B. *Proc Natl Acad Sci U S A* **1989**, *86* (7), 2336-40.
27. Mohammed, R.; Peng, J.; Kelly, M.; Hamann, M. T., Cyclic heptapeptides from the Jamaican sponge *Stylissa caribica*. *J Nat Prod* **2006**, *69* (12), 1739-44.
28. Eder, C.; Proksch, P.; Wray, V.; Steube, K.; Bringmann, G.; van Soest, R. W. M.; Sudarsono; Ferdinandus, E.; Pattisina, L. A.; Wiryowidagdo, S.; Moka, W., New alkaloids from the Indopacific sponge *Stylissa carteri*. *J Nat Prod* **1999**, *62* (1), 184-187.
29. Harvey, A. L.; Edrada-Ebel, R.; Quinn, R. J., The re-emergence of natural products for drug discovery in the genomics era. *Nat Rev Drug Discov* **2015**, *14* (2), 111-29.
30. Ren, J.; Stammers, D. K., HIV reverse transcriptase structures: designing new inhibitors and understanding mechanisms of drug resistance. *Trends Pharmacol Sci* **2005**, *26* (1), 4-7.
31. Pata, J. D.; Stirtan, W. G.; Goldstein, S. W.; Steitz, T. A., Structure of HIV-1 reverse transcriptase bound to an inhibitor active against mutant reverse transcriptases resistant to other nonnucleoside inhibitors. *P Natl Acad Sci USA* **2004**, *101* (29), 10548-10553.
32. Sagar, S.; Kaur, M.; Minneman, K. P., Antiviral Lead Compounds from Marine Sponges. *Mar Drugs* **2010**, *8* (10), 2619-2638.
33. Newman, D. J.; Cragg, G. M., Natural products as sources of new drugs over the last 25 years. *J Nat Prod* **2007**, *70* (3), 461-477.
34. Gerwick, W. H.; Moore, B. S., Lessons from the past and charting the future of marine natural products drug discovery and chemical biology. *Chem Biol* **2012**, *19* (1), 85-98.
35. Gottfredsson, M.; Bohjanen, P. R., Human immunodeficiency virus type I as a target for gene therapy. *Frontiers in bioscience : a journal and virtual library* **1997**, *2*, d619-34.

Dissertation Conclusion

In an effort to bioprospect novel antiviral scaffolds from a Red Sea sponge library, I was able to generate four possible leads from the previously identified compounds known as a Halitoxin, debromohymenialdisine, hymenialdisine and oroidin. Our initial expectation was to find unknown compounds with new activity, assuming that the existing compounds had already been comprehensively screened for their anti-infective potential. Our experimentation provides evidence that the next big step in natural products drug discovery could be achieved by extensively evaluating known compounds for their activity as antivirals. Antibacterial and anti-parasitic, and anticancer screens have yielded a modest number of pharmacophores or “privileged scaffolds” whose modification has contributed to a much larger number of drug leads. Following suit, new tools for acquiring compounds and their derivatives in greater quantities have expanded by the method of genome mining and the subsequent use of heterologous recombination in order to drive the expression of biochemical pathways and biologically engineer pre-existing structures. It is important that while the techniques evolve, that the resulting compounds are also assayed for their activity or we might be sitting on a cure without knowing it. The number of antiviral drug candidates in clinical trials is surprisingly low and it is important to see an increase in approval rates if we are to see less disease and deaths resulting from viral infection.

Manuscripts in preparation

Identification of a 3-alkyl pyridinium from the Red Sea sponge *Amphimedon chloros* as an inhibitor of the West Nile Virus NS3 protease *in vitro*.

Aubrie O'Rourke, Stephan Kremb, Misjudeen Raji, Salim Sioud, Najeh M. Kharbartia, Abdel-Hamid Emwas, William H. Gerwick and Christian R. Voolstra

Alkaloids from *Stylissa carteri* present prospective scaffolds for the inhibition of the Human immunodeficiency Virus-1 (HIV-1)

Aubrie O'Rourke, Stephan Kremb, Theresa Rock, Philippe Schmitt-Kopplin, Ruth Brack-Werner and Christian R. Voolstra

Patent Applications Filed

2014 US Letter Patent Application No. 62/072,292; Invention Disclosure #2014-065: "Novel 3-Alkyl Pyridinium Salt from the Red Sea Sponge Echinochalina with Potent Antiviral Activity."

2014 US Letter Patent Application No. 62/068,716; Invention Disclosure #2014-090: "Bioprospecting of a Red Sea Sponge Stylissa carteri with Novel HIV Inhibitor Scaffolds."